Abstracts 10,617-10,917

SOLID STATE ABSTRACTS

an abstract journal devoted to the theory, production and use of solid state materials and devices

VOLUME 2 NUMBER 3

PHYSICS
METALLURGY
ELECTRONICS

SEMICONDUCTORS
PHOSPHORS
MAGNETICS
DIELECTRICS
SUPERCONDUCTORS
METALS

SOLID STATE ABSTRACTS

VOLUME 2, NUMBER 3

June 1961

Abstracts 10,617–10,917

TABLE OF CONTENTS

Abstracts of the Solid State Literature

Editor: GEOFFREY KNIGHT, JR., Ph.D.

Assistant Editor: JOHN A. MURPHY

PUBLISHED MONTHLY BY

Cambridge Communications Corporation, 238 Main Street, Cambridge 42, Massachusetts, Tel. 491-0710

Subscription Rate: $25.00 per year. Single Copies and Back Issues: $2.50. Advertising Rates on Request.

Cambridge Communications Corp. is not prepared to furnish copies of the articles abstracted. However, there are many libraries throughout the country which maintain photocopying services.

SYMBOLS USED IN THE ABSTRACTS

L: Letter to the Editor. A: Only an abstract is given in the reference. R: Only a review is given in the reference. E: Erratum.

The reference numbers in the indices are the abstract numbers, not the page numbers.

MULTI-LANGUAGE VOCABULARY
for
SOLID STATE TERMS

absorption
1 Absorption
absorption
погощение

acceptor
2 Akzeptor
accepteur
акцептор

activation energy
3 Aktivierungsenergie
énergie d'activation
энергия активации

admittance
4 Scheinleitwert
admittance
адмитанц

aging
5 Alterung
vieillissement
старение

air cooling
6 Luftkühlung
refroidissement par l'air
воздушное охлаждение

alloy
7 Legierung
alliage
сплав

alloyed transistor
8 Legierungstransistor
transistor allié
сплавной триод

alloying method
9 Legierungsverfahren
procédé par alliage
способ легирования

allowed band
10 erlaubtes Band
bande permise
разрешенная зона

ambient temperature
11 Umgebungstemperatur
temperature ambiante
температура окружающей среды

amplifier
12 Verstärker
amplificateur
усилитель

analog transistor
13 Analogtransistor
transistor analogue
аналогичный транзистор

anode
14 Anode
anode
анод

annealing
15 Tempern
frittage
отжигание

apparatus for pulling crystals
16 Kristallzieheinrichtung
apparail de tirage
установка для вытягивания кристаллов

apply
17 aufbringen
appliquer
нанести, наносить

assembly
18 Anordnung
montage, ensemble
установка

atomic bond
19 Atombindung
liaison atomique
атомная связь

atomic lattice
20 Atomgitter
réseau atomique
атомная решетка

avalanche
21 Lawine
avalanche
лавина

back resistance
22 Sperrwiderstand
résistance inverse
обратное сопротивление

barrier height
23 Diffusionsspannung
hauteur de la barrière de potentiel
диффузионное напряжение

barrier layer
24 Randschicht, Sperrschicht
couche de barrage, barrière
запирающий слой

barrier-layer rectifier
25 Sperrschichtgleichrichter
redresseur à couche de barrage
выпрямитель с запорным слоем

base
26 Basis
base
база

base contact
27 Basiselektrode, Basisanschluss
contact de base
контакт базы электрод базы

base current
28 Basisstrom
courant de base
ток базы

base plate
29 Grundplatte
plaque de base
базовая пластинка

base-plate electrode
30 Trägerelektrode
support
нижный электрод основание

base region
31 Basiszone
région de base
область базы

base resistance
32 Basiswiderstand
résistance de base
сопротивление базы

base terminal
33 Basiszuleitung
connexion de base
вывод базы

base zone
34 Basiszone
zone de base
зона базы

bias
35 Vorspannung
polarisation
смещение

binding energy
36 Bindungsenergie
énergie de liaison
энергия связи

branch of the thermoelement
37 Thermoelementschenkel
branche de l'élément thermoélectrique
ветвь термоэлементов

break down voltage
38 Durchschlagspannung, Durchbruchspannung
tension de claquage
пробивное напряжение

capacitance
39 Kapazität
capacité
ёмкость

capsulation
40 Einbau ints Gehäuse
encapsulation, mise en capsule
сборка помещение в корпус

carrier concentration
41 Trägerkonzentration
concentration de porteurs
концентрация носителей

carrier density
42 Trägerdichte
densité de porteurs
плотность носителей

carrier diffusion
43 Trägerdiffusion
diffusion de porteurs
диффузия носителей

carrier injection
44 Trägerinjektion
injection de porteurs
инжекция носителей

carrier mobility
45 Trägerbeweglichkeit
mobilité de porteurs de charge
подвижность носителей тока

cathode
46 Kathode
cathode
катод

cathode sputtering
47 Kathodenzerstäubung
évaporation cathodique
катодное напыление

ceramic case
48 Keramikgehäuse
cartouche céramique
керамический корпус

charge carrier
49 Stromträger, Ladungsträger
porteur de charge
ностель тока

charge carrier concentration
50 Ladungsträgerkonzentration
concentration de porteurs de charge
концентрация носителей тока

charge carrier density
51 Ladungsträgerdichte
densité de porteurs de charge
плотность носителей заряда

charge carrier diffusion
52 Ladungsträger-Diffusion
diffusion de porteurs de charge
диффузия носителей тока

charge carrier injection
53 Ladungsträger-Injektion
injection de porteurs de charge
инжекция носителей тока

chemical compounds of semiconductors
54 chemische Verbindungen der Halbleiterstoffe
composés chimiques des semiconducteurs
химические соединении полупроводников

chemical etching
55 Chemische Ätzung
attaque chimique
химическое травление

coefficient of elasticity
56 Elastizitätskonstante
constante élastique
упругая постоянная

coefficient of expansion
57 Ausdehnungskoeffizient
coefficient de dilatation
коэффициент расширения

cold junction of the thermocouple
58 kalte Lötstelle des Thermoelements, kalte Kontaktstelle des Thermoelements
soudure froide du thermocouple
холодный спай термоэлемента

collector
59 Kollektor
collecteur
коллектор

collector contact
60 Kollektorelektrode, Kollektoranschluss
contact de collecteur
контакт коллектора электрод коллектора

collector current
61 Kollektorstrom
courant de collecteur
ток коллектора

collector region
62 Kollektorzone, Kollektorbereich
région collectrice, région de collecteur
область коллектора

collector resistance
63 Kollektorwiderstand
résistance de collecteur
сопротивление коллектора

collector terminal
64 Kollektorzuleitung
connexion de collecteur
вывод коллектора

collector voltage
65 Kollektorspannung
tension de collecteur
напряжение коллектора

collector zone
66 Kollektorzone
zone collectrice
зона коллектора

common base circuit
67 Basisschaltung
montage base commune
схема с общим основанием

common collector circuit
68 Kollektorschaltung
montage collecteur commun
схема с общим коллектором

common emitter circuit
69 Emitterschaltung
montage émetteur commun
схема с общим эмиттером

conduction band
70 Leitungsband
bande de conduction
зона проводимости

conduction electron
71 Leitungselektron
électron de conductivité
электрон проводимости

conduction type
72 Leitungstyp
type de conductivité
тип проводимости

conductivity
73 Leitfähigkeit
conductivité
проводимость

contact plate
74 Abnahmeelektrode
électrode de prise de courant
контактная шайба

contact potential difference
75 Kontaktpotentialdifferenz
différence de potentiel
контактная разность потенциалов

control electrode
76 Steuerelektrode
électrode de commande
управляющий электрод

controlled rectifier
77 steuerbare Gleichrichterzelle
redresseur commandé
управляемый выпрямитель

cooling
78 Kühlung
refroidissement
охлаждение

cooling fins
79 Kühlrippen
ailettes de réfrigération
охлаждающий ребро

copper-oxide rectifier
80 Kupferoxydulgleichrichter
redresseur à l'oxyde de cuivre
купроксный выпямитель

counter-electrode
81 Gegenelektrode, Deckelektrode
contre-électrode
верхний электрод

covalence crystal
82 Valenzkristall
cristal covalent
ковалентный кристалл

covalent bond
83 Valenzbindung
liaison covalente
ковалентная связь

crucible (melt crucible)
84 Schmelztiegel
creuset
тигель расплава

crucible
85 Tiegel
creuset
тигель

crystal chuck
86 Kristallhalter
porte-cristal
держатель кристалла

crystal growth
87 Kristallwachstum
croissance du cristal
рост кристаллов

crystal holder
88 Kristallhalter
porte-cristal
держатель кристалла

crystal lattice
89 Kristallgitter
réseau cristallin
кристаллическая решетка

crystal preparation in a boat
90 Kristallisation im Tiegel
crystallisation dans une nacelle
кристаллизация в лодочке

crystal pulling
91 Kristallziehen
préparation des cristaux par tirage
вытягивание кристаллов

crystal rectifier
92 Kristallgleichrichter, Kristalldetektor
cristal redresseur
кристаллический диод
кристаллический детектор

crystal structure
93 Kristallstruktur
structure de cristal
кристаллическая структура

crystal wafer
94 Kristallscheibe
lame de cristal
пластинка кристалла

crystallographic plane
95 kristallographische Ebene
plan cristallographique
кристаллографическая плоскость

current density
96 Stromdichte
densité de courant
плотность тока

current gain
97 Stromverstärkung
gain en courant
выигрыш в токе

current gain factor
98 Stromverstärkungsfaktor
gain de courant
коэффициент усиления по току

current multiplication
99 Stromvervielfachung
multiplication de courant
умножение тока

current versus voltage characteristic
100 Strom-Spannungs-Kennlinie
caractéristique courant-voltage
вольтамперная характеристика

dark current
101 Dunkelstrom
courant à l'obscureté
темновой ток

decay time
102 Abfallzeit
temps de décroissance
время потухания

defect electron conduction
103 Defektelektronenleitung, Mangelleitung
conduction par défaut d'électrons
дырочная проводимость

depletion layer
104 Verarmungsrandschicht
couche de barrage
запорний слой

depth of penetration
105 Eindringtiefe
profondeur de pénétration
глубина проникновения

dielectric constant
106 Dielektrizitätskonstante
constante diélectrique
диэлектрическая постоянная

diffused junction
107 diffundierter p-n-Übergang
jonction diffusée
диффузионный переход

diffused transistor
108 Diffusionstransistor
transistor diffusé
диффузионный триод

diffusion coefficient
109 Diffusionskoeffizient
coéfficient de diffusion
коэффициент диффузии

diffusion current
110 Diffusionsstrom
courant de diffusion
диффузионный ток

diffusion length
111 Diffusionslänge
longueur de diffusion
диффузионная длина

diffusion method
112 Diffusionsverfahren
procédé de diffusion
диффузионный метод

diode
113 Diode
diode
диод

dislocation
114 Versetzung
dislocation
дислокация

dislocation density
115 Versetzungsdichte
densité des dislocations
плотность дислокаций

dislocation line
116 Versetzungslinie
ligne de dislocation
линия дислокации

dislocation ring
117 Versetzungsring
boucle de dislocation
кольцо дислокации

distance washer
118 Distanzscheibe
plaque de distance
дистанционная шайба

distribution coefficient
119 Verteilungskoeffizient
coéfficient de distribution
коэффициент распределения

distribution of impurities
120 Störstellenverteilung
distribution des impuretés
распределение примесей

donor
121 Donator
donneur
донор

doping
122 Dotierung
dopage
добавление примесей

doping material
123 Störstellensubstanz
impureté
примесь

doping of the melt
124 Umdotieren der Schmelze
introduction des impuretés dans la fonte
введение примесей в расплав

double-base diode
125 Doppel-Basis-Diode
diode à double base
двубазовый диод

drawing rate
126 Ziehgeschwindigkeit
vitesse de tirage
дырочная проводимость

drift mobility
127 Driftbeweglichkeit
mobilité de déplacement
дрейфовая подвижность

drift transistor
128 Drifttransistor
transistor drift
дрейфовый триод

dry rectifier
129 Trockengleichrichter
redresseur sec
твердый выпрямитель

edge dislocation
130 Stufenversetzung
dislocation coin
краевая дислокация

effective mass
131 effektive Masse
masse apparente
эффективная масса

electric forming
132 elektrisches Formieren
formation électrique
формовка

electrical conductivity
133 elektrische Leitfähigkeit
conductibilité électrique
электропроводимость

electrode
134 Elektrode
électrode
электрод

electrolytic etching
135 Elektrolytische Ätzung
attaque électrochimique
электролитическое травление

electromotive force (emf)
136 elektromotorische Kraft (EMK)
force électromotrice (fem)
электродвижущая сила эдс

electron bombardment
137 Elektronenbeschuss
bombardement électronique
электронная бомбардировка

electron concentration
138 Elektronenkonzentration
concentration des électrons
концентрация электронов

electron conduction
139 Überschusselektronenleitung, Elektronenleitung, Überschussleitung
conduction par excès d'électrons, conduction par électrons
электронная проводимость

electron current
140 Elektronenstrom
courant des électrons
электронный ток

electron density
141 Elektronendichte
densité des électrons
плотность электронов

electron mobility
142 Elektronenbeweglichkeit
mobilité des électrons
подвижность электронов

electron scattering
143 Elektronenstreuung
dispersion des électrons
рассеяние электронов

emitter
144 Emitter
émetteur
эмиттер

emitter contact
145 Emitterelektrode, Emitteranschluss
contact d'émetteur
контакт эмиттера
электрод эмиттера

emitter current
146 Emitterstrom
courant d'émetteur
ток эмиттера

emitter injection efficiency
147 Emitterwirkungsgrad, Emitterwirksamkeit
taux d'injection d'émetteur
область эмиттера

emitter region
148 Emitterzone, Emitterbereich
région émittrice, région d'émetteur
вывод эмиттера

emitter resistance
149 Emitterwiderstand
résistance d'émetteur
к.п.д. эмиттера

emitter terminal
150 Emitterzuleitung
connexion d'émetteur
сопротивление эмиттера

emitter voltage
51 Emitterspannung
tension d'émetteur
напряжение эмиттера

emitter zone
52 Emitterzone
zone émittrice
зона эмиттера

empty band
53 leeres Band
bande vide
незаполненная зона

energy band structure
54 Energiebänderstruktur
structure de la bande d'énergie
структура энергетических зон

energy gap, forbidden band
55 verbotenes Band
bande interdite
запретная зона
запрещенная зона

energy level
56 Energieniveau
niveau énergétique
энергетический уровень

equivalent circuit
57 Ersatzschaltbild
schema équivalent
эквивалентная схема

etch pattern
58 Ätzfigur
figure d'attaque
фигура травления

etch pit
59 Ätzgrube
puits d'attaque
яма травления

eutectic
60 Eutektikum
eutéctique
эвтектика

evaporation
61 Aufdampfen
évaporation
испарение

exciton
62 Exziton
exciton
экцитон

extrinsic conduction
63 Störstellenleitung
conduction extrinsèque
примесная проводимость

extrinsic semiconductor
64 Störstellenhalbleiter
semiconducteur extrinsèque
примусный полупроводник

feeding
165 Speisung
alimentation
питание

Fermi distribution
166 Fermi-Verteilung
distribution de Fermi
распределение Ферми

Fermi level
167 Fermi-Niveau
niveau de Fermi
уровень Ферми

fieldistor
168 Fieldistor
fieldistor, fieldistron
фильдистор

field-effect transistor
169 Feldeffekt-Transistor
transistor à effect de champ
полевой транзистор

filamentary transistor
170 Fadentransistor
transistor filament
нитевидный триод

filled band
171 besetztes Band
bande remplie
заполненная зона

film
172 Film
film
пленка

floating zone melting
173 Tiegelfreies Zonenschmelzen
fusion de zone sans creuset, fusion par zone flottante
бестигельная зонная плавка

foreign atom
174 Fremdatom
atom étranger
посторонний атом
примесный атом

forward current
175 Durchlassstrom, Flussstrom
courant direct
прямый ток

forward direction
176 Durchlassrichtung, Flussrichtung
sens passant
пропускное направление
прямое направление

forward resistance
177 Durchlasswiderstand, Flusswiderstand
résistance directe
прямое сопротивление

forward voltage
178 Spannung in Durchlassrichtung, Durchlassspannung, Flussspannung
tension directe
прямое напряжение

four-terminal network
179 Vierpol
quadripôle
чутырехполюсник

furnace
180 Ofen
four
печь

fused junction
181 Rekristallisations-p-n-Übergang
jonction pn recristallisée
рекристаллизационный p-n-переход

generator
182 Generator
générateur
генератор

germanium rectifier
183 Germaniumgleichrichter
redresseur au germanium
германиевый выпрямитель

germanium transistor
184 Germaniumtransistor
transistor au germanium
германиевый триод

glass capsule
185 Glasgehäuse
cartouche de verre
стекляная коробка

grain boundary
186 Korngrenze
joint de grain, limite des grains
граница зерен

grounded base circuit
187 Basisschaltung
montage base à la masse
схема с заземленным основанием

grounded collector circuit
188 Kollektorschaltung
montage collecteur à la masse
схема с заземленным коллектором

grounded emitter circuit
189 Emitterschaltung
montage émitteur à la masse
схема с заземленным эмиттером

grown junction
190 gezogener p-n-Übergang
jonction par tirage
вытягиваемый p-n- переход

growth rate
191 Wachstumsgeschwindigkeit
vitesse de croissance
скорость роста

Hall effect
192 Hall-Effekt
effet Hall
эффект Холла

Hall generator
193 Hall-Generator
générateur de Hall
генератор Холла

Hall mobility
194 Hall-Beweglichkeit
mobilité de Hall
подвижность Холла

heat conduction
195 Wärmeleitung
conduction thermique
теплопроводимость

heat treatment
196 Tempern, Wärmebehandlung
traitement thermique
термообработка

heteropolar bond
197 heteropolare Bindung
liaison hétéropolaire
гетерополярная связь

heteropolar crystal
198 heteropolarer Kristall
cristal hétéropolaire
гетерополярный кристалл

hole concentration
199 Löcherkonzentration
concentration des trous
концентрация дырок

hole conduction
200 Defektleitung, Löcherleitung
conduction par trous
проводимость дырок

hole current
201 Löcherstrom
courant des trous
дырочный ток

hole mobility
202 Löcherbeweglichkeit
mobilité des trous
подвижность дырок

homopolar bond
203 homöopolare Bindung
liaison homopolaire
гомеополярная связь

homopolar crystal
204 homöopolarer Kristall
cristal homopolaire
гомеополярный кристалл

hot junction of the thermocouple
205 heisse Lötstelle des Thermoelements, heisse Kontaktstelle des Thermoelements
soudure chaude du thermocouple
горячий спай термоэлемента

housing
206 Gehäuse
cartouche, boîtier
корпус

illumination
207 Bestrahlung
illumination
освещение

impedance
208 Scheinwiderstand
impédance
импеданс

imperfection
209 Gitterfehlordnung
imperfection
дефектность

impurity
210 Beimengung, Verunreinigung
impureté
примесь

impurity concentration
211 Störstellenkonzentration
concentration des impuretés
концентрация примесей

impurity content
212 Störstellengehalt
teneur en impureté
содержание примеси

impurity level
213 Störstellenniveau
niveau d'énergie d'impuretés
примесный уровень

index of refraction
214 Brechungsindex
indice de réfraction
показатель преломления

inductance
215 Induktivität
inductance
индуктивность

ingot
216 Barren, Kristall
lingot
слиток

input circuit
217 Eingangskreis
circuit d'entrée
входная цепь

input current
218 Eingangsstrom
courant d'entrée
входной ток

input power
219 Eingangsleistung
puissance d'entrée
входная мощность

input voltage
220 Eingangsspannung
tension d'entrée
входное напряжение

insulating layer
221 Isolierschicht
couche isolante
изолирущий слой

insulating washer
222 Isolierscheibe
disque isolante
изолирующая шайба

intermediate layer
223 Zwischenschicht
couche intermédiaire
прослойка

intermetallic compound
224 intermetallische Verbindung
composé intermétallique
интерметаллическое соединение

interstitial site
225 Zwischengitterplatz
position interstitielle
междоузел

intrinsic conductivity
226 Eigenleitung
conductivité intrinsèque
собственная проводимость

intrinsic semiconductor
227 Eigenhalbleiter
semiconducteur intrinsèque
собственный полупроводник

inversion density
228 Inversionsdichte
densité intrinsèque
инверсионная плотность

ionic bond
229 Ionenbindung
liaison ionique
ионная связь

ionic conduction
230 Ionenleitung
conductivité ionique
ионная проводимость

ionic crystal
231 Ionenkristall
cristal ionique
ионный кристалл

ionic lattice
232 Ionengitter

réseau ionique
ионная решетка

junction (of thermocouple)
233 Lötstelle, Kontaktstelle
soudure (du thermoélément)
спай

lattice
234 Gitter
réseau
решетка

lattice constant
235 Gitterkonstante
constante de réseau
постоянная решетки

lattice defect
236 Gitterfehler
défaut de réseau
дефект решетки

lattice imperfection
237 Gitterstörung
imperfection de réseau
искажение решетки

lattice site
238 Gitterplatz
noeuds du réseau
узел решетки

life time
239 Lebensdauer
durée de vie
время жизни

majority carrier
240 Majoritätsladungsträger
porteur majoritaire
основной носитель тока

material
241 Material
matérial
материал

mean free path
242 mittlere freie Weglänge
libre parcours moyen
средняя длина свободного пробега

melt
243 Schmelze
fonte, bain
расплав

melt-back
244 Rückschmelzen
refusion
метод обратного оплавления

melting point
245 Schmelzpunkt
point de fusion
точка плавления

metal casing
246 Metallgehäuse
cartouche métallique
металлический корпус

metal spraying
247 Aufspritzen
procédé Schoop
шоопирование

metallic bond
248 metallische Bindung
liaison métallique
металлическая связь

metallic crystal
249 Metallkristall
cristal métallique
металлический кристалл

minority carrier
250 Minoritätsladungsträger
porteur minoritaire
неосновной носитель тока

mixed conductivity
251 gemischte Leitfähigkeit
conductivité mixte
смешанная проводимость

mixed crystal
252 Mischkristall
cristal mixte
смешанный кристалл

mobility
253 Beweglichkeit
mobilité
подвижность

modulator
254 Modulator
modulateur
модулятор

molecular crystal
255 Molekularkristall
cristal moléculaire
молекулярныи кристалл

monocrystal
256 Monokristall
monocristal
монокристалл

noise
257 Rauschen
bruit
шум

noise temperature
258 Rauschtemperatur
temperature de bruit
шумовая температура

noise voltage
259 Rauschspannung
tension de bruit
напряжение шумов

non-rectifying contact
260 sperrfreier Kontakt, nicht-gleichrichtender Kontakt
contact non redresseur
незапирающый контакт
невыпрямляющий контакт

n-type conduction
261 n-Leitung
conduction de type n
проводимость типа n

n-type impurity
262 n-Verunreinigung
impureté de type n
примусь типа n

n-type semiconductor
263 Überschussleiter, n-Halbleiter
semiconducteur de type n
полупроводник типа n

oil cooling
264 Ölkühlung
refroidissement par huile
масляное охлаждение

oscillator
265 Oszillator
oscillateur
осциллятор

output circuit
266 Ausgangskreis
circuit de sortie
выходная цепь

output current
267 Ausgangsstrom
courant de sortie
выходной ток

output power
268 Ausgangsleistung
puissance de sortie
выходная мощность

output voltage
269 Ausgangsspannung
tension de sortie
выходное напряжение

pair generation
270 Paarbildung
création d'une paire
образование пары

partially occupied band
271 teilweise besetztes Energieband
bande partiellement occupée
частично заполненная зона

peak reverse voltage
272 Spitzensperrspannung
tension inverse de crête
максимальное обратное напряжение

Peltier's effect
273 Peltier-Effekt
effet Peltier
эффект Пельтье

phase diagram
274 Zustandsdiagramm
diagramme de phases
диаграмма состояния

phonon
275 Phonon
phonon
фонон

photoconduction
276 Photoleitung
photoconduction
фотопроводимость

photoconductivity
277 Photoleitfähigkeit
photoconductivité
фотопроводимость

photocurrent
278 Photostrom
photocourant, courant photoélectrique
фототок

photodiode
279 Photodiode
photodiode
фотодиод

photoelectromotive force
280 photoelektromotorische Kraft
force photoélectromotrice
фотоэлектродвижущая сила

photo emf
281 Photo-EMK
force électromotrice photo-électrique
фотоэдс

photon
282 Photon
photon
фотон

photoresistance
283 Photowiderstand
photorésistance
фотосопротивление

photosensitivity
284 Photoempfindlichkeit
photosensibilité
фоточувствительность

phototransistor
285 Phototransistor
phototransistor
фототранзистор

photovoltage
286 Photospannung
tension photoélectrique
фотонапряжение

photovoltaic cell
287 Photoelement, Sperrschicht-Photozelle
cellule photovoltaique
фотоэлемент с запирающим слоем

photovoltaic effect
288 Sperrschichtphotoeffekt
effet photovoltaique
фотоэффект запирающего слоя

plastic capsulation
289 Kunststoffgehäuse
cartouche plastique
пластмассовый корпус

p-n junction
290 p-n-Übergang
jonction pn
переход p-n

p-n junction crystal
291 p-n-Schichtkristall
cristal à jonction pn
слойстый кристалл типа

p-n junction diode
292 Schichtgleichrichter, Flächengleichrichter
redresseur à jonction
плоскостный выпрямитель

p-n junction transistor
293 Schichttransistor, Flächentransistor
transistor à jonctions
плоскостныи триод

point contact
294 Spitzenkontakt
contact à pointe
точечный контакт

point contact rectifier
295 Spitzengleichrichter
redresseur à pointe
точечный диод

point contact transistor
296 Spitzentransistor
transistor à pointes
точечный транзистор

polycrystal
297 Polykristall
polycristal
поликристалл

potential barrier
298 Potentialschwelle
barriére de potentiel
потенциальный барьер

potential distribution
299 Potentialverteilung
distribution du potentiel
распределение потенциала

potential drop
300 Potentialabfall
chute de potentiel
падение потенциала

potential well
301 Potentialtopf
puits de potentiel
потенциальная яма

power rectifier
302 Starkstromgleichrichter, Leistungsgleichrichter
redresseur de puissance
силовой выпрямитель мощный выпрямитель

power transistor
303 Leistungstransistor
transistor de puissance
мощный транзистор

preparation of crystals
304 Kristallherstellung
préparation des cristaux
приготовление кристаллов

protective gas
305 Schutzgas
gaz de protection
защитный газ

p-type conduction
306 p-Leitung
conduction de type p
проводимость типа p

p-type impurity
307 p-Verunreinigung
impureté de type p
примесь типа p

p-type semiconductor
308 Mangelhalbleiter, Defektleiter
semiconducteur par défaut d'électrons
дырочный полупроводник

pulling apparatus
309 Ziehvorrichtung
appareil de tirage
установка для вытягив ния

pulling rate
310 Ziehgeschwindigkeit
vitesse de tirage
скорость вытягивания

purification
311 Reinigung
purification
очистка

quenching
312 Abschrecken
trempe, refroidissement brusque
закалка замораживание

radiation
313 Abstrahlung

rayonnement
излучение

rate growth
314 Stufenziehen
tirage à vitesse programmée
вытягивание переменного скорости

recombination
315 Rekombination
recombinaison
рекомбинация

recombination center
316 Rekombinationszentrum
centre de recombinaison
рекомбинационный центр

recombination velocity
317 Rekombinationsgeschwindigkeit
vitesse de recombinaison
скорость рекомбинации

recovery time
318 Verzögerungszeit
temps de rétablissement
время восстановления

recrystallisation
319 Rekristallisation
recristallisation
рекристаллизация

rectifier
320 Gleichrichter
redresseur
выпрямитель

rectifier plate
321 Gleichrichterplatte
plaque de redresseur
выпрямительная пластинка

rectifier stack
322 Gleichrichtersäule
pile de redresseurs
выпрямительный столб

rectifying contact
323 gleichrichtender Kontakt
contact rectifiant
выпрямляющий контакт

remelt
324 Rückschmelzen
refusion
метод обратного оплавления

resistance
325 Widerstand
résistance
сопротивление

resistivity
326 spezifischer Widerstand
resistivité
удельное сопротивление

reverse current
327 Sperrstrom
courant inverse
обратный ток

reverse direction
328 Sperrichtung
direction inverse
запирающий направление
запорное направление

reverse voltage
329 Sperrspannung
tension inverse
обратное напряжение

room temperature
330 Zimmertemperatur
temperature ambiante
комнатная температура

rotation rate
331 Rotationsgeschwindigkeit
vitesse de rotation
скорость вращения

sample
332 Probe
échantillon
образец

saturation current
333 Sättigungsstrom
courant de saturation
ток насыщения

screw dislocation
334 Schraubenversetzung
dislocation vis
винтовая дислокация

seed
335 Kristallkeim
germe
затравка

seed chuck
336 Impfkristallhalter
porte-germe
держатель затравки

seed crystal
337 Impfkristall
germe
затравка

seed holder
338 Impfkristallhalter
porte-germe
держатель затравки

segregation coefficient
339 Abscheidungskoeffizient
coefficient de partage, coefficient de ségrégation
коэффициент разделения

segregation from the gas phase
340 Abscheidung aus der Gasphase
ségrégation de la phase gazeuse
осаждение из газовой фазы

selenium rectifier
341 Selengleichrichter
redresseur au sélénium
селеновый выпрямитель

self-diffusion
342 Selbstdiffusion
autodiffusion
самодиффузия

semiconductive wafer
343 Halbleiterscheibe
lame de semiconducteur, plaquette de semiconducteur
пластинка полупроводника

semiconductor
344 Halbleiter
semiconducteur
полупроводник

semiconductor compound
345 Halbleiterverbindung
composé semiconducteur
полупроводниковое соединение

semiconductor device
346 Halbleitergerät
dispositif semiconducteur
полупроводниковый прибор

sensitive to temperature
347 temperaturempfindlich
sensible à la température
термочувствительный

shape of crystal
348 Kristallform
forme du cristal
форма кристалла | вид кристалла

shear stress
349 Schubspannung
cision, contrainte de cisaillement
скалывающее напряжение

signal-to-noise ratio
350 Signal-Rausch-Verhältnis
rapport signal-bruit
отношение сигнал-помеха

silicon rectifier
351 Siliziumgleichrichter
redresseur au silicium
кремниевый выпрямитель

silicon transistor
352 Siliziumtransistor
transistor au silicium
кремниевый триод

single crystal
353 Einkristall
monocristal
монокристалл

slip line
354 Gleitlinie
ligne de glissement
линия скольжения

slip plane
355 Gleitebene
plan de glissement
плоскость скольжения

solar battery
356 Sonnenbatterie
pile solaire
солнечная батарея

solid solution
357 feste Lösung
solution solide
твердый раствор

solid state physics
358 Festkörperphysik
physique de l'état solide, physique du corps solide
физика твердого тела

solidification
359 Erstarrung
solidification
затвердевание

solidifying interface
360 Erstarrungsfläche
surface de solidification
фронт кристаллизации

solvent
361 Lösungsmittel
solvant
растворитель

space charge
362 Raumladung
charge d'espace
пространственный заряд

space charge layer
363 Raumladungsschicht
couche de charges d'espace
слой пространственного заряда

space lattice
364 Raumgitter
réseau d'espace
пространственная решетка

spreading resistance
365 Ausbreitungswiderstand
résistance de divergence
сопротивление распространению

spring contact
366 Abnahmeelektrode
electrode de prise de courant
контактная шайба

state density
367 Zustandsdichte
densité de l'état
плотность состояния

state of equilibrium
368 Gleichgewichtszustand
état d'équilibre
состояние равновесия

surface barrier transistor
369 Randschichttransistor, Sperrschichttransistor, Oberflächensperrschichttransistor
transistor à barrière de surface
поверхностно-барьерный триод

surface conduction
370 Oberflächenleitung
conduction de surface
поверхностная проводимость

surface layer
371 Oberflächenschicht
couche de surface
поверхностний слой

surface recombination velocity
372 Oberflächenrekombinationsgeschwindigkeit
vitesse de recombinaison de surface
скорость поверхностной рекомбинации

surface tension
373 Oberflächenspannung
tension superficielle
поверхностное натяжение

surface treatment
374 Oberflächenbehandlung
traitement de surface
обработка поверхности

thermal conductivity
375 thermische Leitfähigkeit
conductivité thermique
теплопроводность

thermal decomposition
376 thermische Zersetzung
décomposition thermique
термическое разложение

thermal emf
377 Thermo-EMK
pouvoir thermoélectrique
термоэдс

thermal equilibrium
378 thermisches Gleichgewicht
équilibre thermique
термическое равновесие

thermal equilibrium state
379 thermischer Gleichgewichtszustand
état d'équilibre thermique
состояние термической равновесия

thermal expansion
380 thermische Ausdehnung
dilatation thermique
термическое расширение

thermistor
381 Heissleiter
thermistor
термистор

thermobattery
382 Thermobatterie
thermopile
термобатарея

thermocouple
383 Thermoelement
thermo-couple, thermoélement
термопара

thermoelectric power
384 Thermospannung, Thermokraft
pouvoir thermo-électrique
термоэлектродвижущая сила

thermo-electromotive force
385 Thermo-Elektromotorische Kraft
pouvoir thermo-électromotrice
термоэлектродвижущая сила

thermo-junction
386 Thermoelement
thermoélément
термопара

transistor
387 Transistor
transistor, transistron
транзистор, триод

trap
388 Haftstelle
piège
ловушка

tunnel effect
389 Tunneleffekt
effet tunnel
туннельный эффект

twinning
390 Zwillingsbildung
mâclage
двойникование

unipolar transistor
391 Unipolartransistor
transistor unipolaire
униполярный триод

vacancy
392 Fehlstelle, Gitterfehlstelle, Gitterlücke
place vacante de réseau
ваканция

valence band
393 Valenzband
bande de valence
валентная зона

valence bond
394 Valenzbindung
liaison covalente, liaison de valence
ковалентная связь

valence crystal
395 Valenzkristall
cristal covalent
ковалентный кристалл

valence electron
396 Valenzelektron
electron de valence
валентный электрон

vapor diffusion
397 Eindiffusion aus der gasförmigen Phase
diffusion d'impuretés en phase gazeuse
диффузия примесей из газовой фазы

variation of growth rate
398 Änderung der Wachstumsgeschwindigkeit
variation de la vitesse de croissance
изменение скорости роста

varistor
399 Varistor
varistor
варистор

voltage drop
400 Spannungsabfall
chute de tension
падение напряжения

water cooling
401 Wasserkühlung
refroidissement par eau
водоохлаждение

work function
402 Austrittsarbeit
travail de sortie
работа выхода

Zener breakdown
403 Zener-Durchschlag
claquage de Zener
зинеровский пробой

Zener voltage
404 Zener-Spannung
tension de Zener
напряжение Зинера

zone leveling
405 Zonennivellierung
nivellement en zones
выравнивание зон

zone melting
406 Zonenschmelzen
fusion par zone
зонная плавка

zone melting in a boat
407 Zonenschmelzen im Tiegel
fusion par zone dans une nacelle
зонная плавка в лодочке

zone purification
408 Zonenreinigung
purification par fusion par zone
зонная очистка

zone refining
409 Zonenreinigung
purification par fusion par zone
зонная очистка

DEUTSCH

RUSSIAN

ABSTRACTS OF THE SOLID STATE LITERATURE

METALLURGY AND CHEMISTRY OF SOLIDS

THERMODYNAMIC PROPERTIES OF ELEMENTS AND ALLOYS

Indium Antimonide Crystals - See 10,907

10,617 HIGH-TEMPERATURE PHASE STUDIES IN THE TANTALUM-BORON SYSTEM BETWEEN Ta AND TaB by J. M. Leitnaker, M. G. Bowman (U. California), and P. W. Gilles (U. Kansas); J. Electrochem. Soc., Vol. 108, pp. 568-572, June 1961

Phase relationships in the tantalum-boron system between Ta and TaB are described. A phase diagram of the solid portion of the system is shown. Two three-phase equilibria exist within the system: (a) Ta-Ta_2B-Ta_3B_2 at 2040° ± 30°C, and (b) Ta_2B-Ta_3B_2-TaB at 2180° ± 20°C. The chemical composition of the Ta_2B phase is $Ta_{2.4\pm0.2}B$. The composition of the Ta_2B_2 phase is $Ta_{1.60\pm0.05}B$. The melting point of TaB lies above 2800°C. The extreme slowness of reactions within the system has been investigated qualitatively, and the necessity for seeding at temperatures in the neighborhood of 2000°C is noted. The results disagree markedly with data previously reported in the literature.

Phase Diagram of the InAs-In_2Te_3 System - See 10,671

10,618 THERMODYNAMIC PROPERTIES OF II-IV AND V-VI COMPOUNDS by B. W. Howlett and M. B. Bever (MIT); Conf. Ultrapurifi. Semicon. Mat., (A), Apr. 1961

The heats of formation of the II-IV compounds, Mg_2Ge, Mg_2Sn and Mg_2Pb, and of the V-VI compounds, Bi_2Te_3 and Sb_2Te_3, were measured. Metal solution calorimetry was used. In this technique, the difference between the heat of solution in liquid metal (tin or bismuth) of the compound and of a mechanical misture of its components, adjusted for changes in composition of the solvent bath, is the heat of formation of the compound. The heat of fusion and the heat capacity of the compound Bi_2Te_3 were measured in a heat flow calorimeter. A knowledge of the heats of formation and heats of fusion of these compounds permits the evaluation of the free energies of formation.

10,619 ENTROPIES, HEATS OF SUBLIMATION AND DISSOCIATION ENERGIES OF THE CESIUM HALIDES by J. Fine and M. D. Scheer (NBS); Bull. Am. Phys. Soc., Ser. II, Vol. 6, p. 22(A), Feb. 1, 1961

Measurements of the vapor pressures of the crystalline cesium halides in the 700°-900°K temperature range were reported. The salt vapor effusing from a Knudsen effusion cell was collimated accurately into a molecular beam with a well-defined cross-sectional area. Beam intensities were determined from the positive ion currents produced by dissociation of the halide and ionization to Cs^+ on a tungsten surface at 1700°K. From the experimental vapor pressures and heats of sublimation, the crystal entropies, dissociation energies, and heats of sublimation at 298°K were computed using available spectroscopic and thermal data.

10,620 MEASUREMENT OF THE PARTIAL PRESSURE OF CESIUM OVER CESIUM ANTIMONIDES by K. Miyake (Nippon Tel. and Tel.); J. Appl. Phys., Vol. 32, pp. 1132-1136, June 1961

The partial pressure of Cs over cesium antimonides whose compositions are $Cs_{2.95}Sb$, $Cs_{3.00}Sb$, and $Cs_{3.25}Sb$ is evaluated. Results at various temperatures ranging from room temperature to about 180°C are reported. The experimental tube consists of a spherical glass envelope and an ion gauge, the sample being prepared on the inner surface of the spherical envelope. The partial pressure of the Cs dissociated thermally from cesium antimonides is measured by Langmuir's positive ion method. The composition of the samples is determined by comparing their electrical resistivities and thermal activation energies associated with electrical conductivity with those of the cesium antimonides, which had a known composition. The preparation of the sample and the measuring method of the partial pressure are described precisely. The partial pressure of Cs as a function of the absolute temperature can be represented by the equation $\log_{10}p$ (mm Hg) = A-B/T, where A and B are constants. In the case of $Cs_{3.00}Sb$, the values of A and B are 9.040 and 6300°, respectively.

10,621 AN EXPERIMENTAL EQUATION OF STATE FOR SODIUM by R. I. Beecroft and C. A. Swenson (Iowa State U.); J. Phys. Chem. Solids, Vol. 18, No. 4, pp. 329-344, Mar. 1961

An experimental equation of state for Na for pressures to 20,000 atm and for temperatures from 20°K to the melting point is derived. The apparatus used to obtain pressure-volume data which are reliable to ±0.002 in $\Delta V/V_o$ over this range of temperature and pressure is described. The equation of state can be represented to within the above accuracy by an expression derived from the assumption that the isothermal compressibility is linear with volume and has no explicit temperature dependence. A discussion is given of the effect of these assumptions on the validity of calculations of the variation with volume of the temperature dependent contribution to

the thermodynamic functions. Grueneisen constants as obtained from various definitions are calculated as functions of temperature and volume, and the validity of the Mie-Grueneisen equation of state as it applied to Na appears open to question below room temperature. Recent high pressure ultrasonic experiments on Na are interpreted as being in agreement with this conclusion.

10,622 DISSOLVING THE EXCESS OF FERRIC OXIDE IN Ni-Zn-FERRITE by V. V. Latsh, N. G. Minaev, B. Kh. Somin, and N. E. Stepina; Soviet Phys.-Solid State, Vol. 2, pp. 1956-1961, Mar. 1961

The effects of various temperatures of annealing in air and subsequent cooling rates on the solubility of ferric oxide in Ni-Zn ferrite are discussed. In the ferrites studied, NiO/ZnO ranged from 0.43 to 4.0. Upon heating the ferrite in air, excess ferric oxide dissociates to magnetite, at a temperature dependent upon the ratio ferrite:excess ferric oxide. The magnetite enters into a continuous series of solid solutions with the ferrite. During cooling, the magnetite undergoes partial or complete oxidation, to gamma-ferric oxide, with formation of a solid solution, or to alpha-ferric oxide, with formation of a two-phase system.

Thermal Expansion Coefficients of Solid Solutions of Alkali Halides - See 10,750

10,623 BARIUM TITANATE CERAMICS MODIFIED BY ADDITION OF COPPER by L. Castelliz and O. Knop (Nova Scotia Tech. Coll.); Am. Ceram. Soc. Bull., Vol. 40, p. 213(A), Apr. 1961

A study of solid solutions of copper in $BaTiO_3$ was discussed. Transition elements incorporated in the barium titanate lattice impede grain growth, reduce the tetragonal distortion, lower the Curie temperature and, when present in small amounts, reduce the electrical and mechanical loss coefficients. It was found that copper tends to affect these properties in the opposite direction. The observed effects depend quantitatively on the exact stoichiometry of the barium titanate, and they are modified by small amounts of calcium in Ba sites and partially compensated by small additions of Ni. $BaTiO_3$ ceramics containing Cu might find practical application provided the Cu content is low enough to keep the loss tangent reasonably small to benefit from a higher dielectric constant and an increased Curie temperature.

10,624 DISTRIBUTION COEFFICIENTS OF IMPURITIES IN GALLIUM ANTIMONIDE by R. N. Hall and J. H. Racette (GE Res. Lab.); J. Appl. Phys., Vol. 32, p. 856, May 1961

Distribution coefficients of several column II, IV, and VI elements in GaSb are reported. Some of the physical properties of GaSb are discussed briefly.

Migration of Solute Atoms in Tl Solid Solutions During Annealing - See 10,694

10,625 EFFECT OF TEMPERATURE ON DIFFRACTION OF X-RAYS FROM "PERFECT" CRYSTALS by B. W. Batterman (Bell Labs.); Bull. Am. Phys. Soc., Ser. II, Vol. 6, p. 109(A), Mar. 20, 1961

The integrated intensity of the (555) reflection from a "perfect" Si single crystal was measured. Measurements were made in the temperature range from 289° to 698°K, using Moka radiation. A decrease in intensity with increasing temperature was found, which is in qualitative agreement wtih theory. The reduction in intensity from the lowest to the highest temperature was somewhat greater than that calculated from an approximate Debye-Waller treatment, using a Debye temperature of 650°K.

10,626 ON THE ENERGY OF FORMATION OF VACANCIES IN CRYSTALS by H. Amar (Franklin Inst. Labs. and Temple U.); Bull. Am. Phys. Soc., Ser. II, Vol. 6, p. 279(A), Apr. 24, 1961

The basic assumptions and approximations of the Huntington Seitz, and Brooks (HSB) calculation of the vacancy formation energy were discussed. After some criticism of a general nature, specific contributions such as Fermi energy and electrostatic self-energy were singled out and recalculated. This quantitative analysis clearly showed that the uncertainty in some of the items approaches or exceeds the final result. The conclusion was that, while the HSB method is qualitatively illuminating, the quantitative results are of little value in validating experimentally measured parameters.

10,627 THEORETICAL CALCULATIONS OF THE ENTHALPIES AND ENTROPIES OF DIFFUSION AND VACANCY FORMATION IN SEMICONDUCTORS by R. A. Swalin (U. Minnesota); J. Phys. Chem. Solids, Vol. 18, No. 4, pp. 290-296, Mar. 1961

Enthalpies and entropies of vacancy formation and diffusion for elements having the diamond structure are calculated. The potential between nearest neighbor atoms is assumed to have the form of the Morse function. In this fashion kinetic parameters of crystals are calculated by the use of properties determined from equilibrium properties. One of the factors facilitating calculation results from the open nature of the diamond lattice. Because of this, an atom, moving from its equilibrium position into a vacancy, does not pass through a geometric barrier as is the case for more close-packed structures. Calculations yield values for the enthalpies of formation of vacancies of 2.07 ev, 2.32 ev, and 4.16 ev for Ge, Si, and diamond respectively. Experimental results available for Ge yield 2.01 ev. Calculations of the activation enthalpies of self diffusion, assuming a vacancy mechanism, are 3.02, 3.38, and 6.18 ev for Ge, Si, and diamond. Experimental information for Ge indicates a value of 2.98 ev.

Vacancies as Luminescent Centers in ZnS Phosphors - See 10,739

10,628 COLOUR CENTRE IN $BaTiO_3$ SINGLE CRYSTALS by V. Dvorák (Czech. Acad. Sci.); Czech. J. Phys., Vol. B11, pp. 253-260, 1961

The position of the absorption band of a color center formed by one electron trapped on an oxygen vacancy, in a cubic modification of $BaTiO_3$ single crystals, is calculated quantum mechanically.

10,629 ROLE OF DISLOCATIONS IN THE FORMATION OF F CENTERS BY X IRRADIATION by C. L. Bauer and R. B. Gordon (Yale U.); Bull. Am. Phys. Soc., Ser. II, Vol. 6, p. 113(A), Mar. 20, 1961

F-center growth curves in plastically deformed (up to 14 per cent) NaCl and KCl at temperatures ranging from 78° to 325°K were obtained. The rate of formation of F centers can be explained using the two-stage growth model. Colorability of lightly deformed crystals is only enhanced at temperatures where diffusion of F centers is possible; a rapid saturation of this deformation sensitive coloration is observed at lower temperatures. The initial growth rate in a heavily deformed crystal, relative to an undeformed one, becomes larger as the temperature is decreased, and can be explained by the presence of a large number of F centers formed near dislocations. With further x irradiation, this additional contribution saturates. Substantiating the hypothesis that the additional growth is due to F-center formation near dislocations, and that diffusion is necessary for growth to continue, a distinct broadening of the F band is observed which disappears when the crystal is warmed to room temperature.

10,630 OPTICAL ABSORPTION AND EPR AFTER OPTICAL BLEACHING OF F CENTERS by W. E. Bron and R. S. Title (IBM); Bull. Am. Phys. Soc., Ser. II, Vol. 6, p. 113(A), Mar. 20, 1961

The production of R, M, and N centers at the expense of F centers in x-rayed crystals of KCl was described. The crystals were optically bleached at room temperature. The loss of F centers produces a marked shift of the high-energy side of the F band, such that its half-width at 80°K increases from 0.197 to 0.232 ev, and also decreases the width of the room temperature EPR line from 45 to 34 gauss. When the sample is heated for a short period at 140°C to remove all R centers, the half-width of the F band decreases to near 0.200 ev and the width of the EPR line returns to 45 gauss. The half-width of the F band decreases to the original value of 0.197 ev after additional thermal treatment at 140°C to remove M and N centers. The broadening of the F band and the decrease in the width of the EPR line, therefore, appear to result primarily from the presence of R centers. These results also showed that F centers are still present after prolonged optical bleaching and suggested that the R center is paramagnetic, but M and N centers are not.

10,631 POINT-DEFECT MIGRATION AND BINDING IN METALS by A. Sosin (NA Aviation); Phys. Rev., Vol. 122, pp. 1112-1116, May 15, 1961

The kinetics of decay of an excess defect concentration in metals is examined. Special attention is given to the initial stages of decay. A particular case, excess vacancy migration to sinks in a slightly impure metal, is treated in detail. Analog computer plots of isothermal and constant-tempering-rate recovery studies are presented and analyzed. Initial recovery is determined by the migration energy only; final recovery is determined by an energy generally less than the sum of the migration plus vacancy-impurity binding energy but more than the migration energy alone. Initial and final recovery are easily resolved into two annealing stages. The intermediate recovery range may actually give rise to a resistivity increase.

10,632 DISLOCATIONS AND STACKING FAULTS IN ALUMINUM NITRIDE by P. Delavignette, H. B. Kirkpatrick, and S. Amelinckx (Nuclear Energy Center, Mol-Donk, Belg.); J. Appl. Phys., Vol. 32, pp. 1098-1100, June 1961

The nature of dislocations in thin platelets of aluminum nitride grown from the vapor phase is discussed. Some of the dislocations are dissociated into partials of the Shockley type; others are undissociated. A model is given for both types. The stacking fault associated with the dissociated dislocations consists of one lamella of the sphalerite structure. The stacking fault energy is deduced from the width of the ribbons and from the shape of the extended modes; its value is $\gamma \approx 4$ ergs/cm^2.

10,633 DISLOCATION DECORATION INSIDE SILVER CHLORIDE CRYSTALS by L. Slifkin (U. North Carolina) and C. B. Childs (Goddard Space Flight Ctr.); Bull. Am. Phys. Soc., Ser. II, Vol. 6, p. 23(A), Feb. 1, 1961

A method for the decoration of dislocations throughout the interior of large single crystals of silver chloride was described. The method does not require an annealing treatment at elevated temperature. The crystals are moderately loaded with submicroscopic colloidal silver by means of the Haynes-Shockley photoelectric technique. They are then allowed to age for several days at room temperature, during which time much of the silver migrates from random scattering centers into the dislocations. This results in such an increase in the contrast between the decorated dislocations and the background that the dislocation structures then can be examined with ordinary bright-field microscopy and to depths of the order of millimeters. Photographs of various networks and dislocation structures obtained by this technique were shown. Since no high-temperature annealing is necessary, this method suggests the possibility of studies of plasticity effects in the cold-worked state, without the limitation of surface effects.

10,634 SCREW DISLOCATION IN CRYSTALS WITH DIAMOND STRUCTURE by V. Celli (U. Illinois); J. Phys. Chem. Solids, Vol. 19, pp. 100-104, Apr. 1961

A modification of the model of dislocation in a lattice recently proposed by Maradudin is described. The modification is applied to an estimate of the strain energy of a screw dislocation in crystals with the diamond structure, in particular, Si and Ge.

Effect of Linear Dislocations on Energy Band Structure - See 10,665

Dislocation Effects on the Resistivity-Temperature Relationship of Cr - See 10,688

10,635 LOW-TEMPERATURE DISLOCATION DAMPING IN THE ALKALI HALIDES by R. B. Gordon and C. L. Bauer (Yale U.); Bull. Am. Phys. Soc., Ser. II, Vol. 6, p. 113(A), Mar. 20, 1961

Changes in the damping and elastic modulus of plastically deformed rock salt, due to dislocation pinning were described. The changes have been observed during x-irradiation at liquid-helium temperature and during subsequent warmup. The rate at which these changes occur during irradiation at helium temperature is comparable to that at higher temperatures, but the magnitude of the effect is smaller. The decrease in magnitude has been shown to be due to the absence of thermal unpinning. The low-temperature dislocation pinning in NaCl, KCl, KBr, and KI is found to be reversible when the crystals are subjected to illumination in, or near, the visible. The wavelength of the illumination which produces the maximum unpinning increases with increasing lattice constant; the effect disappears when the crystals are warmed to room temperature.

The pinning point is tentatively identified as a jog in close association with an F center whose absorption band is displaced by the dislocation strain field. Ionization of the F center results in recombination of its vacancy with the jog; warmup allows the F center to diffuse beyond recombination range.

10,636 DISLOCATION RELAXATION PHENOMENA IN OXIDE CRYSTALS by R. Chang (Atomics Intl.); J. Appl. Phys., Vol. 32, pp.1127-1132, June 1961

The results of anelastic measurements to study the dislocation relaxation of MgO and Al_2O_3 crystals are analyzed. It is shown that the ratio of Peierls force to shear modulus is about 2×10^{-5} for MgO and possibly also for Al_2O_3. Comparison of the dislocation relaxation phenomena of oxides and metals indicates, rather surprisingly, that the ratio of Peierls force to shear modulus in oxides is about an order of magnitude smaller than that in fcc metals.

10,637 DISLOCATIONS IN SILVER CHLORIDE CRYSTALS by M. G. Miller and L. Slifkin (U. North Carolina); Bull. Am. Phys. Soc., Ser. II, Vol. 6, p. 280(A), Apr. 24, 1961

The study of dislocations in AgCl by means of two distinct techniques was discussed. The techniques are decoration of dislocations in the interior of crystals by forming internal print-out, using the Haynes Shockley technique, and determination of the effect of impurities, defects induced by quenching, and internal print-out on the plastic properties of AgCl, using a "hard" tensile machine. The relative contrast of dislocation decoration has been found to be extremely dependent on impurity content. Currently, no evidence has been found for pile-ups or Frank-Read sources of dislocations in strained AgCl, although bowed out loops have been observed. In copper-doped crystals, the presence or absence of strain aging has been found to be dependent upon whether the impurity is in the divalent or monovalent state. Crystals containing decorated dislocations have been tested in tension and show a slight increase in initial yield point. Quenching experiments indicate that defects thus produced increase the yield point markedly and also decrease the rate of work hardening.

10,638 ON THE PROBLEM OF LARGE ANGLE GRAIN BOUNDARIES II by E. F. Hollander; Czech. J. Phys., Vol. B11, p. 290(A), 1961

The variation of the width of dislocations forming a tilt grain boundary with their mutual distance is derived. A simple model is used. The derived relation is compared with the variation of the dislocation core radius with distance assumed in the derivation of the corrected Shockley-Read formula.

10,639 GRAIN BOUNDARIES AS IMPERFECTIONS OF PLANAR EXTENT, THEIR MODEL AND ELECTRONIC PROPERTIES by H. F. Matare (TE KA DE, Nuremburg); Conf. Ultrapurifi. Semicon. Mat., (A), Apr. 1961

The properties of boundaries or interfaces between two perfect monocrystals of different orientation but equal chemical composition were evaluated. Numerous measurements of their optical and electronic properties in relation to their temperature behavior have been made. The model of these structures, as now established, seems to approximate an arrangement of dislocation-pipes in a lateral superposition. These "imperfections of planar extent" (terminology of Seitz) may be approximated by the Shockley-Read model of an electron gas represented by the overlapping wave functions of the dangling bonds. The resulting degeneracy of the material in the interface has been measured down to liquid helium temperatures. The internal stress field which causes an electronic band gap change in this plane may be associated with the frequency dependence of the photovoltaic effect. Hall-measurements confirm a mobility for holes of about 10^3 cm^2/volt-sec. Capacity measurements and field effect measurements show that the conductivity of the interface is governed by the hole transport in the space charge region along the inversion layer at the interface. The independence of the properties of those structures on temperature variation and impurity content of the mono-crystal sides indicates that the dislocations and their dangling bonds, rather than the chemical impurities in the bulk material, are responsible for the characteristic behavior of these degenerate planes.

10,640 STACKING FAULT PROBABILITY OF NOBLE METAL-ZINC ALLOYS by L. F. Vassamillet (Mellon Inst.); J. Appl. Phys., Vol. 32, pp. 778-782, May 1961

The stacking fault probability on a number of alloys of gold, silver, and copper with varying zinc content is evaluated. The measurements utilized x-rays. By using these probabilities, the relative magnitudes of the stacking fault energies have been deduced.

Stacking Faults in AlN - See 10,632

10,641 A STUDY OF A DILUTE CONCENTRATION OF DISORDER IN THE β-Cu-Zn SUPERLATTICE by J. S. Clark and N. Brown (U. Pennsylvania); J. Phys. Chem. Solids, Vol. 19, pp. 291-298, May 1961

A study of the disorder quenched in β-Cu-Zn is discussed. At low temperatures, 25°-250°C, the predominant defect appears to be a wrong pair of Cu and Zn atoms whose observed value of energy of formation is 7.2-8.0 kcal/mol. The energy of motion during reordering is 14 kcal/mol and it appears that a vacancy is trapped in the vicinity of a wrong pair of atoms.

PURIFICATION OF CRYSTALS

10,642 FREE CONVECTION IN ZONE MELTING by W. R. Wilcox and C. R. Wilke (U. California); Conf. Ultrapurifi. Semicon. Mat., (A), Apr. 1961

The heat transfer conditions upon the degree of purification in zone refining was investigated. Zone melting studies using mixtures of β-naphthol and of benzoic acid in naphthalene were made. These systems were chosen as representative of the two simplest types of binary solid-liquid phase behavior, namely isomorphous and eutectic-forming. The solid mixtures were enclosed in 5 to 20 mm glass tubes and pulled through a stationary heater, which generated the liquid zone. By using the experimental data, correlations were developed which enable estimation of the separation and zone position for various free convection conditions in zone melting.

Purification of Co and Transition Metal Silicides by Zone Refining - See 10,657

10,643 THE PURIFICATION OF TELLURIUM BY DISTILLATION by B. D. Wedlock and F. M. Norton (MIT); Conf. Ultrapurifi. Semicon. Mat., (A), Apr. 1961

The separation of Te and materials of similar vapor pressures from less volatile impurities such as Cu, Sb, and various oxides was discussed. The technique is rapid and economical, and consists of multiple distillation under a continuously pumped vacuum. A mechanical arrangement has been devised which employs a reusable crucible, thereby increasing the speed and reducing the cost of the operation. Preliminary evaluation of this system indicates that one operation will produce Te with an electrically active impurity concentration of about 10^{14} - 10^{15}/cc from material highly doped with antimony and copper. It appears at present that the various oxides have little effect on the electrical conductivity. The measure of their separation is a slag-free end product and successful single-crystal compound semiconductor growth using the purified tellurium.

Purification of Co and Transition Metal Silicides by Filtration - See 10,657

10,644 SYNTHESIS AND GAS CHROMATOGRAPHIC PURIFICATION OF ORGANOMETALLIC COMPOUNDS FOR SEMICONDUCTOR APPLICATIONS by J. I. Peterson, L. M. Kindley, and H. E. Podall (Melpar); Conf. Ultrapurifi. Semicon. Mat., (A), Apr. 1961

Methods for the formation of semiconductor films by deposition of pure elements and element combinations from atmospheres of organic compounds of the elements were discussed. Compounds of boron, gallium, silicon, germanium, tin, phosphorus, arsenic, and bismuth were included, and unusual problems in their synthesis were described. The gas chromatographic approach to achieving high purity of the compounds for vapor deposition was applied. Details, techniques, and applications of this method of purification and analysis were presented.

10,645 ORGANOMETALLIC COMPOUNDS IN THE PREPARATION OF HIGH-PURITY METALS by W. A. G. Graham (A. D. Little); Conf. Ultrapurifi. Semicon. Mat., (A), Apr. 1961

The very limited literature on decomposition of organometallic compounds was reviewed. Four general recovery methods were suggested: pyrolysis, photolysis, electrolysis, and hydrogenolysis. The first three recovery methods have been applied in an effort to prepare samples of high purity magnesium, calcium, gallium, mercury, rhenium, and nickel. In a sample of mercury prepared by photolysis of diethyl-mercury with ultraviolet light, the only detectable impurity was silver at five parts per billion. Rhenium and nickel were prepared by thermal decomposition of their carbonyls. Magnesium can be recovered by electrolysis of organomagnesium compounds in ether, but the physical form of the deposit creates problems. Suitable methods have not yet been found for gallium and calcium.

10,646 ARENE-METAL π-COMPLEXES AND THEIR PURIFICATION by M. Tsutsui (New York U.); Conf. Ultrapurifi, Semicon. Mat., (A), Apr. 1961

The investigation and utilization of metal complexes containing aromatic rings was reviewed. The rapid expansion of this field since 1951 was noted. In addition to metal derivatives of the cyclopentadienyl anion and arenes, a great number of related compounds have been synthesized in which cyclobutadiene tropylium cation, cyclooctatetraene, thiophene, etc. are coordinated via π-electron systems with the metal. In addition the synthesis of many mixed arene-metal complexes and arene-metal carbonyls and nitrosyls has been reported. Arene and olefin π-complex chemistry now covers almost all the elements from group I to group VIII. Purification of π-complexes is accessible by recrystallization, sublimation, chromatography and other techniques which have been utilized in organic and inorganic chemistry. Pyrolysis of some π-complexes yields phoric metals or produces metallic mirrors which are probably ultrapure.

10,647 THE PREPARATION OF HIGH PURITY SILICON FROM SILANE by C. H. Lewis, M. B. Giusto, and S. Johnson (Metal Hydrides); Conf. Ultrapurifi. Semicon. Mat., (A), Apr. 1961

The preparation of high purity Si by a method involving the preparation, purification, and thermal decomposition of silane (SiH_4) was discussed. Quantitative yeilds of silane were obtained by the reduction of SiCl with various hydrides. The reactivity of silane with various purifying agents was studied. Variables in the thermal decomposition of silane were evaluated with regard to purity of the elemental Si produced, and the efficiency of dissociation and deposition rate. Silane was dissociated on an inductively heated single crystal Si substrate to yield high purity Si. Neutron activation analyses for microcrystalline high purity Si as deposited were indicated.

10,648 THE PREPARATION OF SEMICONDUCTOR GRADE SILICON BY THE IODIDE PROCESS by H. Baba and H. Araki (Nippon Tel. and Tel.); Conf. Ultrapurifi. Semicon. Mat., (A), Apr. 1961

The iodide process for preparing semiconductor grade Si was discussed. SiI_4 was prepared from 98 per cent commercial Si, and purified by the combination of recrystallization, sublimation, fractional distillation, and zone refining techniques. The purified iodide was then decomposed to its elemental state inside a quartz tube at 1100°C under reduced pressure. An enlarged experiment for the production of hyperpure Si by this process was conducted to determine its adaptability to industrialization. All of the purifying steps were connected in a closed system to avoid contamination by impurities from the atmosphere. It was clear that the presence of hydrolyzed products suspended in the iodide, which had been produced by contacting the material to water vapor, could improve the refining efficiency of the recrystallization and zone melting of the iodide by virtue of the high adsorptivity for small amounts of the residual impurity elements. The recrystallization process was improved by combining it with the segregational effect simultaneously. The success of this segregational recrystallization technique made this process feasible for industry. Detailed descriptions of the purifying equipments, techniques, yield, and the results of the purity tests of the products were presented, comparing the original and the improved equipments.

10,649 PREPARATION OF CHROMIUM by N. W. Silcox, A. F. Armington, and G. F. Dillon (AF Cambridge Res. Labs.); Conf. Ultrapurifi. Semicon. Mat., (A), Apr. 1961

Two methods for the preparation of pure Cr were described. Both methods involve the formation and decomposition of an intermediate. The first method is a relatively high temperature technique similar to the van Arkel process. The volatile iodide, after synthesis from the elements, is decomposed on a hot substrate. On decomposition a thin film is produced with a total impurity concentration of about 10-15 ppm. The second method, a low temperature technique, involves the preparation and purification of CrO_3 followed by electrolytic decomposition of this material in aqueous media. The CrO_3 is prepared by the hydrolysis of distilled CrO_2Cl_2. Other techniques for the purification of CrO_3 were evaluated and spectroscopic results were reported. This method is primarily for the preparation of Cr metal; however, methods for the

preparation of certain pure chromic salts were given with accompanying analytical data.

Epitaxial Growth of Si from $SiCl_4$ - See 10,659

Purification of Various Elements by Thermal Decomposition - See 10,653, 10,654, 10,655, 10,656, 10,657

10,650 PURIFICATION OF SOME II-VI COMPOUNDS USING ION EXCHANGE RESINS by M. J. Presland (Assoc. Electrical Ind. (Woolwich) Ltd.); Conf. Ultrapurifi. Semicon. Mat., (A), Apr. 1961

The preparation of zinc and cadmium sulphides by precipitation from pure solutions of their salts was described. Methods of purifying the initial solutions by means of ion exchange resins are being investigated. Using chloride and iodide complexes, efficient separations of zinc and cadmium from many other cations are possible.

Purification by Gas Chromatography - See 10,644

10,651 THE POTENTIAL OF GAS CHROMATOGRAPHY FOR PURIFYING SEMICONDUCTOR MATERIALS by J. H. Bochinski, K. W. Gardiner (Bell and Howell Res. Ctr.), and R. Juvet (U. Illinois); Conf. Ultrapurifi. Semicon. Mat., (A), Apr. 1961

The application of gas chromatography for the purification of certain volatile compounds of semiconductor materials was discussed. Continuous or semicontinuous preparative scale chromatographs would be most useful for producing reasonably large quantities of high purity semiconductor elements. On the basis of available data and theoretical considerations it is possible to predict the relative concentrations of impurities that would remain in a chromatographically-treated sample. Chromatographic separations of volatile inorganic compounds of semiconductor materials employing non-volatile molten salts as partitioning solvents holds considerable promise because the inorganic salts available for use as partitioning solvents currently used in conventional organic gas chromatography. A proposed method for applying gas chromatography and a discussion of the operating variables and applicable theoretical considerations were given for several selected systems of semiconductor elements.

10,652 PURIFICATION EFFECTS IN SILICON CARBIDE UNDER THERMAL GRADIENTS by R. S. Braman, E. H. Tompkins, S. Susman, and V. Raziunas (Armour Res. Found.); Conf. Ultrapurifi. Semicon. Mat., (A), Apr. 1961

The effect of thermal gradients upon the movement of impurity elements in single crystal and polycrystalline SiC was discussed. Studies were made at several temperatures from approximately 950°C to the decomposition temperature of SiC in a dc arc. Two different experimental arrangements were required to obtain the desired temperatures. High frequency induction heating was used for temperatures up to approximately 1800°C and a dc spectrographic arc was used for measurements at the decomposition temperature of SiC. In general, impurities diffused toward the cooler portions of the thermal gradients as predicted by a derived equation. The magnitude of the impurity transport was found to be dependent upon the diffusing element and the temperature applied. Polycrystalline rods exhibited impurity diffusion effects only above 1000°C in a two hour heating period. Spectrographic procedures for studying the impurity diffusion were discussed, as well as the use of thermal gradients in purification experiments.

10,653 HIGH PURITY BORON FOR SEMICONDUCTOR RESEARCH by L. Sosnowski, T. Niemyski, and Z. Olempska (Polish Acad. Sci., Warsaw); Conf. Ultrapurifi. Semicon. Mat., (A), Apr. 1961

The preparation of high purity B by purifying and subsequently reducing BCl_3 was described. The purification process is based on the fractional distillation of liquid BCl_3 prepared from boric acid. Gaseous Cl is applied to the boric acid sintered with powdered C. The mixture of Cl and BCl_3 is condensed at a low temperature and BCl_3 is separated by fractional distillation. The BCl_3 fraction is further purified by repeated rectification on a sixty shelf column, and finally shows no impurities in spectral analysis except for traces of Si. The elemental B is prepared by decomposition of chloride in a H_2 atmosphere at 1100°-1250°C. The optimal conditions of decomposition, i.e., temperature and the partial pressure of H_2 have been established. All further processes with B have been carried out in crucibles and containers made of pure BN. B is extremely active at high temperature and reacts with all available materials. It was found that BN is fully stable at the melting point of B and can be used in processes of zone refining, melting and crystallization.

10,654 THE PREPARATION OF HIGH PURITY BISMUTH BY THE REDUCTION OF BISMUTH TRICHLORIDE WITH LITHIUM ALUMINUM HYDRIDE by W. Brenner, C. G. Kumar, H. Hellman, and C. J. Marsel (New York U.); Conf. Ultrapurifi. Semicon. Mat., (A), Apr. 1961

The reduction of bismuth trichloride with lithium aluminum hydride to obtain high purity Bi was described. Data to illustrate the effects of various reaction variables on product purity were presented and optimum reaction conditions were described. Yields of bismuth metal under optimum reaction conditions were in the order of 60 per cent based on the metal content of the trichloride. The products are generally in the form of finely divided powders. Spectroscopic analyses were presented for various runs for both finely divided Bi powder and ingots obtained by fusion of the powders under a He atmosphere.

10,655 THE PREPARATION OF HIGH PURITY GALLIUM BY HYDRIDE REDUCTIONS by Y. Okamoto, W. Brenner, E. Bierig, and C. J. Marsel (New York U.); Conf. Ultrapurifi. Semicon. Mat., (A), Apr. 1961

The preparation of high purity Ga by the synthesis and subsequent decomposition of lithium gallium hydride was described. This intermediate was obtained from the reaction of $GaCl_3$ with LiH. Data are presented to illustrate the mechanism of purification and characterize product quality in terms of spectrographic emission analyses. Some experiments on the reduction of $GaCl_3$ with lithium aluminum hydride are reported. Data have been obtained towards the characterization of the reaction products, and their thermal decomposition behavior is discussed.

10,656 PURIFICATION OF RARE EARTH METALS by B. Love and E. V. Kleber (Nuclear Corp. of Amer.); Conf. Ultrapurifi. Semicon. Mat., (A), Apr. 1961

The state of the art of purification of rare earth metals was considered from two viewpoints - separation of mixed rare earths into constituent chemical species, and reduction of the purified chemical species to high purity metals. Analytical problems are also discussed briefly. Most of the impurities in rare earth metals are introduced during the reduction process. Various reduction methods designed to minimize contamination and

various purification methods designed to remove impurities are discussed. Maximum purity limits are indicated for rare earth metals available commercially and experimentally.

10,657 THE PREPARATION AND PURIFICATION OF TRANSITION METAL SILICIDES by R. M. Ware (Plessey, Ltd.); Conf. Ultrapurifi. Semicon. Mat., (A), Apr. 1961

The two main purification processes employed were discussed. The first consisted of the purification of Co by a chemical method; the second, of the purification of the cobalt silicides by zone refining on a water cooled copper hearth. To obtain pure Co a solution of laboratory grade cobalt chloride was oxidized in the presence of excess ammonia to yield the insoluble cobalt hexammine chloride. Ni, which constituted the main impurity, does not form a hexammine and its pentammine is soluble in water. Filtration of the cobalt hexammine chloride and its reprecipitation from acid solution yielded a material with no spectrographically detectable impurities. Metallic Co was obtained by electrolysis of an aqueous solution of the hexammine onto a tantalum cathode. Impurities in the final product did not exceed 5 ppm. In the second method, the cobalt silicides were prepared by melting the purified Co plate together with pure Si by induction heating on a water cooled copper hearth. Isolation of the stoichiometric compounds and further purification was achieved by zone refining on the copper cold hearth. This method reduces the risk of crucible contamination and is considerably simpler to operate than floating zone refining. The method has been applied to several other transition metal silicides including Cr, Mn, Fe, Ni, Rh, Ir, and appears to be generally applicable to the purification of reactive materials.

INTRODUCTION OF IMPURITIES

Doping Si During Epitaxial Growth - See 10,659

Continuity Equation Analysis - See 10,677

Diffusion Kinetics in Si, Ge, and Diamond - See 10,627

Diffusion of Al into SiC - See 10,775

10,658 POLARIZATION AND DIFFUSION IN A SILICATE GLASS by R. J. Charles (GE Res. Labs.); J. Appl. Phys., Vol. 32, pp. 1115-1126, June 1961

The self-diffusion of alkali ions in alkali silicate glasses is discussed in terms of the formation, migration, and ultimate annihilation of defects. These defects exhibit a combination of the properties exhibited by Frenkel defects in alkali halides and Bjerrum defects in ice; these may be analyzed by techniques which are applicable to defects in crystalline solids. By utilizing the defect concept, relationships between self-diffusion, ac and dc conductivity, and orientational polarization are obtained.

Crystal Structure of the Alkali Antimonides - See 10,691

CRYSTAL GROWTH

10,659 EPITAXIAL SILICON FILMS BY THE HYDROGEN REDUCTION OF $SiCl_4$ by H. C. Theurer (Bell Labs.); J. Electrochem. Soc., Vol. 108, pp. 649-653, July 1961

The growth of epitaxial films of Si with controlled thickness and resistivity, either n- or p-type, is discussed. The process involves the hydrogen reduction of $SiCl_4$ appropriately doped with PCl_3 or BBr_3. The basic chemistry with reaction kinetics pertinent to the growth of these films is discussed in detail.

Formation of Closely Spaced Junctions by Epitaxial Growth - See 10,770

Preparation of $InAs-In_2Te_3$ Alloys - See 10,671

10,660 FERROMAGNETIC COMPLEX OXIDES OF MANGANESE WITH BOTH COBALT AND NICKEL IN THE CRYSTAL LATTICE AND HAVING THE ILMENITE-TYPE CRYSTAL STRUCTURE by T. J. Swoboda (du Pont); U.S. Pat. 2,996,457, Issued Aug. 15, 1961

The preparation of ferromagnetic oxides, $Co_x Ni_{1-x} MnO_3$, which have the ilmenite crystal structure is discussed. A mixture of MnO_2, black NiO, and Co_3O_4 is heated in a platinum corrosion-resistant container under 500 atmospheres and at 500° to 800°C (preferably at 550°-700°C) for 1 to 3 hours. The MnO_2 should constitute 15-85 mole per cent of the total oxide mixture, with the mole per cent calculated using the molecular weights of the NiO and the MnO_2 and one-third the molecular weight of the Co_3O_4. The synthesis can be carried out with a dry mixture of the three oxides or in an aqueous solution. The products exhibit high coercive forces and high Curie temperatures. Eight specific examples of oxide preparation are given.

Coating Process for Improving the Characteristics of Ferrite Cores - See 10,794

10,661 METHOD OF MAKING POLARIZED TITANATE CERAMICS by W. S. Miller (Am. Bosch Arma); U.S. Pat. 2,989,483, Issued June 20, 1961

A ceramic titanate polarized by the presence of certain additives and use of a particular firing schedule is described. Subsequent electric field polarization is unnecessary. The principal components are titanates (primarily Ba) and Li salts. The product exhibits pyroelectric properties, and the nature of a particular additive imparts variability to product use. Addition of tantalum oxide (TaO) is shown to promote infrared absorption (2 to 10 μ) at greater than 45 per cent efficiency.

10,662 PLASTIC TITANATE PIEZOELECTRIC COMPOSITION by W. S. Miller (Am. Bosch Arma); U.S. Pat. 2,989,481, Issued June 20, 1961

The composition and preparation of a titanate body exhibiting piezoelectric and other useful properties, without having been vitrified and polarized, are described. The final product is a moist crystal plastic mass, as opposed to a vitrified ceramic. The starting ingredients include titanates (primarily Ba), and Li compounds. A plasticizer converts the mixture into a slurry, and additional Li is added to promote an endothermic, partial reduction of titantae; the plasticizer may also participate in the reaction. Sixteen compositions, their preparation, properties, and suggested used are listed.

Verneuil Grown Ruby Single Crystals - See 10,735

CRYSTAL SURFACES

Effect of Adsorption and Desorption of Impurity Atoms on Thermionic Emission of Semiconductor Cathode Surfaces - See 10,709

Hydrogen and Oxygen Adsorption to Surfaces - See 10,763

10,663 GOLD ALLOYING TO GERMANIUM, SILICON AND ALUMINUM-SILICON EUTECTIC SURFACES by L. Bernstein (Alloys Unltd. and Hughes Semicon.); Semicon. Prod., Vol. 4, pp. 29-32, July 1961

Large and small area bonds to Ge and Si surfaces are discussed. Metallurgy and choice of backing material to avoid cracking are described. Compositions of Au-Sn offer the most versatile bonds in a variety of atmospheres. Electrode attachments to the Al-Si eutectic region in semiconductor devices, by means of Au or Au alloys, often produce a condition referred to as the "purple plague" (the $AuAl_2$ phase formation) with subsequent mechanical failure. Conditions which promote its formation in addition to the more desirable Au_2Al phase are discussed. Wetting and surface tension problems associated with attachments to the Al-Si surface via Au-Sn, Au-Ge and Au-Si alloys are described in connection with the Au-Al compound formation. Typical photomicrographs and thermal expansion curves for the systems involved are presented.

ENVIRONMENTAL EFFECTS

Migration of Solute Atoms in Tl Solid Solutions During Annealing - See 10,694

Removal of Cu-Impurity Atmosphere from Dislocations in Ge by Heat Treatment - See 10,676

Annealing Effects on Electron-Bombarded Si Tunnel Diodes - See 10,761

Stress-Induced Changes in Superconducting Critical Temperature - See 10,698

Effect of Deformation of Chromium and the Resistivity-Temperature Relationship - See 10,688

Effect of Radiation on Magnets - See 10,798

Carrier Recombination at Radiation-Induced Defects in - See 10,675

Stimulated Spin-Echo Measurement of Cross-Relaxation in Neutron-Irradiated Calcite - See 10,730

Effect of Ion Bombardment on Secondary Emission of W - See 10,709

Influence of Wet and Dry Ambients on Fast States of Ge - See 10,706

CRYSTAL PHYSICS
(including Energy Band Structure)

10,664 A STUDY OF THE BAND STRUCTURE OF TELLURIUM BY MEANS OF TRANSPORT PHENOMENA [in French] by C. Rigaux (Ecole Normale Superieure, Paris); Comptes Rendus, Vol. 253, pp. 81-82, July 3, 1961

Transport properties of Te in the extrinsic and intrinsic regions in zone refined, large single crystals are discussed. Galvanomagnetic coefficients and thermoelectric power were measured in a 5 kgauss applied field and conduction phenomena were studied in fields up to 16 kgauss. Piezoresistive and Hall effects were also investigated. The experimental results are interpreted using a 12-ellipsoid model, each ellipsoid representing a valence band constant energy surface. Principal effective masses and angular orientation of the ellipsoid axes are listed, as well as electron-hole mobility ratios in the extrinsic and intrinsic regions.

10,665 THE THEORY OF ELECTRON STATES CONNECTED WITH DISLOCATIONS I. LINEAR DISLOCATIONS by V. L. Bonch-Bruevich and V. B. Glasko (Moscow State U.); Soviet Phys. Solid State, Vol. 3, pp. 26-33, July 1961

The effect of linear dislocations on the energy spectrum of a system of electrons in a semiconductor is considered. Studies were made of the overall form of the spectrum; within the limits of a given model a clear determination has been made of the number of dislocation zones and the position of their boundaries for various concentrations of free current carriers and temperature of the specimen.

Effect of Grain Boundaries on Band Gap - See 10,639

Measurement of Internal Strain Energy in Ferromagnetic Crystals - See 10,719

Energy Gaps of InAs-In_2Te_3 Alloys - See 10,671

Effect of Temperature on Surface States in Ge - See 10,710

Influence of Wet and Dry Ambients on Fast States of Ge - See 10,706

10,666 DIRECT EXPERIMENTAL MEASUREMENT OF THE MAGNETIC FIELD DEPENDENCE OF THE SUPERCONDUCTING ENERGY GAP OF ALUMINUM by D. H. Douglass, Jr. (Lincoln Lab.); Phys. Rev. Lett., Vol. 7, pp. 14-16(L), July 1, 1961

Measurement of the magnetic field dependence of the superconducting energy gap of aluminum films as a function of the ratio of film thickness to penetration depth is discussed. The critical gap was found to be zero for values of this ratio less than 1.9 and equal to a finite value for values greater than 2.4. Good agreement from this experiment and the Ginzburg-London-Gor'kov theory was obtained for ratios up to 2.8.

Energy Levels in Superconducting Cylinders - See 10,693

Conduction Electron Energy Gap in Superconductors - See 10,699

10,667 ELECTRIC FIELD GRADIENTS IN POINT-ION AND UNIFORM-BACKGROUND LATTICES by F. W. DeWette (U. Illinois); Phys. Rev., Vol. 123, pp. 103-112, July 1, 1961

The lattice contribution to the field gradient in ionic crystals and metals is discussed. This is a quantity which has a well-defined value; however, for an actual evaluation, the field gradient is usually broken up into a number of conditionally convergent series with poor convergence. Rapidly convergent expressions for these series, and consequently, for the field gradient can be obtained by applying the method of plane-wise summation. This method is applied to the field gradient in ionic crystals with tetragonal and hexagonal symmetry and to the field gradient in tetragonal and hexagonal close-packed metal structures. As an example, an expression for the field gradient at the position of the anion is derived for ionic crystals with the CdI_2 structure. This expression is numerically evaluated for $CoBr_2$, $FeBr_2$, $MgBr_2$, $MnBr_2$, CaI_2, CdI_2, FeI_2, GeI_2, MgI_2, and MnI_2. Rather extensive numerical results are also presented for both close-packed metal structures, including values for the field gradient in Li, Be, Zn, In, and Rh.

Phonon Saturation Mechanism in Masers - See 10,801

10,668 DEBYE-WALLER FACTOR IN MÖSSBAUER INTERFERENCE EXPERIMENTS by H. J. Lipkin (Weizmann Inst. Sci., Rehovoth); Phys. Rev., Vol. 123, pp. 62-63, July 1, 1961

A simple calculation of the effects of lattice dynamics on interference between Mössbauer processes and corresponding atomic processes, i.e., between Mössbauer and Rayleigh scattering, or between internal conversion of Mössbauer radiation and the photoelectric effect is presented. When the energy of the emitted γ ray or electron is not measured, it is necessary to sum over all possible final states of the lattice. The interference contribution is found to be attenuated by the same "Debye-Waller" factor as the ordinary Mössbauer contribution, depending only upon the momentum of the incident γ ray. If the energy of the emitted γ ray is measured (e.g., by a Bragg scattering experiment), the atomic contribution is attenuated by the usual x-ray Debye-Waller factor, depending upon the momentum transfer, the Mössbauer contribution by the square of the usual Mössbauer factor, and the interference term by the geometric mean of the atomic and Mössbauer factors.

10,669 ASPHERICAL 3d ELECTRON DISTRIBUTION IN BODY-CENTERED CUBIC METALS by F. Stern (U. S. Naval Ord. Lab.); Phys. Rev. Lett., Vol. 6, pp. 675-677(L), June 15, 1961

The asphericity of the 3d electron atomic scattering factor for x-ray and polarized neutron diffraction in body-centered cubic metals on the basis of a simple energy-band model is estimated. The results agree with the neutron observations on iron, which indicate a departure of the 3d charge distribution from spherical symmetry. The asphericity of metallic iron is estimated using the charge density near the peak of the radial wave function and the results of a cohesive energy calculation in which energy values and wave functions were found for each of the five 3d bands for thirteen nonequivalent points of high symmetry in the Brillouin zone. The total charge density near the peak at 0.4 Bohr radii is found to have 44 per cent e_g symmetry and 56 per cent t_{2g} symmetry. A spherically symmetric charge distribution would be 40 per cent e_g. The net spin-up charge density near the peak is 52 per cent e_g. Two corrections, neither of which has a large effect on the results for iron, must be made to the calculated asphericity: (1) exchange polarization which contracts the wave functions of spin-up electrons relative to those of spin-down, and (2) the explicit crystal field shift.

Nuclear Polarization of Impurities in Fe from Conduction Electron Polarization - See 10,720

ELECTRICAL PROPERTIES (General)

Effect of Grain Boundaries on Electronic Properties - See 10,639

10,670 ELECTRIC BREAKDOWN STRENGTHS OF SINGLE AND LAMINATED FILMS OF VINYL CHLORIDE-ACETATE by R. G. Greenler and R. M. Kay (Allis-Chalmers); J. Appl. Phys., Vol. 32, pp. 1252-1255, July 1961

The electric breakdown strengths of thin, unsupported vinyl chloride-acetate films 1200 to 50,000 A thick are discussed. No dependence of breakdown strength on thickness is found in this region. Composite films composed of alternate layers of plastic film and thin conducting layers of silver show essentially the same breakdown strength as do single films. Five and six layer laminates which do not contain metal layers show a breakdown strength that is greater by a factor of 2 than the breakdown of single films of the same total thickness.

10,671 ELECTRICAL AND OPTICAL PROPERTIES OF InAs-In_2Te_3 ALLOYS by J. C. Woolley, B. R. Pamplin, and J. A. Evans (U. Nottingham); J. Phys. Chem. Solids, Vol. 19, pp. 147-154, Apr. 1961

The production of suitable InAs-In_2Te_3 alloys by annealing and by directional freezing methods is considered and the relevance of the second method to the phase diagram of the system is discussed. The results of measurements of Hall effect, conductivity, thermoelectric power and infrared absorption are given for the whole composition range, and values of carrier density n, mobility μ and optical energy gap E_g are obtained. It is seen that the behavior is similar to that of InSb-In_2Te_3 alloys in that the InAs-rich alloys are highly degenerate, having $n \approx 5 \times 10^{19}/cm^3$. Explanations of this behavior in terms of solubility of tellurium in InAs and of the band structure of InAs are discussed. The variation of μ with composition and hence possible scattering mechanisms and types of conduction occurring in the alloys are considered. Assuming certain scattering effects, attempts are made to use the values of thermoelectric power in conjunction with the measured values of E_g to determine the variation of intrinsic energy gap throughout the composition range.

DIELECTRIC PROPERTIES

10,672 NONLINEARITY AND MICROWAVE LOSSES IN CUBIC STRONTIUM-TITANATE by G. Rupprecht, R. O. Bell, and B. D. Silverman (Raytheon); Phys. Rev., Vol. 123, pp.

97-98, July 1, 1961

The complex dielectric constant of single-crystal strontium-titanate measured from 90° to 230°K at microwave frequencies is discussed. The real part of the dielectric constant consists of a large field-independent contribution which obeys a Curie-Weiss law over the entire range of measurement plus a smaller anisotropic field-dependent contribution. These results are shown to be in qualitative agreement with the theory of ferroelectricity in perovskite structures as proposed by Slater. The observed loss tangent consists of a contribution which is quadratic in an applied biasing field plus a field-independent contribution. The field-independent loss tangent goes through a minimum at about 170°K with a much steeper slope on the low-temperature side of the minimum than on the high-temperature side. The origin of the behavior of the field-independent loss tangent is discussed.

10,673 DIELECTRIC PROPERTIES OF $BaTiO_3$ SINGLE CRYSTALS IN THE PARAELECTRIC STATE FROM 1 KC/SEC TO 2000 MC/SEC by E. Stern and A. Lurio (IBM Watson Lab.); Phys. Rev., Vol. 123, pp. 117-123, July 1, 1961

The dielectric constant of $BaTiO_3$ single crystals in the region above the 120°C Curie point, measured at several frequencies in the range from 1 kc to 2000 Mc, is discussed. The B coefficient in Devonshire's equation for the free energy has been studied at 500 Mc. It is shown that the crystal is completely clamped with respect to the measuring field at 500 Mc so that the coefficient of the P^4 term in Devonshire's equation is positive and agrees with the expected theoretical result of $B_F{}^c = 2.23 \times 10^{-13}$ cgs unit.

Pyroelectric Effects in Polarized Titanates - See 10,661

Ferroelectric Properties of $BaTiO_3$ with Cu Additive - See 10,623

Ferroelectric Properties of $(NH_4)_2(BeF_4)_x(SO_4)_{1-x}$ and Other Systems - See 10,733

Piezoelectric Properties of a Plastic Titanate - See 10,662

Properties of Piezoelectric Transducing Elements - See 10,809

CARRIER PROPERTIES

10,674 ON THE STUDY OF VOLUME RECOMBINATION OF EXCESS CHARGE CARRIERS IN SEMICONDUCTORS WITH THE AID OF PHOTOCONDUCTANCE by B. H. Schultz (Philips); Philips Res. Rep., Vol. 16, pp. 175-181, Apr. 1961

A method for the elimination of surface effects on measurements of volume-recombination times with the aid of photoconductance is described. The measurements indicate directly whether or not it is possible to deduce a reliable value for the volume-recombination time.

Bulk and Surface Lifetime Measurements for a Si Solar Cell - See 10,780

Carrier Lifetime in Solar Cells - See 10,782

10,675 VOLUME RECOMBINATION OF CURRENT CARRIERS IN n-TYPE SILICON CONTAINING RADIATION-INDUCED STRUCTURAL DEFECTS by G. N. Galkin, N. S. Rytova and V. S. Vavilov (Acad. Sci. of USSR); Soviet Phys.-Solid State, Vol. 2, pp. 1819-1823, Mar. 1961

Data relating to the capture of current carriers by the deep-lying levels of radiation-induced defects in n-type silicon irradiated by high-energy electrons are presented. The location of the recombination levels and their cross sections for capture of electrons and holes are determined.

10,676 THE EFFECT OF A COPPER-IMPURITY ATMOSPHERE AT DISLOCATIONS IN GERMANIUM ON RECOMBINATION by S. G. Kalashnikov and A. K. Mednikov; Soviet Phys.-Solid State, Vol. 2, pp. 1847-1852, Mar. 1961

The effect of a copper-impurity atmosphere at liner dislocations in germanium on recombination velocity is discussed. It is shown that creation of an impurity atmosphere at dislocations decreases the effect of the dislocations on recombination. It is also demonstrated that, in addition to the formation of thermal acceptors, the effect of heat treatment on recombination in germanium may also be due to the removal of the impurity atmosphere from dislocations.

Charge Carrier Effective Masses in Single Crystal Te - See 10,664

Effective Mass of Conduction Electrons in InAs - See 10,703

10,677 ALTERNATIVE APPROACH TO THE SOLUTION OF ADDED CARRIER TRANSPORT PROBLEMS IN SEMICONDUCTORS by J. P. McKelvey, R. L. Longini, and T. P. Brody (Westinghouse Res. Labs.); Phys. Rev., Vol. 123, pp. 51-57, July 1, 1961

A novel method of solving added carrier transport problems in semiconductors is presented. Equations embodying conservation of flux (with due allowance for generation and recombination) which incorporate the proper boundary conditions from the outset are solved in the steady-state one-dimensional case to yield a Green's function for the desired carrier fluxes directly. The method is more general than the commonly used continuity equation formulation in that the physical dimensions of the system and the diffusion lengths are not restricted to be large compared to the mean free path; in particular it is unnecessary to assume Fick's law for diffusion processes. Otherwise the method is equivalent to the continuity equation analysis. An example involving carrier generation in a plane region bounded on one side by a surface of arbitrary reflection coefficient (or recombination velocity) and on the other by a collecting p-n junction is worked out. The results are shown to reduce to those obtained via the continuity equation in the appropriate limiting case.

10,678 CURRENT-CARRIER TRANSPORT WITH SPACE CHARGE IN SEMICONDUCTORS by W. van Roosbroeck (Bell Labs.); Phys. Rev., Vol. 123, pp. 474-490, July 15, 1961

Differential equations giving a general formulation of current carrier transport including the effects of space charge are discussed. The inclusion of space charge is necessary since the widely used approximation of electrical neutrality frequently does not apply for carrier injection and transport in semiconductor material of high resistivity. Arbitrary dependencies of diffusivities and magnitudes of drift velocities on electrostatic field are considered and extension is made for applied magnetic field. The exact electron and hole distributions are obtained in closed form for the linear small-signal case and the condition for linearity is given. The two principal types of

solutions, τ_0 (τ the diffusion-length lifetime) greater or less than the dielectric relaxation time are discussed and the respective hole-electron distributions are derived.

Space-Charge-Limited Currents in Rutile - See 10,686

10,679 IBM 704 FORTRAN PROGRAM FOR EVALUATING SEMICONDUCTOR SURFACE TRANSPORT INTEGRALS by E. G. Thomas (Naval Ord. Lab.); U.S. Gov. Res. Rep., Vol. 36, p. 114(A), July 5, 1961 AD-255 720

An IBM 704 computer FORTRAN program for the numerical evaluation of the final mobility formula in a theoretical study of surface transport in semiconductors is described. The mobility formula has the form of an integral of a transcendental function of an integral. Evaluation is required for a finite number of values of the lower limit of the outer integral and of a parameter occurring in the integrand of the inner integral.

10,680 MICROWAVE MEASUREMENT OF MOBILITY: ANALYSIS OF APPARATUS by S. H. Liu, Y. Nishina, and R. H. Good, Jr. (Iowa State U.); Rev. Sci. Instr., Vol. 32, pp. 784-789, July 1961

Measurement of the microwave mobility in a semiconductor is discussed. The mobility can be determined by mounting a sample in a bimodal cavity with an applied static magnetic field and then measuring the power transfer which is produced by the Faraday rotation in the sample. An analysis of the effect based on the field distributions in the cavity and the wave propagation in the sample is presented. The dependence of the power transfer on the static applied magnetic field, on the mobility and conductivity of the sample, and on an effective sample size is obtained.

10,681 VARIATION OF FIELD EFFECT MOBILITY AND HALL EFFECT MOBILITY WITH THE THICKNESS OF THE DEPOSITED FILMS OF TELLURIUM by S. K. Ghosh (Indian Inst. Tech.); J. Phys. Chem. Solids, Vol. 19, pp. 61-65, Apr. 1961

Experimental results of the variation of conductivity, Hall mobility and field effect mobility with the thickness of the evaporated films of tellurium are discussed. A tentative explanation of the experimental results is offered. The low values of Hall mobility are explained to be mainly due to the scattering of the carriers at the intercrystalline boundaries.

10,682 MICROWAVE MEASUREMENT OF HALL MOBILITY: EXPERIMENTAL METHOD by Y. Nishina and G. C. Danielson (Iowa State U.); Rev. Sci. Instr., Vol. 32, pp. 790-793, July 1961

Measurements of Hall mobilities of germanium single crystals at a frequency of 9000 Mc over the temperature range 30°-300°K are discussed. A rectangular sample occupied the central part of a wall of a rectangular cavity, which was doubly degenerate in the TE_{101} mode and in the TE_{011} mode at a single resonance microwave frequency. The external magnetic field and the microwave field associated with one of the two modes gave rise to the other mode of oscillation. The theoretical analysis by Liu, Nishina, and Good was verified by measurements on an n-type sample having a room temperature resistivity of 0.40 ohm cm. The measured Hall mobility at microwave frequencies (with a size correction) was compared with the dc Hall mobility between 30° and 300°K. The agreement was excellent.

Mobilities of Charge Carriers in InSb - See 10,704

Electron-Hole Mobility Ratios in Single Crystal Te - See 10,664

10,683 ACOUSTIC-MODE SCATTERING OF HOLES by M. Tiersten (Columbia U.); IBM J. Res. and Dev., Vol. 5, pp. 122-131, Apr. 1961

Matrix elements for acoustic-mode scattering of holes in the valence band structure typified by germanium are calculated. Whitfield's generalization of the deformation potential theorem is used to calculate the electron-phonon interaction and his method is extended to include the spin-lattice coupling. A general expression for the electron-phonon interaction matrix element is obtained, and calculations for some special directions in k-space are presented.

Scattering Mechanisms in Longitudinal Magnetoresistance in n-type Ge - See 10,702

Contribution of Scattering between Nonequivalent Valleys to the Free Carrier Infrared Absorption in Semiconductors - See 10,736

Ultrasonic Attenuation in Magnetite - See 10,753

CONDUCTIVITY

Thickness Dependence of Conductivity in Thin Evaporated Films of Te - See 10,681

10,684 MECHANISM OF IMPURITY CONDUCTION IN SEMICONDUCTORS by J. Mycielski (Polish Acad. Sci., Warsaw); Phys. Rev., Vol. 123, pp. 99-103, July 1, 1961

A proposed mechanism of impurity conduction in semiconductors at low temperatures is discussed. The conductivity is attributed to the carrier jumps over the Coulomb potential wall from the occupied impurity centers to the empty ones. The activation energy of conductivity and, in the case of strong carrier-phonon interaction, the conductivity itself is calculated and compared with Fritzsche's experimental data for the so-called "ϵ_2 anomaly" in p- and n-type germanium.

Measurement of Resistivity of High Resistance Semiconductors - See 10,701

10,685 IMPURITY ZONES IN P- AND N-TYPE GALLIUM ARSENIDE CRYSTALS by O. V. Emel'yanenko, T. S. Lagunova, and D. N. Nasledov (Inst. Phys. Tech., Leningrad); Soviet Phys. Solid State, Vol. 3, pp. 144-147, July 1961

The electrical conductivity and Hall coefficient of monocrystalline samples of p- and n-type gallium arsenide measured at temperatures ranging from 2° to 600°K are discussed. In strongly alloyed samples in agreement with the already published results, the Hall coefficient is constant and there is little change in the electrical conductivity as the temperature decreases. For p-type samples with a carrier concentration $p \leq 4 \times 10^{18}$ cm^{-3} the curve showing the temperature dependence of the Hall constant has a maximum at low temperatures and the electrical conductivity falls sharply. A pure n-type sample ($n = 20 \times 10^{16}$ cm^{-3}) exhibits the same type of behavior. At low temperatures an anomalous decrease in the resistance of n-type samples in magnetic fields was observed. The results

are discussed on the basis of our understanding of conductivity in the impurity band.

10,686 NONOHMIC BEHAVIOR IN NEAR-STOICHIOMETRIC RUTILE (TiO_2) by E. H. Greener and D. H. Whitmore (Northwestern U.); J. Appl. Phys., Vol. 32, pp. 1320-1324, July 1961

Experimental observations of the isothermal current-voltage relationships in rutile (TiO_2) over the temperature range 632° to 908°C are discussed. It was found that currents in excess of ohmic currents can be drawn through small, single crystals of near-stoichiometric composition. These currents have been identified as space-charge-limited currents analogous to those observed in the case of a vacuum diode. An increase in the ambient specimen temperature had the effect of displacing the potential for transition from ohmic to nonohmic behavior to greater values so that, at 908°C, near-stoichiometric rutile exhibited only ohmic currents even at the largest fields employed.

10,687 ELECTRICAL CHARACTERISTICS OF FOUR TERNARY PLATINUM-RHODIUM-BASE ALLOYS CONTAINING CHROMIUM, COBALT, OR RUTHENIUM by H. H. Lowell, H. W. Allen, and J. E. Jenkins (NASA); U.S. Gov. Res. Rep., Vol. 36, p. 86(A), July 5, 1961 AD 255 531

The resistivities of small specimens of 5Co-15Rh-80Pt, 5Cr-15Rh-80Pt, 10Cr-15Rh-75Pt, and 5Ru-15Rh-80Pt determined for temperatures up to 900°C are discussed. Resistance to progressive oxidation was observed in the Co- and Cr-containing alloys. The Co-containing alloy exhibited a shallow minimum of resistivity between about 200° and 400°C, but stability was not attained. The Cr-containing alloys exhibited very high and nearly constant rates of change of resistivity with temperature up to low-temperature reversible transformation points and were electrically stable at all temperatures. The Ru-containing alloy exhibited a linear and stable change of resistivity throughout its (lower) useful temperature range.

10,688 ELECTRICAL RESISTIVITY OF CHROMIUM IN THE VICINITY OF THE NÉEL TEMPERATURE by M. J. Marcinkowski (U.S. Steel Res. Ctr.) and H. A. Lipsitt (Wright-Patterson AFB); J. Appl. Phys., Vol. 32, pp. 1238-1240, July 1961

The observation of a sharply cusped minimum in the resistivity-temperature relationship for fully recrystallized chromium at the Néel temperature (35°C) and of the elimination of this minimum by plastic deformation is discussed. Plastic deformation also produces a pronounced change in the resistivity-temperature relationship over a wide range of temperatures centered about the Néel temperature. The results agree with those of other workers. This behavior is analyzed and interpreted in terms of the strong dependence of the Néel temperature on hydrostatic stresses which are thought to arise from the presence of dislocations in the deformed material.

Temperature Dependence of the Electrical Resistivity of $MnSn_2$ - See 10,718

Piezoresistive Effect in Single Crystal Te - See 10,664

10,689 ELECTRICAL CONDUCTIVITY OF NaCl DURING HIGH-TEMPERATURE CREEP by R. W. Christy and W. E. Daniels, Jr. (Dartmouth Coll.); J. Appl. Phys., Vol. 32, pp. 1265-1268, July 1961

Measurements made on the electrical conductivity of NaCl in the intrinsic range during and after deformation by creep are discussed. The conductivity is proportional to the diffusion coefficient for Na. At about 550°C, no change in conductivity was observed, even at steady-state creep rates approaching 10%/min. This negative result is shown to be in accord with theoretical estimates.

10,690 PINCH EFFECT IN INDIUM ANTIMONIDE by A. G. Chynoweth and A. A. Murray (Bell Labs.); Phys. Rev., Vol. 123, pp. 515-520, July 15, 1961

The critical current at which pinching occurs in indium antimonide is discussed. The critical current has been measured by three independent methods: (a) by noting the current at which the pinched current-voltage characteristics deviate from the unpinched characteristics that are obtained in the presence of a longitudinal magnetic field H, using crystals of sufficiently high resistance for the avalanche breakdown current to be considerable, before pinching sets in, as the electric field is increased; (b) by noting the current at which the magneto resistance, as a function H, shows a change in its behavior; and (c) from a study of the critical current as a function of H. The three methods lead to a value for the critical pinching current of 4-5 amp. This current is the same for both single-crystal and polycrystalline samples, and is insensitive to small changes in the donor concentration or cross-sectional area of the crystal. The value of the critical current leads to a mean carrier temperature of 0.04 ev in avalanche breakdown. An irregular form of noise is observed when the crystal is operated in the transition region between the pinched and unpinched conditions, and it is thought that this noise is caused by pinching-unpinching instabilities.

10,691 CRYSTAL STRUCTURES AND ELECTRICAL PROPERTIES OF ALKALI ANTIMONIDES by J. Chikawa, S. Imamura (Japan Broadcasting, Tokyo), K. Tanaka and M. Shiojiri (Kyoto U.); J. Phys. Soc. Japan, Vol. 16, pp. 1175-1180, June 1961

X-ray and electrical measurement performed simultaneously on the antimonides of potassium, sodium, cesium, and rubidium in a vacuum are discussed. In K-Sb and Na-Sb, the crystallization into the hexagonal structure from the amorphous state and the transition from p-type semiconductor to n-type occur simultaneously with successive activation by alkali metal. Cs-Sb, however, remains p-type even after crystallization into the cubic structure from the amorphous state. In Rb-Sb the amorphous → cubic → hexagonal transition occurs and n-type conduction appears in the hexagonal structure. In order to explain these facts, the relation between the excess alkali atoms and the crystal structure is considered. The cubic phase of Rb_3Sb is found to be the same as the structure of Cs_3Sb.

10,692 SINGLE-CRYSTAL AND POLYCRYSTAL RESISTIVITY RELATIONSHIPS FOR YTTRIUM by J. K. Alstad, R. V. Colvin, and S. Legvold (Iowa State U.); Phys. Rev., Vol. 123, pp. 418-419, July 15, 1961

Different proposals for calculating polycrystal resistivities from single-crystal values are applied to yttrium metal. It is shown that a simple average yielding $\rho_{poly} = (2\rho_{\perp} + \rho_{\parallel})/3$ gives the best fit to experimental data.

10,693 THEORETICAL CONSIDERATIONS CONCERNING QUANTIZED MAGNETIC FLUX IN SUPERCONDUCTING CYLINDERS by N. Byers and C. N. Yang (Stanford U.); Phys. Rev. Lett., Vol. 7, pp. 46-49 (L), July 15, 1961

Some theoretical aspects of the quantized magnetic flux in a superconducting cylinder are discussed. By examining the energy eigenfunction for the superconducting electrons and the wave equation subject to boundary conditions, it is deduced that (1) the energy levels are periodic in the magnetic flux, Φ, with a period ch/e, (2) the energy levels are even functions of Φ, (3) the macroscopic partition function, Q, of the system is an even periodic function of Φ with period ch/e, and (4) the superconducting state is given by the maxima of InQ as a function of Φ. However, for the microscopic consideration it is seen that the trapped flux Φ is related to the original flu.. Φ_o in integral units of Φ_o/ch/2e.

Quasi-Particle Model of a Superconductor - See 10,711

Paramagnetic Effect in Superconductors - See 10,729

Magnetic Field Dependence of the Energy Gap of Superconducting Aluminum Films - See 10,666

10,694 STUDY OF THE SUPERCONDUCTING TRANSITION TEMPERATURE IN DILUTE THALLIUM SOLID SOLUTIONS by D. J. Quinn and J. I. Budnick (IBM Res. Lab.); Phys. Rev., Vol. 123, pp. 466-469, July 15, 1961

The superconducting transition temperature T_c, measured in dilute solid solutions of In, Bi, and Pb in Tl is discussed. The transition temperature is found to increase in all cases, thus exhibiting a behavior opposite to that observed by Serin, Lynton, and co-workers in their studies of solid solutions of Sn, In, and Al. Some loss in residual impurity scattering which occurs upon annealing suggests the migration of solute atoms to grain boundaries in the dilute alloys.

10,695 ULTRASONIC ATTENUATION IN TIN SINGLE CRYSTALS AT LOW TEMPERATURES by K. Kamigaki (Tohoku U.); J. Phys. Soc. Japan, Vol. 16, pp. 1141-1144, June 1961

The ultrasonic attenuation coefficient and velocity in the superconducting and the normal states of tin single crystals measured at temperatures between 1.5° and 4.2°K are discussed. It was found that (1) anisotropy of ultrasonic attenuation in different crystallographic direction exists in the case of comparatively long wavelengths (the product of the mean free path of conduction electrons and wave number of sound waves is less than unity) and (2) the ratio of longitudinal to shear wave attenuation is larger than that predicted from the free electron model.

10,696 EXPERIMENTAL PROOF OF MAGNETIC FLUX QUANTIZATION IN A SUPERCONDUCTING RING by R. Doll and M. Nabauer (Bayerischen Akad. Wissenshaften, Germany); Phys. Rev. Lett., Vol. 7, pp. 51-52 (L), July 15, 1961

Experimental verification of magnetic flux quantization is described. The samples were prepared by evaporating lead onto 10 μ quartz fibers of approximately 1 mm length. Flux measurement was made by suspending the superconducting cylinders on a torsion fiber inside a pickup coil. The samples were heated above the transition temperature, then a known axial field was applied and after recooling below the transition temperature, the field was switched off. The resonance amplitude was then determined to measure the trapped flux. The obtained interval was found to be about 40 per cent of the expected value.

10,697 EXPERIMENTAL EVIDENCE FOR QUANTIZED FLUX IN SUPERCONDUCTING CYLINDERS by S. Deaver, Jr. and W. M. Fairbank (Stanford U.); Phys. Rev. Lett., Vol. 7, pp. 43-46 (L), July 15, 1961

Measurements of the net flux in superconducting tin cylinders made by oscillating the cylinders at a known frequency and amplitude between two small pickup coils are discussed. The experiment was carried out by cooling the sample through the transition temperature in an axially applied field and subsequently observing the rise in flux after the field is reduced to zero. The observed flux is apparently quantized in units of hc/2e or one-half the value predicted by London and Onsager.

10,698 SIZE EFFECTS IN THIN SUPERCONDUCTING INDIUM FILMS by A. M. Toxen (IBM Res. Ctr.); Phys. Rev., Vol. 123, pp. 442-446, July 15, 1961

Measurements of residual resistivity, superconductive critical temperature, and critical magnetic field carried out on indium films ranging in thickness from 650 to 126,000 A are discussed. The thickest films had the bulk critical field and critical temperature. The variation of residual resistivity with thickness is consistent with Fuchs' model if one assumes an intrinsic resistivity ρ_0 of 1.31×10^{-8} Ω cm and an intrinsic mean free path l_0 of 152,000 A. The value of $\rho_0 l_0$ so obtained was 2.0×10^{-11} Ω cm^2. The critical temperature was found to be a systematic function of film thickness, increasing with decreasing thickness. The magnitude of this change in critical temperature is in good agreement with a simple model relating critical temperature to elastic stresses in the films. The penetration depth, as calculated from the critical field by means of the London theory or the Ginzburg-Landau theory, was found to increase with decreasing film thickness. This result is consistent with a nonlocal model and implies a coherence length of ~2600 A.

10,699 ELECTRON TUNNELING AND SUPERCONDUCTIVITY by S. Shapiro, P. H. Smith, J. L. Miles, and J. Nicol (A. D. Little); Program Cryogenic Engrg. Conf., pp. 33-34(A), Aug. 1961

The voltage dependence of currents produced by electron tunneling through thin dielectric layers between superconducting metal films was discussed. In the first experiments, Al and Pb were separated by Al_2O_3; later work has involved organic monolayers between films of Pb, Sn, and In. The voltage-current characteristics are exceedingly nonlinear and, under properly chosen conditions, exhibit a region of negative resistance. A theoretical analysis provides excellent quantitative agreement with the data and demonstrates that the experiment provides a simple and accurate means of measuring the conduction electron energy-gap in super-conducting metals under the influence of various parameters. While the research program is still in an early stage of development, the form of the characteristics and their sensitivity to temperature and magnetic field have suggested many interesting circuit applications of the Tunneltron, either alone or in combination with other superconducting circuit elements such as the Cryotron.

MAGNETOELECTRIC PROPERTIES
(Galvanomagnetic)

10,700 GALVANOMAGNETIC EFFECTS IN SEMICONDUCTORS AT HIGH ELECTRIC FIELDS by E. M. Conwell (Genl. Tel. Electronics Lab.); Phys. Rev., Vol. 123, pp. 454-463, July 15, 1961

A treatment of magnetoconductivity for high electric fields and general energy-band structure using a partial solution of the Boltzmann equation in a form similar to that set up by McClure for low electric fields is developed. The present treatment is valid when the scattering processes are such that the distribution function varies but a small amount over an entire constant-energy surface, or, in the case of the many-valley band structure, over the part of a constant-energy surface within each valley. In the latter case, different distribution functions must be used for the different valleys. The elements of the magnetoconductivity matrix that results are expressed in terms of carrier concentrations, total or within each valley, and averages over the carriers of a quantity involving the momentum relaxation time and the S tensor defined by McClure. This tensor, which depends on the shape of the constant-energy surfaces and on the magnetic-field strength, is evaluated for the individual valleys in a nondegenerate many-valley semiconductor. The magnetoconductivity matrix is then in a form convenient for calculation of conductivity and galvomagnetic effects for either low or high fields. It is used to obtain expressions for anisotropy voltage and Hall coefficient in high electric fields involving the number of carriers in each valley, orientation of the valleys, and valley averages over quantities involving relaxation time and energy.

10,701 APPARATUS FOR THE MEASUREMENT OF GALVANOMAGNETIC EFFECTS IN HIGH-RESISTANCE SEMICONDUCTORS by G. Fischer, D. Greig, and E. Mooser (Natl. Res. Counc., Ottawa); Rev. Sci. Instr., Vol. 32, pp. 842-846, July 1961

An apparatus for the measurement of galvanomagnetic effects in high resistance semiconductors is described. The apparatus allows the resistivities of samples whose resistances fall within the range 10^{-1} to 10^{12} Ω to be measured. The Hall coefficients of these samples can also be determined with the apparatus as long as the charge carrier mobilities of the samples exceed 1 cm^2/v sec. The fundamental limitations of Hall coefficient measuring equipment is discussed.

10,702 LONGITUDINAL MAGNETORESISTANCE IN n-TYPE GERMANIUM: THEORETICAL by S. C. Miller and M. A. Omar (U. Colorado); Phys. Rev., Vol. 123, pp. 74-80, July 1, 1961

Calculations for the longitudinal magnetoresistance of n-type Ge for high magnetic fields where Landau levels are important are discussed. The scattering mechanisms considered are acoustic and ionized impurity scattering. Comparison is made with experiment for acoustic scattering and is found to be satisfactory for sufficiently high fields.

Magnetoresistive Measurements in Ge Resistance Thermometers - See 10,790

Temperature Dependence of Hall Coefficient in GaAs - See 10,685

10,703 INFRARED CYCLOTRON RESONANCE IN n-TYPE InAs AND InP by E. D. Palik and R. F. Wallis (U.S. Naval Res. Lab.); Phys. Rev., Vol. 123, pp. 131-134, July 1, 1961

Cyclotron resonance of conduction electrons in InAs and InP measured in the far infrared spectral region is discussed. The effective masses obtained for InAs show a variation with magnetic field indicative of the nonparabolic nature of the conduction band of this material.

10,704 CORBINO DISK MAGNETORESISTIVITY MEASUREMENTS ON InSb by M. Green (USASRDL); J. Appl. Phys., Vol. 32, pp. 1286-1289, July 1961

Magnetoresistivity measurements employing "Corbino disk" geometry made at temperatures of 77°, 203°K, and at approximately room temperature, on a slice of fairly high-purity, single-crystal, n-type InSb (probably compensated) with excess impurity concentration $N_D - N_A$ of about 7×10^{15} are discussed. In a series of measurements the ratios of the resistance at 20 kgauss to that at zero field, for the temperatures and in the order listed above, were found to be approximately 23, 23, and 33. The maximum magnetic coefficients of resistance, in the same order, were approximately 0.87, 0.70, and 0.50 per kgauss occurring approximately at fields of 0.7, 1.0, and 2.6 kgauss, respectively. Mobilities were determined by both Hall effect and low-field magnetoresistivity, and were found to agree within a few per cent. The values were, in the same temperature order, 7.3, 5.3, and 4.5 m^2/v sec. Temperature cycling and aging appear to cause a reduction in area of soldered contacts to the specimen. Very slight variations of magnetoresistance with the polarity of current through the specimen were observed. An explanation is given. The calculations are of the same order of magnitude as experimental observations.

Galvanomagnetic Coefficients of Single Crystal Te - See 10,664

ELECTRICAL PROPERTIES OF SURFACES

10,705 INVESTIGATION OF THE SURFACE PROPERTIES OF GERMANIUM AT DIFFERENT TEMPERATURES I. AMPLITUDE CHARACTERISTICS by V. G. Litovchenko and V. I. Lyashenko (Phys. Inst., Kiev), Soviet Phys.-Solid State, Vol. 3, pp. 44-52, July 1961

Investigations of the surface properties of germanium at temperatures of 170°-305°K are discussed. Additional data have been obtained supporting the discrete distribution of surface levels in the forbidden zone for a real germanium surface. The temperature dependences have been determined for the parameters of "fast" and "slow" surface states, and also the surface potential and work function.

10,706 INFLUENCE OF WET AND DRY AMBIENTS ON FAST SURFACE STATES OF GERMANIUM by Y. Margoninski and H. E. Farnsworth (Brown U.); Phys. Rev., Vol. 123, pp. 135-140, July 1, 1961

Simultaneous measurements of surface recombination velocity and added trapped charge density in the fast states as a function of surface potential, carried out on n-type Ge, are reported. The Ge was subjected to the following gaseous ambient cycles: (a) room air-vacuum, (b) dry air-vacuum, (c) dry oxygen-vacuum, (d) dry nitrogen-vacuum, (e) wet nitrogen-vacuum, and (f) wet oxygen-vacuum. The most important results of these measurements were: (1) Dry nitrogen had no influence

whatsoever on any of the surface-state parameters, (2) dry oxygen affected only the density of states and the unperturbed surface potential, and (3) wet nitrogen and wet oxygen had almost the same and most pronounced effect on the fast surface states.

10,707 THE THEORY OF NONSTATIONARY THERMOEMISSION OF A SEMICONDUCTOR CATHODE by A. A. Ostroukhov (Kiev State U.); Soviet Phys.-Solid State, Vol. 3, pp. 1-8, July 1961

The kinetics of electron processes in the bulk and at the surface of a semiconductor, which can be used to describe the impulse thermoemission effect of a semiconductor cathode is discussed. The case in which the time of relaxation of the bulk charge and the effective time of surface recombination is much less than the time of bulk recombination of the current carriers, i.e., when the time relationship of all values are due to the slow change in the concentration of gas on the bulk donors is discussed. Calculations are made of the volt-ampere characteristics of the cathode and the start and finish of a semi-infinite impulse of the anode voltage. In the general case, an approximate method was used to study the relationship between the thermal stream and the time and the effect on this relationship of the anode voltage and the parameters of the semiconductor. Studies were also made of the effect of desorption and adsorption of impurity atoms at the surface of the cathode on the size of the thermal stream impulse.

Emission from Cesium Coated Cathode Surfaces - See 10,787

10,708 TEMPERATURE-DEPENDENT BISMUTH-CESIUM PHOTOSURFACES by R. J. Zollweg and C. R. Taylor (Westinghouse Res. Labs.); J. Appl. Phys., Vol. 32, pp. 1316-1319, July 1961

An investigation of the temperature dependence of the yield of bismuth-cesium photosurfaces is discussed. This effect has been found to be dependent upon the presence of oxygen and upon the size of the aggregates making up the photosurface. The photoelectron energy spectra are also examined. It is concluded that the temperature dependence probably arises from a change in escape depth with temperature because of phonon collisions, but that the principal photoelectron energy loss may occur at oxygen impurity sites.

Photoemission Spectra of ZnS:Cu - See 10,741

10,709 EMISSION FROM TUNGSTEN INDUCED BY CERTAIN POSITIVE IONS by N. N. Petrov and A. A. Dorozhkin (Leningrad Polytech. Inst.); Soviet Phys.-Solid State, Vol. 3, pp. 38-43, July 1961

Secondary emission from a tungsten target bombarded by ions of certain gases (He^+, Ne^+, A^+), nitrogen (N_1^+, N_2^+) and calcium (Ca^+) is discussed. From the data obtained conclusions are drawn as to the effect of electron shell structure of the ion on the ion-electron emission.

10,710 INVESTIGATION OF THE SURFACE PROPERTIES OF GERMANIUM AT DIFFERENT TEMPERATURES II. KINETICS OF THE PROCESSES by V. G. Litovchenko and V. I. Lyashenko (Phys. Inst., Kiev); Soviet Phys.-Solid State, Vol. 3, pp. 53-64, July 1961

An investigation and comparison of the kinetics of the field effect and the kinetics of the photoconductivity at 170°-305°K are discussed. The effect of temperature on the capture cross section and other parameters of the surface electron states has been determined.

OTHER ELECTRICAL PROPERTIES

Noise in the Transition Region Between the Pinched and Unpinched States in InSb - See 10,690

Generation-Recombination Noise Mechanism - See 10,769

Current-Carrier Transport with Space Charge in Semiconductors - See 10,678

10,711 TUNNELING FROM AN INDEPENDENT-PARTICLE POINT OF VIEW by W. A. Harrison (GE Res. Lab.); Phys. Rev., Vol. 123, pp. 85-89, July 1, 1961

A method for calculating wave functions through regions of varying band structure is developed. This method is applied to tunneling problems using the transition-probability approach of Bardeen. It is found that the experiments of Giaever involving tunneling into superconductors cannot be understood strictly in terms of an independent quasi-particle model of the superconductor. The observed proportionality of the tunneling probability to the density of states depends upon the matrix elements being constant which, in turn, depends upon a many-particle feature of the problem. This feature does not carry over to fluctuations in the density of states arising from band structure, and contributions to the current are not expected to be proportional to the density of states in that case. Instead, a projection in wave-number space of the appropriate constant-energy surface enters. Tunneling systems which involve semiconductors, semimetals, and transition metals as well as simple metals are discussed.

Tunneling between Superconductors - See 10,699

MAGNETIC PROPERTIES

10,712 INDIRECT EXCHANGE MODEL FOR FERROMAGNETIC METALS by S. H. Liu (IBM); Phys. Rev., Vol. 123, pp. 470-474, July 15, 1961

The ferromagnetic properties of rare-earth metals and their alloys are discussed in terms of the indirect exchange model. It is shown by the molecular-field approximation that, in calculating Curie temperatures of these metals, the simple theory of Fröhlich and Nabarro and Zener is applicable. The second-order energy terms calculated by Ruderman and Kittel, Kasuya, and Yosida are important in discussing the low-temperature properties. Some numerical results which are in good agreement with the experiments are obtained.

10,713 TECHNIQUES FOR MEASURING THE ANGULAR DISPERSION OF THE EASY AXIS OF MAGNETIC FILMS by T. S. Crowther (Lincoln Lab.); U.S. Gov. Res. Rep., Vol. 36, p. 114(A), July 5, 1961 AD 255 697

Two methods for using a B-H looper in the measurement of the angular dispersion of the easy axis are presented. Results of the two methods agree within a factor of two. For a typical evaporated film 50% of the material is oriented within ±0.5

degrees of the mean of the distribution and 98% within ±2.0 degrees of the mean.

10,714 MAGNETIC SPECTRUM OF MIXED NICKEL, ZINC AND COPPER FERRITE IN A STATE OF RESIDUAL MAGNETISM AT VARIOUS TEMPERATURES by L. A. Fomenko; Soviet Phys.,-Solid State, Vol. 3, pp. 95-101, July 1961

An investigation of the temperature dependence of the magnetic spectra of Ni-Zn-Cu ferrite (21% NiO, 4%CuO, 26% ZnO and 49% Fe_2O_3, molar per cent, baking temperature 1140°C, Curie temperature 238°C), measured in the absolute null state and in a state of residual magnetism at temperatures ranging from -80° to 232°C is discussed. The reversible magnetization of ferrites at higher temperatures may be explained by the processes involved in the rotation of the magnetization vector in an effective field having isotronic inner stresses. The observed dispersion is apparently associated with diffusion processes. At other temperatures the dominating role is probably that of the processes involved in the shift of the boundaries which is undoubtedly the major factor at temperatures of -80° to 100°C. The resonant character of the spectra is described by the resonance of the boundaries, according to Dering. A comparison made of the results of the investigation with Kersten's foreign body theory and Kondorskii's stress theory indicates that the latter manner of describing the phenomena is more accurate.

Effect of Radiation on Magnets - See 10,898

10,715 MAGNETIZATION PROCESS IN SMALL PARTICLES OF CrO_2 by F. J. Carnell (du Pont); J. Appl. Phys., Vol. 32, pp. 1269-1274, July 1961

Initial magnetization curves, remanence, coercivity, reversible susceptibility, and rotational hysteresis measured in small particles of CrO_2 are discussed. The measurements allow rough division into three types of behavior with decreasing particle size: multidomain, or bulk behavior, for $\sim$ 100 μ particles; few-domain behavior for $\sim$1 - 10-μ particles; and single-domain behavior for particles with a length/diameter ratio $\sim$5 and a diameter $\leq$ 0.2 μ. The smaller particles studied were acicular and showed coercivity dominated by shape anisotropy.

10,716 ADIABATIC DEMAGNETIZATION WITH YTTRIUM-RARE EARTH ALLOYS by D. T. Nelson and S. Legvold (Iowa State U.); Phys. Rev., Vol. 123, pp. 80-84, July 1, 1961

An investigation of yttrium alloys with 0.3 and 1.0 at. per cent gadolinium, 1.0 at. per cent dysprosium, and 0.6 and 1.0 at. per cent holmium to determine their usefulness as the working substance for adiabatic demagnetization is discussed. In addition, single crystals of 0.6 and 1.0 at. per cent holmium-yttrium alloys were studied. Those alloys which exhibited paramagnetic susceptibility behavior in the temperature range 1.2°-4.2°K were demagnetized adiabatically from about 11 koe and 1.25°K. The lowest temperature attained was 0.76°K for the single crystal of 1.0 at. per cent holmium with the magnetic field parallel to the a-axis of the hexagonal crystal. Magnetization measurements obtained for the single crystals in the temperature range 1.2°-4.2°K indicated strong anisotropy with the a-axis as the easy axis of magnetization. Hysteresis was observed in the magnetization of the 1.0 at. per cent holmium single crystal with the a-axis parallel to the field. Entropy removal during magnetization was calculated from the magnetization data for the single crystals and found to be only about 15 per cent of that expected if the alloy behaved like a ideal paramagnetic substance.

10,717 FERROMAGNETISM IN SOLID SOLUTIONS OF SCANDIUM IN INDIUM by B. T. Matthias, A. M. Clagston, H. J. Williams, E. Corenzwit, and R. C. Sherwood (Bell Labs.); Phys. Rev. Lett., Vol. 7, pp. 7-9(L), July 1, 1961

The observation of ferromagnetism at temperatures below 6°K in a solid solution of approximately 24 at. per cent indium in scandium is discussed. This effect is reported to occur over an extremely narrow range of only 0.4 at. per cent of indium. The susceptibility, x for these solid solutions is strongly temperature dependent and can be fitted approximately to a Curie-Weiss law of the form $x = N\mu_B^2 p_{eff}^2/3k(T-\theta)$, where N is the number of magnetic centers, μ_B the Bohr magneton, p_{eff} is the effective magnetic moment per atom, and θ is the Curie temperature. Data are given for Curie temperature as a function of x.

Coating Process for Improving the Characteristics of Ferrite Cores - See 10,694

10,718 ABRUPT MAGNETIC TRANSITION IN $MnSn_2$ by J. S. Kouvel and C. C. Hartelius (GE Res. Lab.); Phys. Rev., Vol. 123, pp. 124-125, July 1, 1961

The magnetic susceptibility and the electric resistivity of the intermetallic compound $MnSn_2$ are discussed. They are found to decrease precipitously as the temperature is lowered through 73°K. Both these abrupt changes exhibit a small temperature hysteresis and are highly suggestive of a first-order transition. From 73°K down to 4.2°K, the susceptibility is essentially constant; above 73°K, the susceptibility rises slowly to a maximum (at 86°K) and then decreases in a manner consistent with the Curie-Weiss relation. It is tentatively concluded that the abrupt transition at 73°K involves only a partial disordering of an antiferromagnetic state.

Temperature Dependence of the Magnetic Susceptibility of Ferrites - See 10,725

10,719 MAGNETIZATION OF NICKEL SINGLE CRYSTALS by L. Tterlikkis and A. W. Jenkins, Jr. (U. Denver); J. Appl. Phys., Vol. 32, pp. 1293-1296, July 1961

The magnetization curves of nickel single crystals are calculated by the method of Lawton and Steward for arbitrary orientation of the crystal in the field. The anisotropy coefficients are calculated from experimental curves with the applied field in symmetry directions, and it is found that only K_1 can be determined reliably with the data used. The calculated off-axis curves agree well with experimental results. A correcting field determined from the easy-axis magnetization curve is utilized to compensate for internal strain effects. The relation between the calculated field minus the observed field and the easy-axis field suggests a possible method for measuring internal strain energy in ferromagnetic crystals.

10,720 NUCLEAR POLARIZATION OF IMPURITIES IN FERROMAGNETS by F. J. Blatt and R. J. Elliott (Clarendon Lab., Oxford); Bull. Am. Phys. Soc., Ser. II, Vol. 6, p. 54(A), Feb. 1, 1961

The nuclear polarization of impurities in iron was estimated.

The polarization, arising from the contact interaction with the polarized conduction electrons, is deduced by determining the charge density and conduction electron polarization in the impurity cell. The estimates of the nuclear polarization, based on these calculations and on hyperfine structure data, agree reasonably well with recent experimental results provided the conduction electrons in iron are assumed only partially s-like.

10,721 DEVICE FOR THE RAPID MEASUREMENT OF MAGNETIC ANISOTROPY AT ELEVATED TEMPERATURES by H. Zijlstra (N. V. Philips); Rev. Sci. Instr., Vol. 32, pp. 634-638, June 1961

A method for the rapid measurement of magnetic anisotropy is described. The instrument consists of a self-exciting torsion pendulum containing the magnetic sample, which is suspended in a magnetic field in a furnace. The resonance frequency of the pendulum, which depends in a known way on the anisotropy energy, lies between 10 and 100 cps so that the time required for a measurement is shorter than in other methods. The instrument is therefore capable of following a rapidly changing anisotropy, e.g., during magnetic annealing of the sample. The measurement of the anisotropy of a single crystal of Ticonal G magnet steel during cooling from 900° to 400°C in a magnetic field is described as an example.

10,722 GYROMAGNETIC RATIO OF NICKEL FERRITE by G. G. Scott (GM); Phys. Rev., Vol. 123, p. 434, July 15, 1961

The gyromagnetic ratio of the ferrite $NiOFe_2O_3$ determined by measurements of the Einstein-deHaas effect is discussed. The g' value of 1.849 ± 0.002 indicates that the magnetization is largely due to the Ni^{++} ions as in the Néel model. Comparison with values of g determined by ferromagnetic resonance investigations furnishes evidence as to the validity of the Kittel-Van Vleck relation for ferrites.

10,723 WEAK FERROMAGNETISM IN β-$NaFeO_2$ by H. Watanabe (Tohoku U.) and M. Fukase (Konishiroku Photo Ind.); J. Phys. Soc. Japan, Vol. 16, pp. 1181-1185, June 1961

The high temperature modification of sodium ferrite, β-$NaFeO_2$, which exhibits a weak ferromagnetism and a Curie temperature of about 450°C is discussed. The magnetic property resembles that of $LaFeO_3$. The origin of weak ferromagnetism of β-$NaFeO_2$ can be attributed to the presence of the Dzyaloshinsky type interaction in this compound.

10,724 PRIMITIVE THEORY OF FERRIMAGNETIC RESONANCE FREQUENCIES IN RARE-EARTH IRON GARNETS by J. H. van Vleck (Harvard U.); Phys. Rev., Vol. 123, pp. 58-62, July 1, 1961

The effective g factor for ferrimagnetic resonance frequencies in rare-earth iron garnets is calculated by direct inspection of eigenvalues rather than study of the equations of motion. The rare-earth ions are treated as captive in the exchange field from the iron, but subject to decomposition of their energy levels by crystalline fields and/or spin-orbit interaction. With a crystalline field, the problem is tractable in a simple way only if these decompositions are large or small compared to those which could be produced by the exchange field acting alone. Anisotropy, actually very important at low temperatures, is neglected except insofar as it can be represented by an anisotropy field. The concept of "fictitious spin" is useful, and the spectroscopic splitting factors turn out to be more relevant than the true gyromagnetic ratios. For europium garnet, the theory becomes essentially that of Wolf. It is shown that Kittel's formula $g_{eff} = 2(M_{Fe} + M_{RE})/M_{Fe}$ has approximate validity if most of the magnetic moment of the rare earth arises from nondiagonal matrix elements joining ionic energy levels with separations large compared with the Zeeman energy in the exchange field. The fact that in certain cases the experimental results are represented fairly well by Kittel's formula is hence not necessarily to be construed as evidence that the rare-earth ion is highly damped by spin-lattice interaction as in his original model.

10,725 TEMPERATURE RELATIONSHIPS OF THE WIDTH OF THE RESONANCE CURVE AND PROCESSES OF RELAXATION IN FERRITE MONOCRYSTALS by A. G. Gurevich, I. E. Gubler, and A. G. Titova (Inst. Semicon., Leningrad); Soviet Phys.-Solid State, Vol. 3, pp. 13-22, July 1961

Measurements of the width of the resonance curve and the magnetic susceptibility during resonance in the temperature range from -196°C to the Curie points for Y ferrite with a structure of the garnet type and Mn- and Mg-Mn-Ferrites with a spinel type structure are discussed. The measurements were made on spheres with various surface treatment. Studies were made on Y-ferrite monocrystals grown from Y oxide of varying purity. On the basis of the obtained results, several conclusions were drawn as to the role of various relaxation processes and on the temperature dependences of parts of the width of the resonance curve $2\Delta H$ caused by these processes. It was shown that the part $2\Delta H$ connected with the roughness of the surface of the specimens is approximately proportional to the magnetization. The part $2\Delta H$ caused by the noncoherent relaxation process near the Curie point on the temperature according to a law close to $1/\sqrt{T_c - T}$ (T_c is the Curie temperature). The frequency of relaxation of ions of the rare-earth impurities was determined for Y ferrite.

10,726 ELECTROMAGNETIC THEORY OF SPIN WAVE RESONANCE by M. H. Seavey, Jr. (Lincoln Lab.); U.S. Gov. Res. Rep., Vol. 36, p. 33(A), July 5, 1961 AD 255 342

An electromagnetic theory of spin wave resonance which applies mainly to situations in which the DC magnetic field is perpendicular to the planar surface of a medium is discussed. The consequence of introducing the exchange anisotropy field into the equation of motion are worked out. It is first shown that, in general, two resonant modes of propagation exist in the perpendicular case and that one of these modes is a spin wave. The degree of excitation of the spin wave mode is shown to depend on the boundary condition, e.g., whether the spins are pinned or unpinned at the surface. The theory is then applied to a semi-infinite medium metal and approximate permeability expressions are obtained. Evidence for a large normal surface anisotropy is presented. Finally, spin wave resonance in a thin film is discussed and a phenomenological model of the process is described. Approximate permeability expressions are obtained and exact theoretical spin wave resonance curves are discussed and compared briefly with experiment.

Determination of the Gyromagnetic Ratio of $NiOFe_2O_3$ by Ferromagnetic Resonance - See 10,722

10,727 SUPERPOSITION OF ANTIFERROMAGNETISM AND SUPERPARAMAGNETISM IN A VERY SMALL CRYSTAL [in

French] by L. Néel (Inst. Fourier, Grenoble); Comptes Rendus, Vol. 253, pp. 9-12, July 3, 1961

The mean magnetic moment, M, of a very small antiferromagnetic crystal having a permanent magnetic moment which is placed in a magnetic field is calculated. The case in which the variations of the coupling energy in the antiferromagnetic direction with respect to the crystal matrix are negligible in comparison with the thermal excitation energy is treated. M is assumed to be large compared to the Bohr magnetron, classical Boltzmann statistics are assumed, and the final result is simply obtained in terms of the error function $\Phi(x)$. Special cases considered include the case for which $S_{11} = 0$, the case for which the permanent magnetic moment of M is zero, and two asymptotic approximations, valid for very weak and very strong applied fields, respectively.

10,728 ANTIFERROMAGNETIC RESONANCE IN FeF_2 AT FAR-INFRARED FREQUENCIES by R. C. Ohlmann and M. Tinkham (U. California); Phys. Rev., Vol. 123, pp. 425-434, July 15, 1961

Antiferromagnetic resonance observed in single crystals of FeF_2 between 1.5° and 66°K (T_N = 78.4°K) in the far-infrared region is discussed. The resonance frequency at $T \approx 0$ was found to be $\tilde{\nu}(0) = 52.7 \pm 0.2$ cm^{-1}. Using the antiferromagnetic resonance relation derived by Kittel, Nagamiya, Keffer, and others, and the experimental value for the static susceptibility, the uniaxial anisotropy constant at absolute zero, K(0), was inferred to be 1.1×10^8 ergs/cm^3 (40 cm^{-1}/atom). Measurements of the splitting of the line caused by an external magnetic field gave $g_{11} = 2.25 \pm 0.05$. The anisotropy energy in FeF_2, being primarily due to the crystalline field-spin-orbit interaction, may be described by a term $\Sigma_i DS_{zi}^2$ in the Hamiltonian. By including this interaction in the molecular-field treatment it has been found that $D = -9 \pm 2$ cm^{-1}, and the temperature dependences of the sublattice magnetization, the anisotropy constant, the resonance frequency, and the line width have been calculated. The last two were compared with the experimental results and found to be in reasonable agreement. The linewidths were found to follow a T^4 law above 15°K. The search over a frequency region of 13-70 cm^{-1} for the absorption lines expected in the paramagnetic region was unsuccessful, possibly indicating a relaxation time of less than 10^{-12} sec.

10,729 DIFFERENTIAL PARAMAGNETIC EFFECT IN SUPERCONDUCTORS by R. A. Hein and R. L. Falge, Jr. (U.S. Naval Res. Lab.); Phys. Rev., Vol. 123, pp. 407-415, July 15, 1961

The magnetic moment and the differential magnetic susceptibility of two spherical samples of tin and tantalum as a function of magnetic field and temperature are discussed. The differential paramagnetic effect (DPE) is observed in both ac and dc mutual inductance measurements provided the sample exhibits a good Meissner effect. For a superconducting sample in which the infinite conductivity behavior dominates the Meissner effect, the DPE does not appear in the ac measurements but does, under certain conditions, show up in dc measurements. The results of the dc mutual inductance measurements are used to classify the DPE as reproducible or nonreproducible. The former is characteristic of ideal Meissner-type superconductors while the latter is more characteristic of superconductors whose macroscopic magnetic properties are dominated by the classical infinite electrical conductivity behavior. The superconducting-to-normal transitions obtained by the three techniques are compared and the data discussed in view of (a) occurrence of the DPE; (b) magnitude of the DPE; (c) ability of these data to give information about the volume participation of the sample; and (d) relation of the "characteristic magnetic fields" determined by these transitions and the bulk critical field of the sample.

Parametric Susceptibility in Y-Rare Earth Compounds - See 10,716

10,730 STIMULATED SPIN-ECHO MEASUREMENT OF CROSS-RELAXATION IN NEUTRON-IRRADIATED CALCITE by L. K. Wanlass and J. Wakabayashi (U. California); Phys. Rev. Lett. Vol. 6, pp. 271-273(L), March 15, 1961

Measurements of the cross-relaxation decay curve of stimulated spin-echoes in radiation-damaged calcite are discussed. The stimulated echoes at a frequency of 8807 Mc are a paramagnetic analog of those obtained at nuclear frequencies by Hahn. The first echo, the eight ball echo, relaxed in a time characterized by the spin-spin relaxation time of about 18 μsec at 1.5°K. The stimulated echo (due to storage parallel to the Z axis) following the recollection pulse decayed with a time constant of 600 μsec, nearly 8000 times faster than predicted by the spin-lattice relaxation time of 5 ± 2 sec. This rapid relaxation is undoubtedly due to cross-relaxation since the calcite spectrum consists of three spectral lines with a separation of about three gauss when equally spaced.

Temperature Dependence of NMR in Ferroelectric Compounds - See 10,733

Effects of Crystal Phase Transitions on NMR - See 10,733

Paramagnetic Resonance Detection of Luminescent Centers and Traps in ZnS Phosphors - See 10,739

Color Center Paramagnetic Resonance in KCl - See 10,630

10,731 ULTRASONIC EXCITATION IN NUCLEAR MAGNETIC RESONANCE IN KI by A. H. Silver (Ford Motor); Bull. Am. Phys. Soc., Ser. II, Vol. 6, p. 234(A), Apr. 24, 1961

Changes which occur in the NMR absorption spectrum of I^{127} in KI as a function of acoustic excitation were discussed. The NMR line, observed at $\nu = 5$ Mc/sec with a Pound-Watkins type detector, is inhomogeneously broadened by strain. Longitudinal acoustic waves with $\nu_A = 10$ Mc/sec are generated by an X-cut quartz transducer and propagated along a [100] direction perpendicular to H_0. This distortion of the lattice induces $\Delta m = \pm 2$ quadrupolar transitions resulting in saturation of some of the five $\Delta m = \pm 1$ magnetic dipole transitions and in enhancement of others. Because the six levels are not all equally spaced, some of the spin-spin relaxation processes are attenuated. The nuclei do not assume a Boltzmann distribution in the presence of the acoustic excitation. The change in absorption at the center of the line is a function of the satellite distribution and is observed by varying $(\nu_A - 2\nu_0)$. For $\nu_A = 2\nu_0$, the absorption is reduced to 45 per cent of its equilibrium value in the sample studied. The effects of shear waves and of mechanical resonance were also discussed.

10,732 NUCLEAR RESONANCES IN TaC AND NbC by L. H. Bennett (NBS); Bull. Am. Phys. Soc., Ser. II, Vol. 6, p. 233 (A), Apr. 24, 1961

Measurements of the nuclear magnetic resonance of Ta^{181} in

TaC powder and Nb^{93} in NbC powder at room temperature were discussed. Each shows a small (about 0.1 per cent) diamagnetic shift. Since both TaC and NbC are metallic conductors at room temperature, and NbC is considered a superconductor at helium temperatures, these negative Knight shifts are unusual. Diamagnetic shifts previously observed in alloys (or intermetallic compounds) containing transition metals concern the nontransition element only. The transition element, vanadium, displayed paramagnetic shifts of the same order of magnitude as the Knight shift in metallic vanadium. The resonance results on the carbides were discussed with relation to other physical properties of these materials and the problem of sample characterization was considered.

10,733 NUCLEAR MAGNETIC RESONANCE IN $(NH_4)_2(BeF_4)_x(SO_4)_{1-x}$ AND OTHER FERROELECTRIC SYSTEMS by G. Burns (IBM); Phys. Rev., Vol. 123, pp. 64-66, July 1, 1961

The temperature dependence of fluorine and proton nuclear magnetic resonance (NMR) in polycrystalline samples of the solid solution $(NH_4)_2(BeF_4)_x(SO_4)_{1-x}$ measured for several x is discussed. This solid solution is ferroelectric for high and low x and is paraelectric in between. A sharp transition in the second moment of the F^{19} resonance was observed but found to be independent of x, while the ferroelectric properties are dependent on x. The proton NMR showed the nonequivalence of the NH_4 groups, but again the temperature dependence could not be correlated with the ferroelectric properties. Thus, the ferroelectric behavior of this system cannot be associated with the appealing hypothesis of the freezing in the vibrating NH_4 or BeF_4 groups. The temperature dependence of the proton NMR was also observed in the ferroelectric compounds $(NH_4)_2Cd_2(SO_4)_3$ and NH_4HSO_4. Similar conclusions can be drawn from these measurements as those given above. In some of the alums, the crystallographic phase transition is again not accompanied by any change in the proton resonance line. However, in N_2H_5Al alum and NH_3OHAl alum, there is a very abrupt change in the NMR line at the temperature of the phase transition.

OPTICAL PROPERTIES

Absorption Spectra of ZnS-Cu - See 10,741

Absorption Coefficients of Ge and CdTe - See 10,746

Four Specimen Liquid Helium Cryostat for Measuring Absorption Spectra - See 10,740

Orientation Polarization of Absorption in Cu_2O - See 10,747

Impurity Absorption in NaCl, KCl, and KBr - See 10,738

Energy of Longitudinal Optical Phonons in InSb - See 10,743

10,734 THE COMPLEX NATURE OF THE F-BAND IN KCl CRYSTALS by N. G. Politov (Acad. Sci. USSR); Optics and Spectrosc., Vol. 10, pp. 87-89, Feb. 1961

Experimental data indicating the complex nature of absorption and phosphorescence excitation spectra in colored KCl crystals and 520 mμ are superposed on the "pure" F-band $\lambda_m \cong 560$ mμ. These bands were observed at low F-band intensities, since they are masked when the F-band is strong.

Absorption by Color Centers in KCl - See 10,630

10,735 ULTRAVIOLET ABSORPTION SPECTRA IN RUBY by A. Linz, Jr. and R. E. Newnham (MIT); Phys. Rev., Vol. 123, pp. 500-501, July 15, 1961

The optical properties of highly doped rubies are discussed. Al_2O_3 and Cr_2O_3 form a complete solid-solution series; single crystals containing up to 5 mole per cent chromia were grown by the Verneuil technique. The optical absorption of a group of ultraviolet crystal-field bands near 3400 A was studied as a function of temperature, crystal orientation, and chemical composition. The intensity of these absorption bands varies with the square of the Cr concentration, perhaps indicating strong chromium-pair interactions.

10,736 CONTRIBUTION OF LATTICE SCATTERING BETWEEN NONEQUIVALENT VALLEYS TO FREE-CARRIER INFRARED ABSORPTION IN SEMICONDUCTORS by H. Risken (Deutsche Philips) and H. J. G. Meyer (Philips Res. Labs.); Phys. Rev., Vol. 123, pp. 416-418, July 15, 1961

The contribution of scattering between nonequivalent valleys of the conduction band to the absorption of infrared radiation by free carriers is discussed. The absorption induced by this scattering process results in a transfer of the electrons from the <111> valleys to the <100> valleys of the [000] valley. A quantum mechanical calculation has been made of the partial absorption constant μ_i^* due to this scattering on the basis of a deformation-potential type theory. The final formula obtained for μ_i^* is similar to that derived previously for the partial absorption constant μ^{opt} due to optical intravalley scattering. The physical significance of some limiting forms of μ_i^* at low temperatures is discussed.

Infrared Absorption of Titanates Having TaO Additive - See 10,661

10,737 ABSORPTION SPECTRUM OF PHOTOCHEMICALLY COLORED SILVER HALIDES by F. Moser (Eastman Kodak); J. Opt. Soc. Am., Vol. 51, pp. 603-608, June 1961

The work of E. A. Kirillov and co-workers reporting the existence of a pronounced fine structure in the absorption spectrum of weakly colored emulsion layers and a variety of other silver-containing systems is reviewed. These authors conclude that the fine structure is characteristic of small aggregates of silver. Attempts to observe this fine structure in the spectrum of exposed Lippmann emulsions and in silver hydrosols are summarized. No structure has been observed. These results indicate that the absorption spectrum of small aggregates of silver does not necessarily exhibit the general features reported by Kirillov.

10,738 OPTICAL ABSORPTION AND FLUORESCENCE OF OXYGEN IN ALKALI HALIDE CRYSTALS by J. Rolfe, F. R. Lipsett, and W. J. King (Natl. Res. Council, Ottawa); Phys. Rev., Vol. 123, pp. 447-454, July 15, 1961

The optical absorption, fluorescence excitation, and fluorescence emission spectra of single crystals of NaCl, KCl, and KBr grown from the melt in an oxygen atmosphere measured at 300°, 77°, and 4.2°K are discussed. The weak absorption band caused by oxygen was the same in all three crystals, and did not vary with temperature. The band had maximum absorption at 5.0 ev and a half-width of 1.0 ev. All fluorescence excitation spectra contained a component identical to this absorption band. The fluorescence emission spectra consisted of a series of peaks in the wavelength range 4000 - 10,000 A, with an approximately equal energy separation of 1000 cm^{-1}. At 300°K, 12 to 15 peaks were resolved, and at 4.2°K each of these peaks split into 4 to 6 components. From these optical results and from paramagnetic resonance experiments, it is concluded that O_2-molecule-ions located in anion sites in the crystal are responsible for the absorption and fluorescence.

10,739 PARAMAGNETIC RESONANCE DETECTION OF LUMINESCENT CENTERS AND TRAPS IN SELF-ACTIVATED ZnS PHOSPHORS by P. H. Kasai and Y. Otomo (Hitachi Cent. Res. Lab.); Phys. Rev. Lett., Vol. 7, pp. 17-18(L), July 1, 1961

The paramagnetic resonance observed in zinc sulfide phosphors prepared in a flux of NaCl or NaBr on irradiation with 3650 A ultraviolet light at 77°K is discussed. The observed resonance confirms a model similar to that proposed by Prener and Williams in which the centers in question are Zn^{++} ion vacancies with one of their charge compensating ions (Cl^-, Br^-, I^-, Al^{+++}, or Ga^{+++}) associated at the nearest possible lattice sites. Two resonance peaks were observed, one of which was symmetric (associated with un-ionized donors) and the other showing an anisotropic g value. The width of the latter peak is dependent upon the magnetic moment of the appropriate halogen species.

10,740 FOUR-SPECIMEN LIQUID HELIUM CRYOSTAT FOR FLUORESCENCE by F. R. Lipsett (Natl. Res. Counc., Ottawa); Rev. Sci. Instr., Vol. 32, pp. 840-841, July 1961

A cryostat in which the fluorescence spectra of four solid specimens may be obtained by rotating each specimen in turn into focus by means of a tube operated externally is described. Although designed primarily for obtaining fluorescence spectra in "reflection," the cryostat may also be used to obtain such spectra in "transmission" or for the measurement of conventional absorption spectra. Helium is used as a transfer gas and the temperature is determined by a Bourdon pressure gauge used as a gas thermometer. The level of liquid helium in the reservoir is determined with the help of carbon resistors. The specimens are mounted on a small cage which may easily be removed from the cryostat and sealed back into place with an indium gasket. The cryostat is made of metal and is easily demountable.

Phosphorescence Excitation Spectra in Colored KCl Crystals - See 10,734

10,741 A COMPARATIVE STUDY OF INFRARED LUMINESCENCE AND SOME OTHER OPTICAL AND ELECTRICAL PROPERTIES OF ZnS:Cu SINGLE CRYSTALS by I. Broser and H. -J. Schulz (Fritz-Haber Inst., Berlin); J. Electrochem. Soc., Vol. 108, pp. 545-548, June 1961

The optical transitions which produce infrared luminescence in ZnS-Cu are discussed. Many optical and electrical properties, such as emission spectra of the infrared and visible luminescence, excitation and quenching spectra of luminescence and photoconductivity as well as optical absorption spectra, have been investigated on the same single crystal within the temperature range between 4° and 300°K. Most of the experimental results are explained in terms of a relatively simple energy band scheme which differs in some respects from those published during the last few years.

10,742 FLASHLIKE RISE OF LUMINESCENCE II. ZnS-Co AND ZnS-Ag, Co PHOSPHORS by N. A. Tolstoi, A. A. Anufriev, P. G. Deineka, L. A. Rusinov, V. A. Sokolov, and A. A. Spartakov (Acad. Sci. USSR); Optics and Spectrosc., Vol. 10, pp. 90-92, Feb. 1961

The properties and rules of the flashlike rise of luminescence of cobalt-activated and silver, cobalt-activated zinc sulfide phosphors are described. The nature of the phenomenon is shown to be connected specifically with the kind of activator present.

10,743 OSCILLATORY PHOTOCONDUCTIVITY IN InSb by W. Engeler, H. Levenstein, and C. Stannard, Jr. (Syracuse U.); Phys. Rev. Lett., Vol. 7, pp. 62-63(L), July 15, 1961

Photoconductive spectral response measured in samples of InSb doped with Ag, Au, and Cu are discussed. All spectra showed an oscillatory phenomenon whose energy minima versus the number of minima gave straight lines of slope 0.0244 ev. These slopes are interpreted as the energy of the longitudinal optical phonon emitted on excitation of a hole from the impurity state to the valence band corresponding to successive thresholds. This value is found to be in good agreement with the value obtained by Hall, Racette, and Ehrenreich of 0.024 ev from tunneling experiments.

10,744 NOTES ON CUMULATIVE PHOTOVOLTAGES by J. A. Swanson (IBM); IBM J. Res. Dev., Vol. 5, pp. 210-217, July 1961

The large photovoltages observed by Cheroff and Keller in ZnS crystals are discussed. These photovoltages are theoretically plausible and can result from a wide class of different mechanisms. Conversely, the conditions under which a photoconductor with periodic inhomogeneities does not show a cumulative photovoltage are shown to be very restrictive and improbable. General theorems concerning the magnitude of the photovoltage are proved and remarks on its directionality are made.

10,745 HIGH-VOLTAGE PHOTOSENSITIVE THIN FILMS (Air Information Div.); U.S. Gov. Res. Rep., Vol. 36, p. 116(A), July 5, 1961 AD 255 795

Photosensitive CdTe films with photoelectromotive forces as high as 150 to 180 v/cm obtained by alloying components and/or by introducing an arsenic impurity are discussed. The dependence of the magnitude of the output voltage in films

on such process factors as film thicknesses and base temperatures was investigated. Optimum results were obtained in film thicknesses of the order of 1.5 microns. In addition to CdTe films, studies were made of binary and ternary chalcogenides of Sb and Be. With these materials it was also possible to obtain high-voltage output considerably exceeding the width of the forbidden zone. It was found that high-voltage output depends on high resistivity.

Temperature Dependence of Yield of Bi-Cs Photosurfaces - See 10,708

PEM Effect Solar Energy Converter - See 10,784

Antireflection Coatings for Si, Ge, InAs, InSb - See 10,785

Methods of Reducing Reflection Loss in Si Photocells - See 10,783

10,746 DETERMINATION OF THE OPTICAL CONSTANTS OF Ge AND CdTe BY THE REFLECTION METHOD by N. K. Kiseleva and N. N. Pribytkova (Acad. Sci. USSR); Optics and Spectrosc., Vol. 10, pp. 133-134(L), Feb. 1961

The optical constants of Ge and CdTe determined by a reflection method are discussed. Liquids of known refractive index were used at the interface of the sample to be measured and a suitable standard was used as reference. From these measured data the variation of absorption coefficient, κ, and refractive index, n, as a function of wavelength in the range 300 to 800 mμ, were obtained.

Diffraction Studies on 3d Electron Distribution in bcc Metals - See 10,669

10,747 POLARIZATION IN THE ABSORPTION SPECTRUM OF CUBIC CUPROUS OXIDE by I. S. Gorban' and V. B. Timofeev (Lenin State U., Kiev); Soviet Phys.-Solid State, Vol. 2, pp. 1863-1864, Mar. 1961

Polarization of a line related to the yellow hydrogen-simulated series in cubic cuprous oxide is discussed. Quantitative measurements of the absorption of polarized light whose oscillations are oriented parallel to the (110) plane, as well as in successive displacements of 10° from that plane, are plotted. Polarization of at least 90 per cent is indicated by comparing the light intensity (maximum) for absorption parallel to (110) with the intensity (minimum) for absorption perpendicular to (110). Polarization of the line was observed both in single crystal and polycrystalline samples, but not in very fine crystalline specimens.

Optical Properties of InAs-In_2Te_3 Alloys - See 10,671

THERMAL PROPERTIES

10,748 SPECIFIC HEATS OF DELTA-PHASE Zr-H AND Zr-D by W. J. Tomasch (Atomics Intl.); Phys. Rev., Vol. 123, pp. 510-514, July 15, 1961

The specific heats of fcc $ZrH_{1.58}$ and $ZrD_{1.58}$ measured in the temperature interval 30° - 500°C are discussed. The data are interpreted in terms of a harmonic oscillator model for the H and D specific heat contributions. This model is in accord with recent inelastic neutron scattering studies and predicts an isotopic depression of the deuteride Einstein temperature by a factor of $1/\sqrt{2}$ relative to the hydride value. Over the interval 30° - 200°C, the data and model are quantitatively consistent. At higher temperatures, the deuteride specific heat is somewhat smaller than anticipated. Quantities of noncubic γ-phase material are known to be present in the samples used, particularly in the deuteride, and this is thought to be a likely cause for the deviations. The hydride Einstein temperature calculated from the difference between deuteride and hydride specific heats at 150°C is 1500 ± 300°K, as compared with the inelastic neutron scattering value of 1500 ± 60°K.

Specific Heat and Entropy of Na in Equation of State Derivation - See 10,621

Specific Heat of Bi_2Te_3 - See 10,618

10,749 A PRELIMINARY DIGITAL COMPUTER PROGRAM (FORTRAN) FOR THREE-DIMENSIONAL HEAT CONDUCTION by W. M. Burley, Jr. (Naval Ord. Lab.); U.S. Gov. Res. Rep., Vol. 36, p. 115(A), July 5, 1961 AD 255 722

A FORTRAN coded program developed to calculate temperature distributions due to transient or steady-state conduction heat transfer in one, two, or three-dimensional systems is discussed. Calculations in the program are based on a finite difference solution of the conduction equation in cylindrical coordinates. The system may be made of a group of different materials and may have distributed sources of heat. Applicability of a given problem to the program depends primarily on the boundary conditions available in the program. The program is written to provide for a choice of surface temperature or surface conductance for the boundary condition on the cylindrical surface when the conductance subroutine is included.

Thermoelectric Power of Single Crystal Te - See 10,664

Thermoelectric Power of InAs-In_2Te_3 Alloys - See 10,671

10,750 THERMAL EXPANSION OF ALKALI HALIDES AND THEIR SOLID SOLUTIONS by H. A. McKinstry and W. R. Buessem (Penn. State U.); Am. Ceram. Soc. Bull., Vol. 40, p. 195(A), Apr. 1961

The thermal expansion coefficients of LiF, NaCl, KCl, KBr, RbCl, and RbBr determined by an x-ray diffraction method in the temperature region from room temperature to approximately 500°C are discussed. The temperature dependence of the thermal expansion coefficient was found to be more compatible with other physical properties (specific heat and compressibility) when compared with previous measurements, using the Grueneisen equation of state. The four solid solutions studied showed a nonlinear variation of the thermal expansion coefficient with composition.

10,751 PROPOSED METHOD OF MEASURING THERMAL DIFFUSIVITY AT HIGH TEMPERATURES by R. D. Cowan (U.

California, Los Alamos); J. Appl. Phys., Vol. 32, pp. 1363-1370, July 1961

A method for determining the thermal diffusivity, α, of a thin solid plate, mounted in a vacuum and heated to incandescence by means of a high-energy electron beam impinging on one face of the plate, or heated by thermal radiation from an arc-imagining furnace, is discussed. The beam energy is modulated by either a square wave or a sine wave, and the resulting temperature modulation of the faces is observed photoelectrically. A theoretical study is made of the possibility of deducing the thermal diffusivity of the solid from amplitude and/or phase measurements. The most practical method seems to be that which involves sine wave modulation, and measurement of the phase difference between the temperatures of the two faces of the plate. With a plate thickness of about 1 mm and frequencies of the order of 0.01 - 300 cps (depending on the value of α), it should be possible to measure thermal diffusivities, especially of the poorer conductors (α less than about 0.1 cm^2/sec), for temperatures from 1000°K or less to the point where sublimation becomes troublesome.

MECHANICAL PROPERTIES

10,752 ELECTRONIC EFFECT IN THE ELASTIC CONSTANTS OF GERMANIUM by L. J. Bruner and R. W. Keyes (IBM); Phys. Rev. Lett., Vol. 7, pp. 55-56(L), July 15, 1961

The elastic constants for two samples of germanium, one pure and the other heavily doped with arsenic, measured by an ultrasonic pulse technique, are discussed. The pure sample contained less than 10^{14} carriers/cm^3 whereas the heavily doped sample contained 3.5×10^{19} arsenic donors/cm^3. Only C_{44} changed by a significant amount, becoming some 5.5 per cent smaller for the heavily doped specimen. It is concluded that the change in elastic constants results from the addition of electrons to the conduction band.

Changes in Elastic Modulus of Plastically Deformed Rock Salt - See 10,635

10,753 ULTRASONIC ATTENUATION IN MAGNETITE AT LOW TEMPERATURES by K. Kamigaki (Tohoku U.); J. Phys. Soc. Japan, Vol. 16, pp. 1170-1174, June 1961

The ultrasonic attenuation coefficients in magnetite crystals measured over the temperature range 4.2° - 300°K are discussed. Two kinds of attenuation peaks were observed below the transformation temperature of ionic ordering. The attenuation is attributable to the relaxed electron diffusion between Fe^{2+} and Fe^{3+} ions on the octahedral sites in the ordered lattice of magnetite. The electron diffusion processes are classified into the single electron process and the coupled transition. The activation energy of the former process is determined to be 0.055 ev and the latter 0.36 ev.

Changes in Damping of Plastically Deformed Rock Salt - See 10,635

10,754 A THEORY OF ABSORPTION OF SOUND IN UNIAXIAL FERROMAGNETIC DIELECTRICS by M. I. Kaganov and Ya. M. Chikvashvili (Tbilisi State U., Kharkov); Soviet Phys.-Solid State, Vol. 3, pp. 200-204, July 1961

The theory of spin waves is used to calculate the temperature and frequency dependences of the absorption coefficient of sound in a ferromagnetic dielectric (a ferrite) at temperatures far below the Curie point.

SOLID STATE DEVICES

DIODES

10,755 DEVELOPMENT OF PRODUCTION PROCESSES AND TECHNIQUES FOR HIGH VOLTAGE SILICON RECTIFIERS by W. D. Bryan (Texas Instr.); U.S. Gov. Res. Rep., Vol. 36, p. 38(A), July 5, 1961 AD 255 750

High-voltage silicon rectifiers in the 20,000, 30,000 and 60,000 P.I.V. range for use as clipper diodes in ground and airborne electronic applications are described. Successful operation of the rectifiers at extremely high voltages was made possible by resolution of the problems associated with avalanche breakdown, junction forming by diffusion, arcing, stacking of basic cells and packaging. Solution to the problem of arcing under evacuated conditions and packaging contributed most to the success of the program. Test samples furnished to a contractor for application in a fire control system were satisfactory under all conditions.

10,756 SELENIUM RECTIFIER by G. Eannarino and R. Parsons (Sarkes Tarzian); U.S. Pat. 2,841,749, Issued July 1, 1958

The formation of the barrier layer between the selenium and the counter electrode by the use of certain organic amines and certain inorganic and organic acids is discussed. Several examples of solutions which produce desirable selenium rectifiers are included. Resulting rectifiers display longer operating life, and are stable against high humidity, high temperature and high voltages.

Germanium Varactor Diodes - See 10,908

Point Contact Varactor Diodes - See 10,762

Negative Resistance Oscillation Modes of Tunnel Diodes - See 10,843

10,757 GALLIUM ANTIMONIDE ESAKI DIODES FOR HIGH-FREQUENCY APPLICATIONS by C. A. Burrus (Bell Labs.); Proc. IRE, Vol. 49, p. 1101(L), June 1961

Esaki diodes capable of operation into the millimeter wave region, made from both p- and n-type GaSb are discussed. The p-type diode with a resistivity of about 0.0011 Ω-cm, exhibited a peak current at 0.07-0.09 v with the valley at 0.2-0.3 v. Peak-to-valley ratios were commonly 6:1 to 12:1 but frequently exceeding 15:1. Current densities in excess of 50,000 a/cm^2 are reported. Fundamental oscillations to frequencies of 50 kMc were observed. N-type GaSb diodes doped with tellurium or selenium showed considerably lower peak-to-valley ratios. Their somewhat higher peak currents produced fundamental oscillation frequencies to 62.5 kMc.

10,758 GALLIUM ARSENIDE ESAKI DIODES FOR HIGH-FREQUENCY APPLICATIONS by C. A. Burrus (Bell Labs.); J. Appl. Phys., Vol. 32, pp. 1031-1036, June 1961

Esaki diodes which show promise of usefulness into the millimeter-wave region fabricated from both p- and n-type gallium arsenide are described. Both diodes were alloyed junctions having point contact geometry and dimensions. The fabrication of these diodes is briefly described, and their initial performance as oscillators in mechanically simple circuits is discussed. Fundamental oscillations to 103 kMc have been obtained.

10,759 HIGH-FREQUENCY POWER IN TUNNEL DIODES by G. Dermit (Genl. Tel. Electronics Labs.); Proc. IRE, Vol. 49, pp. 1033-1042, June 1961

An expression for HF tunnel diode power employing a simple dissipative load and for signals confined within the nearly linear range of the diode negative resistance is discussed. The existence of maximum power output for a given frequency of operation, and for an optimum peak current-to-capacitance ratio is demonstrated. The power and the inductance appear in the equations as a product, and consequently, the higher-power output diodes require the lower inductances. The results are plotted for germanium as well as for gallium arsenide in the form of charts with the ratio of peak current-to-capacity and the operating frequency as coordinates. These charts present two families of curves which cross each other, one referring to constant products of power times inductance and the other referring to constant products of capacity times inductance. The presented data cover a wide operational range of tunnel diodes. For a diode oscillating at 10 kMc and having a resistive cut-off frequency of 30 kMc, the maximum power-inductance product is 0.0224 (mw)(mμh) for a voltage swing of 0.15 v in the nearly linear range.

10,760 THE EQUIVALENT NOISE CURRENT OF ESAKI DIODES by R. A. Pucel (Raytheon); Proc. IRE, Vol. 49, pp. 1080-1081 (L), June 1961

A theoretical analysis of the noise performance of Esaki semiconductor diodes used in amplifiers and mixers derived from the voltage-dependence of the net (measured) tunnel current is discussed. Measurement involves practical difficulties, although measurement is possible by shot-noise techniques. Quite general considerations give expressions so that each tunnel component, and hence the sum of these components, can be calculated simply in terms of tunnel diode current for the voltage range excluding the "excess" current region. The results apply equally well for "reverse" or forward bias voltages and encompasses most of the negative differential conductance region of the I-V characteristic. Direct and indirect tunneling in semiconductors, and tunneling between normal and superconducting metals separated by an insulating film are also described.

Fabrication of Tunnel Diode Arrays - See 10,776

10,761 ELECTRON BOMBARDMENT DAMAGE IN SILICON ESAKI DIODES by R. A. Logan, W. M. Augustyniak, and J. F. Gilbert (Bell Labs.); J. Appl. Phys., Vol. 32, pp. 1201-1205, July 1961

The density and distribution of states introduced into the forbidden gap by electron bombardment are discussed. The excess current in silicon Esaki diodes has been shown to be a sensitive indicator of these states. Both the effects of bombardment and the annealing properties of the radiation damage have been found to depend upon the specific donor in the n-type region of the diode. The average bombardment dose of 1-Mev electron/cm^2 needed to increase the excess current density by 1 amp/cm^2 at a bias of 0.3 v is 1.2×10^{16} for P-doped diodes and 0.8×10^{16} for Sb- or As-doped diodes. Upon annealing in an inert atmosphere, at temperatures in the range 300° - 400°C, the bombardment diode is restored to its original characteristics. While the annealing studies reveal novel interactions, they show considerable similarity with other work where the radiation damage was monitored by carrier lifetime or conductivity measurements. Structures observed in the I-V characteristics during the annealing indicate that the bombardment-induced levels at $E_V + 0.27$ and $E_V + 0.06$ are due to pairing of a primary defect (probably a vacancy) with an arsenic and a phosphorus impurity atom, respectively.

10,762 HIGH-FREQUENCY SILICON VARACTOR DIODES by C. A. Burrus (Bell Labs.); J. Appl. Phys., Vol. 32, pp. 1166-1167(L), June 1961

By reducing the zero bias junction capacitance of silicon varactor diodes, the high frequency limit up to which these diodes are useful has been extended. A point contact of suitable group III or V doping elements can be electroplated or evaporated onto electrolytically pointed wires. These wires, usually 1-2 mils in diameter, may then be formed into the usual "s" shaped contacts. Electrically forming the contact to the appropriately etched surface can be done by discharging a current pulse from a 0.01-0.1 μf capacitor charged at 6-10 v. Zero bias junction capacitance from less than 0.02 μμf to over 0.3 μμf have been obtained by this technique. Both p- and n-type silicon diodes have been made which provide broad band gain and oscillation to 30 kMc in parametric amplifier circuits.

10,763 SOME EXPERIMENTS USING A VACUUM-CLEANED SILICON P-N JUNCTION by J. T. Law (Bell Labs.); J. Appl. Phys., Vol. 32, pp. 848-855, May 1961

Measurements of the junction characteristics and the transport properties on either side of a vacuum-cleaned silicon p-n

junction are presented. The changes in these properties during the adsorption of oxygen and hydrogen have also been investigated. In the clean condition, the value of $(E_F - E_V)$ for both 21.5 ohm-cm n-type and 27 ohm-cm p-type was found to be 0.13-0.14ev. When the silicon surface was clean, a large excess current across the junction was observed which disappeared during the adsorption of gas.

Avalanche Breakdown in Silicon Rectifiers - See 10,755

Diffused Junction Silicon Rectifier - See 10,755

Al Diffusion of Junctions in SiC - See 10,775

10,764 MICROMINIATURE SEMICONDUCTOR DEVICES by C. E. Maiden and E. E. Maiden (Pacific Semicon.); U. S. Pat. 3,002,133, Issued Sept. 26, 1961

Microminiature packages for semiconductor diodes are described. Ohmic contacts are soldered to both regions of the diode. For example, gold plated nickel leads can be attached by heating under a pressure of 800 to 1000 psi at about 450°C. Flat ribbon-shaped electrodes which cover essentially the whole semiconductor surface are used. The electrodes extend in opposite directions from the two surfaces. A thin protective film is formed on the exposed semiconductor regions and the device is encapsulated by coating it with either an epoxy resin, a polysiloxane, glass, or ceramic. The resultant device is only slightly larger than the diode itself.

Package for High Temperature Rectifier - See 10,909

High Voltage Rectifier Packaging - See 10,755

TRANSISTORS

Fabrication of 108 Mc Transistor - See 10,771

Triple Diffused, High Power Silicon Transistor - See 10,772

10,765 PROFILES IN FAILURE RATE VS APPLICATIONS by R. E. Pratt (Raytheon); Solid State J., Vol. 2, pp. 30-35, Aug. 1961

Failure rate profiles used by design engineers to obtain optimum circuit design by trading off end-of-life points and operating conditions to meet stated reliability requirements are discussed. Methods of providing these profiles are described and a typical application of the technique is given.

10,766 A LOSS AND PHASE SET FOR MEASURING TRANSISTOR PARAMETERS AND TWO-PORT NETWORKS BETWEEN 5 AND 250 MC by D. Leed, and O. Kummer (Bell Labs.); Bell Sys. Tech. J., Vol. 40, pp. 841-884, May 1961

An insertion loss and phase measuring set, developed for making small-signal measurements on transistors and general two-port networks with maximum inaccuracy of 0.1 db and 0.5 degree over a frequency range from 5 to 250 Mc is described. In order to realize accuracy substantially independent of test frequency, the measurement information is heterodyned to a fixed intermediate frequency, where detection is performed with the aid of adjustable loss and phase-shift standards. Use of a rapid sampling technique to compare the unknown with a high-frequency standard eliminates errors from circuit drifts and also reduces the magnitude of the "instrument-zero line" to a small value. Problems related to purity of terminations as seen from the unknown, automatic control of beat oscillator frequency, conversion, signal-to-noise, and design of loss and phase standards are also discussed. Particular attention is given to the features of the set which especially adapt it to the measurement of transistor parameters.

10,767 SWITCHING TIME FORMULAE FOR SINGLE DIFFUSED MESA TRANSISTORS by E. Severin (Texas Instr.); Semicon. Prod., Vol. 4, pp. 37-42, June 1961

Formulae necessary to calculate the four switching times (delay, rise, storage, and fall) from either data sheets or easily measurable steady state quantities are derived. Values calculated from these expressions should, with careful choice of parameters, be within 20 per cent of measured values for single-diffused mesa units. Some or all the formulae can be applied with some success to other type devices; the accuracies to be expected are included in the explanation of each derivation.

10,768 A NEW DYNAMIC RATING FOR THE EMITTER-BASE DIODE by J. A. Ekiss (Philco); Solid State J., Vol. 2, pp. 34-38, June 1961

The maximum rating of the base-emitter diode, considered as the reverse power dissipated in the diode rather than the breakdown voltage is discussed. A rating curve is derived whereby in switching circuits utilizing a speed-up capacitor, the emitter-base breakdown voltage may be exceeded on a transient basis. The design of RTL circuits is also affected by the rating philosophy presented here.

10,769 NOISE PERFORMANCE OF TRANSISTORS by D. G. Peterson (Lockheed Aircraft); U.S. Gov. Res. Rep., Vol. 36, p. S-35(A), July 5, 1961 PB 154 287

The accuracy with which the Beatie lumped model represents transistor noise performance is experimentally verified. The statistical properties of transistor noise are studied using a laboratory-constructed amplitude-probability density analyzer. The noise model consists of three statistically independent shot-noise generators connected across the lumped elements representing the generation-recombination and diffusion mechanisms of the transistor. In addition, a thermal-noise generator is used to represent the noise contributed by the base spreading resistance. By comparing measurements with calculations based on the model, not only is good over-all agreement obtained, but it becomes evident that certain bias and source conditions allow separate confirmation of the internally postulated noise generators.

10,770 SEMICONDUCTOR DEVICE WITH CONTROLLED ZONE THICKNESS by J. C. Marinace (IBM); U. S. Pat. 3,000,768, Issued Sept. 19, 1961

The production of closely spaced parallel junctions is described. A junction is formed on one surface of the wafer by a technique such as alloying or diffusion. The wafer is then immersed in an electrolytic etch after a mask is applied and a reverse bias is applied to the junction. The reverse bias is of such magnitude that a depletion region extends across the semiconductor to the desired location of the second junction. A depression is etched in the unmasked region of the surface opposite the junction. The etching is stopped when the depletion region is reached, which point is indicated by a sudden drop in current in the etch bath. The mask is removed and the second junction is formed by the epitaxial deposition of the properly doped semiconductor in the depression.

10,771 108-MC, 10-WATT SILICON TRANSISTORS by W. A. Bosenberg (RCA); U.S. Gov. Res. Rep., Vol. 35, p. 732(A), June 16, 1961 PB 154 479

The design and fabrication of a 108 Mc, 10 w, silicon transistor is discussed. N-p-ν-n configuration and comb-structure geometry are employed in the device and impurity distributions are shown. Fabrication involves the use of photolithographic, metalizing, and thermocompression bonding techniques. Silver is reported to be the most promising material for metalizing; new apparatus for bonding has been constructed and is described.

10,772 RESEARCH AND DEVELOPMENT OF HIGH-POWER SILICON TRANSISTORS (Pacific Semicon.); U.S. Gov. Res. Rep., Vol. 36, p. 30(A), July 5, 1961 AD 255 236

A survey of semiconductor devices which might be useful in power amplifiers is discussed. Conclusions reached are that the triode transistor is presently the best choice. The design theory for such power transistors is described. A survey of possible semiconductor materials is given, with the conclusion that silicon is by far the best choice. A process is described for fabrication of this family of very high power transistors. The basic structure in an n^+-p-n-n^+ triply-diffused silicon transistor with interdigitated (comb) emitter and base-contact layers produced photographically. A simple scaling principle is employed to make a variety of transistors with a wide range of current and power ratings. A description of tests and their results are given for 30 transistors of each type delivered to the Wright-Patterson Air Development Division. Manufacturing problems, particularly in the larger size transistors, are discussed.

Au Alloyed Contacts to Ge and Si - See 10,663

10,773 NOVEL HEADER OF SEMICONDUCTOR DEVICES by B. Cornelison, J. H. Eddleston, A. D. Evans, M. Shepherd, Jr., R. L. Trent, and E. A. Wolff, Jr. (Texas Instr.); U.S. Pat. 2,990,501, Issued June 27, 1961

A header capable of containing a semiconductor device which allows a space between the bottom of the header and its mounting surface to relieve the danger of solder bridging conductive parts when the assembly is being used with a printed circuit board is described. The header consists of a standard type header into which a "stand-off" peg of a grangible material (glass, ceramic, etc.) is fused into the insulating portion in a way that it projects outwardly normal to the bottom surface. An annular score mark near the point of attachment enables the peg to be easily broken when it is not needed as a spacer.

10,774 THE FIELD-EFFECT TETRODE by H. A. Stone, Jr. and R. M. Warner, Jr. (Bell Labs.); Proc. IRE, Vol. 49, pp. 1170-1183, July 1961

A new device consisting of a thin N region adjacent to a comparably thin P region is described. Two contacts are made on the N side and two to the P side so that currents can be passed through each thin region parallel to the single junction of the device. The two currents do not mix because reverse bias is maintained on the junction. A current in either side affects the resistance of the other side, and hence the current in the other side, through the medium of the depletion layer; this mutual interaction of currents gives the device its unique properties. The field-effect tetrode has applications as a gyrator and isolator. In a two-terminal connection it exhibits voltage-controlled negative resistance. Also, it can be applied as a truly linear, yet electronically variable, resistor. Equations are developed for its behavior in these applications and experimental results are discussed. In the models to data, the thin regions were shaped by rather tedious mechanical and chemical procedures. Epitaxial film techniques may be well adapted to its fabrication in the future.

10,775 STUDY, DEVELOPMENT AND APPLICATION OF TECHNIQUES NECESSARY TO FABRICATE ACTIVE SILICON CARBIDE DEVICES by H. -C. Chang, L. F. Wallace, and C. Z. LeMay (Westinghouse); U.S. Gov. Res. Rep., Vol. 36, p. S-81(A), July 5, 1961 PB 154 358

Fundamental techniques developed for the fabrication of SiC devices in general and unipolar field-effect transistors in particular are discussed. The diffusion of Al vapor in alpha-SiC was quantitatively investigated and the diffusion-junction process was developed. Hexagonal SiC was grown in the form of thin platelets which are ready for device fabrication. Device fabrication processes include the single- and double-gate fused junctions, single-gate grown junctions, and single- and double-gate diffused junctions. Only the double-gate diffused junction process produced unipolar transistors which exhibit power gain. These devices are still in a primitive stage of development and will require further development before they become practical. An experimental model of a SiC double-gate unipolar transistor was developed that exhibited ac power gain as high as 380 at room temperature and 7 at 500°C.

FUNCTIONAL UNITS

10,776 RESEARCH IN MICRO FLIP-FLOPS by T. V. Sikina (Philco); U.S. Gov. Res. Rep., Vol. 35, p. 731(A), June 16, 1961 PB 171 566

The feasibility of applying thin-film techniques to microminiature circuit plates or functional circuit blocks is described. Both active and passive elements are fabricated by solid-state techniques on a silicon substrate. The active component, or transistor, which is unilaterally constructed, is found fully compatible with the one-sided approach to microminiaturization. Excellent switching characteristics are achieved with this active device and further improvement in switching times should be attainable. GaAs tunnel diode arrays are highly reproducible for the peak current range of 10 to 20 ma. The best uniformity of characteristics and reproducibility of diodes is achieved by the "forced alloying" technique. Two methods are developed for achieving the desired peak and valley current. They are: (1) controlled electrolytic etching, and (2) temperature controlled re-alloying.

MAGNETOELECTRIC DEVICES

10,777 PROPERTIES OF HALL EFFECT MULTIPLIERS by S. P. Denker (MIT); Semicon. Prod., Vol. 4, pp. 32-34, June 1961

The properties of Hall effect multipliers such as geometry, terminal characteristics, power limitations and temperature variation of output voltage are discussed. Formulations for these various properties are derived.

Hall Effect Components in Solid State Synchros - See 10,900

Magnetoresistive Devices - See 10,809

CRYOGENIC DEVICES

10,778 THE SILICON CRYOSAR by H. Izumi (Nippon Tel. and Tel.); Proc. IRE, Vol. 49, pp. 1313-1314 (L), Aug. 1961

Silicon cryosars of uncompensated impurity Si crystals demonstrating negative resistance characteristics at 4.2°K are discussed. A wide range of Si wafer thickness and resistivities were investigated using Sb-doped Au alloyed n-type contacts and Al or Ga-doped Au contacts for p-type wafers. The dc voltage-current characteristics of the devices at 4.2°K show four distinct regions. Dynamic characteristics for the negative resistance region were obtained and switching times of 50 μsec with max-min voltage ratios of 7 are reported.

PHOTODEVICES

10,779 SEMICONDUCTORS by D. N. Nasledov [Translated from Russian by Aerospace Tech. Intelligence Ctr.]; U.S. Gov. Res. Rep., Vol. 36, p. 108 (A), July 5, 1961 AD 255 388

The use of semiconductors in infrared techniques, photoconductive materials, thermal radiation detection, photoresistors, heat seekers, infrared communications, germanium phototubes, infrared receivers, thermoelectrical triode cooling, photoresistor cooling, infrared optics, and infrared ray modulation is reviewed.

Cumulative Photovoltages in Photoconductors - See 10,744

High Voltage Photovoltaic Films - See 10,745

10,780 SPECTRAL RESPONSE OF SOLAR CELLS by B. Dale and F. P. Smith (Transitron); J. Appl. Phys., Vol. 32, pp. 1377-1381, July 1961

An analysis of the spectral response of a solar cell which includes the effect of the electric field present in the diffused surface region is given. Results are presented which show the variation of response with junction depth and with carrier lifetime in both surface and bulk regions. By curve fitting, it is found that in a typical silicon cell the bulk lifetime is in the range 1 - 15 μsec, while the surface region lifetime is between 10^{-9} and 10^{-10} sec. Bombardment with a total flux of 3.3×10^{14} electrons/cm^2 of 2-Mev electrons reduced the n region lifetime by a factor of 300, and the p region lifetime by a factor of 6 in a particular case.

10,781 HIGH-TEMPERATURE, IMPROVED-EFFICIENCY PHOTOVOLTAIC SOLAR ENERGY CONVERTER by J. J. Wysocki, J. J. Loferski, and P. Rappaport (David Sarnoff Res. Ctr.); U.S. Gov. Res. Rep., Vol. 35, p. 721 (A), June 16, 1961 PB 154 525

Current work describing attempts to achieve higher-efficiency GaAs solar cells by fabrication improvements is cited. Best results obtained were a 5 per cent overall conversion efficiency on cell 1/4 cm^2 in area. Surface erosion of GaAs is one cause of low efficiency. Diffusion of phosphorus and nickel did not lead to appreciable improvement. An analysis of the spectral response of a photovoltaic cell is presented with some experimental examples showing how it can be used to study the lifetime in a finished cell. Improvements in spectral response are described using post diffusion processing.

10,782 INVESTIGATION OF HIGH-TEMPERATURE PHOTOVOLTAIC SOLAR ENERGY CONVERTER by J. J. Wysocki, J. J. Loferski, and P. Rappaport (David Sarnoff Res. Ctr.); U.S. Gov. Res. Rep., Vol. 36, p. S-32 (A), July 5, 1961 PB 154 474

Temperature measurements on comparable efficiency GaAs and Si solar cells are cited. The results show that GaAs is generally superior above 150°C. Higher-efficiency silicon cells are superior at higher temperatures. Further analysis of contact and sheet resistance shows the former to be more serious, although both are capable of limiting cell output. Experimental results indicate contact and sheet resistance are negligible and that carrier lifetime is the limiting factor in present cells. Spectral response curves are shown to be a useful analytical tool in determining diffusion length of processed cells and on predicting limiting efficiencies. Results on InP cells are reported with best efficiency of 3 per cent obtained. Preliminary work on GaP shows V_{max} of 1.2 v, but no photo effect due to internal photo emission.

10,783 RESEARCH ON EFFICIENT PHOTOVOLTAIC SOLAR ENERGY CONVERTERS by B. Dale (Transitron); U.S. Gov. Res. Rep., Vol. 36, p. S-40 (A), July 5, 1961 PB 171 270

The performance of a variable energy gap solar cell compared with that of a single gap cell is described. It is found that no major advantage is offered by the variable gap cell, although small improvements could be obtained provided that the lifetimes could be maintained comparable with those in the single gap cell. Two methods of reducing the reflection loss from the surface of a solar cell are described. One uses the principle of destructive interference between light reflected from either

side of a quarter wavelength film of silicon monoxide. The other uses a specially shaped silicon surface which requires an incident beam to be reflected several times before escaping. Both methods reduce the reflectivity to a very low value.

10,784 HIGH-TEMPERATURE, IMPROVED-EFFICIENCY, PHOTOVOLTAIC SOLAR ENERGY CONVERTER by J. J. Wysocki, J. J. Loferski et al. (David Sarnoff Res. Ctr.); U. S. Gov. Res. Rep., Vol. 35, p. 721 (A), June 16, 1961 PB 154 526

A new type of zinc diffusion process for GaAs using an open furnace yielding cells having 5.2 per cent efficiency is discussed. This process is promising since present surface concentrations are a tenth of what they should be. Progress has been made on improved ohmic contacts. Spectral response curves show that lifetime is the limiting factor in the GaAs solar cells. The use of spectral response curves in determining lifetime is also discussed. Spectral response on n and p surface layer silicon cells are presented. An analysis of the PEM effect as a solar energy converter is presented showing it to be an inefficient conversion process with efficiencies of the order of 10 per cent. This has been verified experimentally.

10,785 INFRARED FILTERS OF ANTIREFLECTED Si, Ge, InAs, AND InSb by J. T. Cox, G. Hass and G. F. Jacobus (USAERDL); J. Opt. Soc. Am., Vol. 51, pp. 714-718, July 1961

Vacuum-deposited single-, double-, and triple-layer infrared antireflection coatings for Si, Ge, InAs, and InSb developed for the 1-μ to 15-μ region are discussed. MgF_2, didymium fluoride, SiO, ZnS, CeO_2, and Si were used for the preparation of the coatings. All of the coatings are hard and durable and can be cleaned and boiled in water for several hours with little or no damage. With these coatings, the transmittance of Si and Ge plates can be increased to a maximum value of nearly 100%, and stays above 90% over a wavelength interval the limits of which are in the ratio of 1.5:1, 27:1, and 3:1 for single-, double-, and triple-layer coatings, respectively. InAs and InSb are slightly absorbing, but more than 90% transmittance can be obtained with sufficiently thin antireflected plates. The temperature dependence of absorption in all four of these materials has been measured in the range from 25°C to 250°C.

THERMAL DEVICES

Thermoelectric Devices - See 10,779

10,786 NEW CONCEPTS IN THERMOELECTRIC DEVICE DESIGN by W. H. Clingman (Texas Inst.); Proc. IRE, Vol. 49, pp. 1155-1160, July 1961

An analysis of the effects of the thermal and electrical circuit on entropy production within a thermoelectric device is presented. The design problem is analyzed by comparing the relative contribution of various parts of the system to the total entropy production. This irreversible thermodynamic approach is illustrated with examples concerning several different design questions. Many qualitative conclusions are drawn.

10,787 OPTIMIZATION OF EMISSION LIMITED THERMIONIC GENERATORS by A. Schock (Republic Aviation); U.S. Gov. Res. Rep., Vol. 36, p. 35 (A), July 5, 1961 AD 255 550

Equations describing the performance of space charge neutralized thermionic converters with negligible transport effects are described. For a given anode work function and cathode temperature, optimization of the other system parameters leads to an expression for the maximum attainable conversion efficiency, in terms of the fundamental physical constants e, m, c, and k, (e and m, the charge and mass of an electron; k, Boltzmann's constant and c, the velocity of light). The calculated results, presented graphically, suggest several distinct modes of high efficiency operation, and lead to a number of interesting conclusions about converters with cesium coated cathodes.

10,788 THERMOELECTRIC AIR CONDITIONER FOR SUBMARINES by J. R. Andersen (RCA); RCA Rev., Vol. 22, pp. 292-304, June 1961

The design and experimental development of a thermoelectric air conditioner for submarines is discussed. The basic design concept is discussed in terms of performance, pressurization, sea-water corrosion, and simplicity. A working theory which expresses the performance of a "real" thermoelectric refrigeration machine leads to a discussion of the design parameters for such a machine. The results of design optimization studies are then displayed showing, specifically, the size of the machine and the weight of thermoelectric material required as a function of maximum coefficient of performance for a variety of thermopile configurations. The final design, based on these considerations, is presented and its expected performance is discussed. Experimental performance data obtained from a one-ton model, constructed according to this design, is discussed and compared with predicted performance, and some difficulties are mentioned. It is concluded that large-capacity, compact thermoelectric air conditioners for special applications are feasible.

10,789 USE OF $PrCl_3$ IN A SOLID STATE INFRARED QUANTUM COUNTER by J. F. Porter, Jr. (Johns Hopkins U.); J. Appl. Phys., Vol. 32, pp. 825-826, May 1961

Two suitable schemes for the production of an infrared quantum counter utilizing $PrCl_3$ are discussed. One is employed for detection at 2.33 μ and the second for detection at 104 μ. Consideration is given to isolation of the final detector from the pumping signal and a suitable experimental arrangement for unambiguously determining proper operation is shown.

10,790 GALLIUM-DOPED GERMANIUM RESISTANCE THERMOMETERS by F. J. Low (Texas Instr.); Program Cryogenic Engrg. Conf., p. 43 (A), Aug. 1961

Germanium resistance thermometers, designed to cover the temperature interval 1° to 40°K, were discussed. Two types were described, the RT104, hermetically sealed in glass and the RT104A, encapsulated but not sealed. At 2°K the thermal conductance between the sensing element and the surroundings is 1000 μw/°K for type RT104 and 25,000 μw/°K for type RT104A. Two electrical leads are used so that 2, 3, or 4 lead resistance bridges may be employed. Below 5°K the sensitivity T/R (dR/dT), is approximately 5, above 15°K it is about 3, with a gradual transition between 5° and 15°K. Repeated rapid immersion in liquid helium at the boiling point produces shifts in the temperature calibration no greater than 0.05%. A description was given of a simple procedure for accurately determining the reproducibility of resistance thermometers without the use of a highly stabilized bath. At 4.2°K the time constant of type

RT104A is < 0.05 sec. Both transverse and longitudinal magnetoresistance measurements at various temperatures were reported. The thermometer is non-magnetic except for a minute quantity of solder which becomes superconducting below 4.2°K. A calibration procedure accurate to 0.1% in temperature was devised which covers the range from 1° to 40°K.

10,791 GERMANIUM RESISTANCE THERMOMETRY by R. L. Powell, L. P. Caywood, Jr., and J. L. Harden (NBS); Program Cryogenic Engrg. Conf., p. 43 (A), Aug. 1961

Preliminary tests and calibrations for commercially available, encapsulated, germanium resistance thermometers were presented. The properties tested at liquid hydrogen and helium temperatures include reproducibility after both rapid and slow thermal cycling, resistance change caused by self-heating from measuring current, and drifting of resistance with time without intermediate thermal cycling. Complete resistance vs temperature calibrations are included for the liquid hydrogen and helium temperatures; preliminary results were also given for intermediate temperatures. The thermometers appear to be equally well suited for both engineering and instrumentation and high precision temperature scale research between 2° and 50°K.

FERRITE DEVICES

10,792 THEORY OF DIELECTRIC-LOADED AND TAPERED-FIELD FERRITE DEVICES by R. F. Soohoo (Lincoln Lab.); IRE Trans., Vol. MTT-9, pp. 220-224, May 1961

By means of combined boundary-value and perturbation-theory approach, a theoretical analysis of transverse-field ferrite device performance is developed. It is shown that dielectric-loading and tapered-field techniques increase the bandwidth of isolators and phase shifters, the isolation-to-insertion loss ratio of the former, and the phase shift of the latter.

Ferrite X-Band Isolator - See 10,910

10,793 OCTAVE-BANDWIDTH UHF/L-BAND CIRCULATOR by F. Arams, B. Kaplan, and B. Peyton (Cutler-Hammer); IRE Trans., Vol. MTT-9, pp. 212-216, May 1961

Test data on two aluminum-substituted yttrium-iron-garnet (YIG) materials that have low-saturation magnetizations that permit the extension of ferrite devices well into the UHF/VHF region are presented. One composition has a saturation magnetization of 300 gauss and a line width of 50 oe. Measurements are presented that compare the new materials with previously available higher-saturation magnetization materials. A broadband UHF/L-band four-port circulator that operates over a 2-to-1 frequency band has been developed, using this 300 gauss material. Insertion loss is 1 db or less from 665 to 1320 Mc (with constant magnetic field) and 0.5 db or less from 800 to 1150 Mc. A compact and favorable circulator package design was obtained by using coaxial hybrids and dielectric-loaded strip transmission line. Data on the broadband magic-tee used in the circulator are included. Isolator measurements down to 200 Mc are reported. Reverse-to-forward magnetic-loss ratios of 36 at 600 Mc and 12 at 300 Mc were obtained.

10,794 PROCESS OF MAKING A FERROMAGNETIC BODY by P. Robinson and A. Sommer (N.A. Philips); U. S. Pat. 3,002,930, Issued Oct. 3, 1961

The improvement of the characteristics of a ferrite core by coating the prefired core with an oxide of nickel, cobalt, zinc, or copper prior to the final firing is discussed. The divalent metal oxide is applied to the prefired core as a suspension of finely divided particles of the oxide in a lacquer such as a cellulose nitrate or cellulose acetate lacquer. The ferrite with the layer of the divalent metal oxide is then refined at 1100 to 1500°C. Manganese-zinc ferrites, for example, prepared by this technique (with a coating of nickel oxide) were found to have higher initial permeabilities, lower losses, and were denser than uncoated ferrites. The coated ferrites were also free of cracks.

10,795 MAGNETICALLY-TUNABLE MICROWAVE FILTERS USING SINGLE-CRYSTAL YTTRIUM-IRON-GARNET RESONATORS by P. S. Carter, Jr. (Stanford U.); IRE Trans., Vol. MTT-9, pp. 252-260, May 1961

A new type of magnetically-tunable band-pass microwave filter that makes use of ferrimagnetic resonance in single-crystal yttrium iron garnet is presented. The 3-db bandwidth can be adjusted from about 6 Mc to 100 Mc at X band, and the center frequency can be tuned over a wide range of frequencies, by means of a varying dc field. A theoretical analysis of the operation and behavior of this type of filter is presented. Descriptions of single-resonator and two-resonator filters which can be tuned over the X-band frequency range are given and experimental data are presented showing their tuning range, insertion loss, and bandwidth.

Design and Fabrication of Ferrite Filters - See 10,866

YIG in Microwave Filters - See 10,865

Ferroresonant Regulation in Power Supplies - See 10,894

10,796 SMALL SIGNAL IMPEDANCE OF A SOLID CORE INDUCTANCE by F. Kollar and R. D. Russell (U. Brit. Columbia); Brit. J. Appl. Phys., Vol. 12, pp. 307-310, June 1961

The small signal impedance of an electromagnet is calculated. The effects of eddy currents are considered but nonlinearities in the magnetizing curve of the iron are ignored. It has been possible to use typical values for the relative incremental permeability and conductivity of iron to obtain a rather good estimate of its impedance over four decades above the lowest frequency for which reactive components of impedance are significant. There is a change in slope in the curve of the magnitude of the impedance at a frequency corresponding to a skin depth equal to approximately three-quarters of the radius of cross section of the core. Above this frequency the magnitude of impedance rises at 3 db per octave and the phase angle approaches 45°. At much higher frequencies the existence of stray capacities causes deviations from this predicted behavior.

10,797 DESIGN AND CONSTRUCTION OF A SYSTEM OF PULSED MAGNETS by R. L. Kuskowski, T. B. Novey, and S. D. Warshaw (Argonne Natl. Lab.); Rev. Sci. Instr., Vol. 32, pp. 674-682, June 1961

A system of two pulsed iron-free magnets, designed for an experiment in high energy physics, is described. One of these is a small solenoid, with a working volume of about 35 cm^3, pulsed at 200 kgauss; the other is a large magnet with a volume of about 6 liters, pulsed at a nominal 15 kgauss. Construction details, working lifetimes, and detail of switch gear are discussed.

10,798 NUCLEAR RADIATION EFFECTS IN PERMANENT MAGNETS by R. S. Sery, D. I. Gordon, and R. H. Lundsten (Naval Ord. Lab.); U.S. Gov. Res. Rep., Vol. 36, p. S-36 (A), July 5, 1961 PB 155 913

The effect of radiation upon the properties of permanent magnets is discussed. Permanent magnets exposed to 10^{17} fast nvt at 90°C in the BNL Reactor showed no measurable changes in magnetic properties. The materials irradiated were: 3-1/2 Cr Steel, 36 Co Steel, Alnico II, V, and XII, Cunico, Cunife, Silmanal, fine irons, platinum-cobalt, and oriented and unoriented barium ferrites. Pre- and post-irradiation measurements of (a) demagnetization curves and (b) open magnetic circuit induction were made. Unirradiated controls, held at 90°C for 12 days were also measured. Because of induced radioactivity in the irradiated samples, post-irradiation measurements were made remotely, using the NRL hot-cell facility.

10,799 A NONDIRECTIONAL FERRITE ROD ANTENNA ARRANGEMENT SUITABLE FOR AM RADIOS by O.K. Nilssen (Ford); Proc. IRE, Vol. 49, pp. 1222-1223 (L), July 1961

A ferrite rod antenna arrangement which provides an essentially nondirectional polar pattern is described. Two mutually-perpendicular, separately-tuned antennas add in quadrature to provide a circular polar pattern. The addition angle can deviate from 90° by as much as ±35° and the resulting polar pattern is still circular within ±3 db. The antennas are critically coupled through mutual inductance. The voltage induced in one tuned circuit couples across to the other with a 90° phase shift. The output can be taken from either antenna.

MASERS AND LASERS

10,800 SOLID-STATE MASER by W. B. Mims (Bell Labs.); U.S. Pat. 3,001,142, Issued Sept. 19, 1961

A maser in which continuous wave operation can be achieved by utilizing a pump of lower frequency than the signal frequency is described. A magnetic field is applied to the active material so that four energy levels exist with the separation between one pair of levels equal to a whole number times the separation of a second pair of levels and a third pair of levels whose separation is greater than the separation of the second pair. A negative temperature between the third pair of levels can be obtained by applying a pump of a frequency corresponding to the separation of the second pair of levels. A signal with a frequency corresponding to the separation of the third pair of levels can then be amplified. An experimental arrangement is shown and some experimental results obtained are presented.

10,801 RESEARCH ON PARAMAGNETIC RESONANCES by R. L. Kyhl and M. W. P. Strandberg (MIT); U.S. Gov. Res. Rep., Vol. 36, p. S-80 (A), July 5, 1961 PB 154 391

A solid-state single-cavity X-band maser operated with a 20 Mc bandwidth at 10 db gain and a bath temperature of 4.2°K is described. The present system is tunable from 8400 Mc to 9700 Mc. The performance of this maser is offered as further experimental support of the phonon saturation mechanism.

10,802 A TRAVELING-WAVE MASER USING CHROMIUM-DOPED RUTILE by E. S. Sabisky and H. J. Gerritsen (RCA Labs.); Proc. IRE, Vol. 49, pp. 1329-1330 (L), Aug. 1961

The structure and characteristics of an X-band traveling-wave maser amplifier using chromium-doped rutile as the paramagnetic material are described. The device displays an appreciable gain-per-unit length with a very large tunable bandwidth. The normalized power curves, P_{out}/P_{in} vs frequency, are included.

10,803 AMPLIFICATION THROUGH STIMULATED EMISSION-THE MASER by R. A. Smith (RRE); Brit. J. Appl. Phys., Vol. 12, pp. 197-206, May 1961

The various factors which determine the ultimate sensitivity of a radio receiver are considered. External sources of noise (random electromagnetic fluctuations) are examined and the conditions determined under which ultimate sensitivity is limited by noise generated in the receiver itself. The physical principles of emission and absorption of radiation are examined with particular reference to their application to the microwave region of the electromagnetic spectrum. The use of stimulated emission for amplification (Maser action) is considered and various methods for its exploitation are discussed. Different types of Maser amplifiers are described and an elementary method of calculating their noise factors is given. Recent applications of Maser amplifiers to radio astronomy and communications are described and some figures given to illustrate the large gain in ultimate sensitivity which has been obtained. Thus it is now possible to design an amplifier with noise equivalent to the input from a load at a temperature of only a few degrees K, and a whole system, including antenna and external noise from outer space, with noise equivalent to the input from a load at about 20°K.

10,804 INFRARED AND OPTICAL MASERS by A. L. Schawlow (Bell Labs.); Solid State J., Vol. 2, pp. 21-29, June 1961

The ways in which maser operation can be obtained at infrared and optical frequencies, with special emphasis on solid state optical masers is described. Optical masers produce light which is far more monochromatic, directional, coherent and powerful than light produced by other sources. The reasons for these properties are discussed and the experimental results are summarized.

10,805 CROSS-DOPING AGENTS FOR RUTILE MASERS by P. F. Chester (Westinghouse Res. Labs.); J. Appl. Phys., Vol. 32, pp. 866-868, May 1961

The EPR spectra of nonstoichiometric rutile and rutile doped with tantalum, niobium, and cerium is examined at helium temperatures. Ta^{4+} and Nb^{4+} have short spin-lattice relaxation times and appear to be suitable for cross doping in maser applications.

10,806 D.C. PUMPED SOLID STATE MASER by W.S. Boyle and G.E. Smith (Bell Labs.); U.S. Pat. 3,002,156, Issued Sept. 26, 1961

The use of single crystals of the semimetals Bi, Sb, or As as the active material in masers is discussed. Continuous wave maser operation can be achieved by using a dc electric field as the pump rather than pumping at a frequency higher than the signal frequency. Since the conduction electron population of Bi is high, large differences in the level population can be achieved. This results in large power handling capacities. A typical maser system employing Bi is shown. Amplification of a signal at 300 kMc can be achieved by applying a magnetic

field of 15,000 gauss and a dc electric field of approximately 10^{-3} v/cm to refrigerated Bi in a resonant cavity.

OTHER SOLID STATE DEVICES

10,807 AN ANTENNA ARRAY OF LONGITUDINALLY-SLOTTED DIELECTRIC-LOADED WAVEGUIDES by E.D. Sharp and E.M.T. Jones (Stanford Res. Inst.); U.S. Gov. Res. Rep., Vol. 36, p. 37 (A), July 5, 1961 AD 255 747

An investigation concerning the design of an antenna made up of an array of dielectric-loaded rectangular waveguides with common narrow walls is presented. Longitudinal slots were cut in the center of each broad wall. The preferred form of the antenna utilized a slab of dielectric placed over all the slots, although it also operated when dielectric was placed within each guide. An approximate theory is discussed and empirical design data are presented from which an experimental model of this antenna was designed. Empirical data are also given for cases in which dielectric was placed inside the waveguides. The radiated H-field from this antenna was parallel to the antenna aperture, and the main beam was directed up from the aperture at an angle equal to the arc cosine of the velocity of light divided by the slotted-waveguide phase velocity. An experimental antenna was constructed using standard 0.900 by 0.400-inch waveguide, and had an aperture 9 inches wide by 20 inches long. At the design frequency of 10 kMc the E-plane and H-plane beamwidths were 5.4 and 8.0 degrees, respectively, and the E-plane and H-plane first-sidelob levels were -22.0 db and -23 db, respectively. Good radiation patterns were obtained from 8 to 11 kMc.

10,808 ENERGY STORAGE CAPACITORS, HIGH DIELECTRIC CONSTANT (Erie Resistor); U.S. Gov. Res. Rep., Vol. 35, p. 724 (A), June 16, 1961 PB 153 723

Twelve sample capacitors made using the stacked plate method and tested according to contract specifications are discussed. Degradation of the ceramic under high temperature-high voltage conditions caused the units to fail life test. The degradation was traced to an electrochemical reduction of the ceramic and subsequently high leakage. The ability of the ceramic to withstand high constant voltage conditions at elevated temperatures during earlier testing indicates that the constant pulsing of the voltage was the cause of failure, but also indicates that the ceramic can be improved to withstand the additional stress engendered by the pulsing. Those units which were not subjected to life test met the remaining electrical tests reasonably well in most instances. In those cases where failures occurred or questionable results were obtained, the difficulties appeared attributable to the types of jacketing materials employed. The use of rigid jacketing compounds appears unsuited to this type of unit unless provisions are made to closely match the coefficient of thermal expansion of the jacket material to that of the ceramic over the operating temperature range. The use of plasticized materials of flexible materials would be probably more desirable.

Tunneltron Theory and Analysis - See 10,669

10,809 RESEARCH INTO SOLID STATE TRANSDUCING TECHNIQUES by W. Welkowitz, R. Downs et al. (Gulton Ind.); U.S. Gov. Res. Rep., Vol. 35, p. 726 (A), June 16, 1961 PB 153 567

Measurements of pressure, acceleration, temperature, and heat flow by employing solid state devices is cited. The major areas of investigation were the following: piezoresistance, magnetoresistance, piezocapacitance, heat transfer measurement using thermetric films, heat transfer measurement using thermetric films, and heat transfer measurement using ultrasonic pulse techniques. Preliminary investigations were carried out on the use of magnetic transitions for temperature measurement, measurement of temperature using the pyroelectric phenomenon, measurement of heat transfer using a transverse thermomagnetic effect, the acoustoelectric effect, and plastic composite piezoelectric materials. In the area of piezoresistance, a miniature piezoresistive pressure gage was built and tested.

BASIC SOLID STATE DEVICE CIRCUITS

GENERAL

10,810 ON THE FACTORIZATION OF RATIONAL MATRICES by D. C. Youla (Brooklyn Polytech.); IRE Trans., Vol. IT-7, pp. 172-189, July 1961

Several algorithms for affecting the factorization of a matrix-valued function of a complex variable p for the class of rational matrices G (p), i.e., matrices whose entries are ratios of polynomials in p, are presented. Many problems in electrical engineering, such as the synthesis of linear n ports and the detection and filtration of multivariable systems corrupted by stationary additive noise, depend upon such decompositions for their solutions. The methods employed are elementary in nature and center around the Smith canonic form of a polynomial matrix. Several nontrivial examples are worked out in detail to illustrate the theory.

Measurement of Two-Port Network Parameters - See 10,766

10,811 POTTING, EMBEDMENT, AND ENCAPSULATION OF WELDED ELECTRONIC CIRCUITS by C. G. Clark (Space Tech. Labs.); U.S. Gov. Res. Rep., Vol. 36, p. S-37 (A), July 5, 1961 PB 155 775

Information on the wide variety of available methods, materials, and techniques for the potting, embedment, and encapsulation of electronic circuits is summarized. The proper use of these techniques to protect electronic circuits against the effects of severe environmental conditions requires full consideration of the effects of the casting resin on electronic parts, methods of mounting and packaging of equipment, handling and repair of modules, costs, and thermal effects. The characteristics of seven principal classes of casting resins are discussed, together with the use of resin modifiers including fillers, diluents, and flexibilizers. Various types of molds and molding processes are described as well as the techniques for preprocessing, mixing, pouring, curing, and finishing. A discussion of quality control considerations is included.

Fabrication of Thin Film Functional Units - See 10,776

Analysis of Tunnel Diode Switching Circuits - See 10,846

10,812 CIRCUIT CONTROL OF TUNNEL DIODE NEGATIVE-RESISTANCE CHARACTERISTICS by W. N. Carr and A. G. Milnes (Carnegie Inst. Tech.); Proc. IRE, Vol. 49, pp. 1204-1205 (L), July 1961

Controlling the negative resistance curve of a distributed junction tunnel-diode by lateral current flow in one degenerate region, provided with two ohmic contacts, is described. Current in the resistances biases the individual functions and results in output characteristics with controlled variation of negative resistance. The resistances are approximately equal to the negative resistance of a single junction. The required control current is of the same magnitude as the peak tunnel current controlled. Curves of unusual shape may be produced by mismatching the diodes. Negative resistance control makes possible variable gain amplification, variable swing relaxation oscillators and variable threshold switching gates.

Noise in Tunnel Diode Amplifiers - See 10,817

Shot Noise in Tunnel Diode Amplifiers - See 10,818

10,813 TRANSISTOR PROTECTIVE CIRCUIT by W. N. Carroll (IBM); U.S. Pat. 2,993,128, Issued July 18, 1961

A common emitter circuit which prevents damage to transistors in the event of control voltage failure is described. The circuit consists of a voltage divider network between the base bias supply and the collector supply, with a diode connected between the base and the voltage divider network. Failure of the base supply biases the diode on and drives the transistor into saturation. If the collector supply fails, the voltage divider network limits the reverse collector potential to a safe value.

10,814 TRANSISTOR CIRCUIT HAVING REVERSE BASE CURRENT SUPPLY MEANS by F. R. Noll (Intl. Tel. and Tel.); U.S. Pat. 2,993,127, Issued July 18, 1961

The use of an additional driving transistor to supply reverse base current to an output transistor, reducing the power supply drain, is described. The output transistor base is in series with a diode and the collector of a driving transistor which supplies the normal base current. The diode is shunted by the base and emitter of a second driving transistor which provides the reverse base current. If the input signal does not require an output current less than the current produced by the cutoff current, the additional transistor remains off. When the output current falls below this value, the second transistor is turned on, blocking the diode, and supplies reverse base current to the output transistor.

AMPLIFIERS

AGC in Automatic Direction Finder - See 10,863

Multistage Amplifier in Remote Control Unit - See 10,901

10,815 NOISE MEASURE OF DISTRIBUTED NEGATIVE-CONDUCTANCE AMPLIFIERS by A. Van Der Ziel (U. Minn.); Proc. IRE, Vol. 49, pp. 1212-1213 (L), July 1961

The concept of the noise measure of an amplifier stage, introduced by Haus and Adler, is discussed. The case of distributed negative-conductance circuits in which the characteristic impedance has a reactive part is included. The calculations are developed on a current basis, not a power basis. The result for the lossless case is completely equivalent with the noise measure of the lossless lumped-circuit case, whereas the result for the lossy active line is fully comparable to that of the lossy lumped-circuit case. The proper definition for the noise measure of a distributed active circuit is developed.

10,816 A THEORETICAL COMPARISON OF AVERAGE - AND SPOT - NOISE FIGURE IN TRANSISTOR AMPLIFIERS by J. A. Ekiss and J. W. Halligan (Philco); Proc. IRE, Vol. 49, pp. 1216-1217 (L), July 1961

Calculation of the average noise figures of a transistor from an assumed functional relationship for the spot-noise figure is presented. Equations are derived which relate the average-noise figure to the spot-noise figure. For both the low and high frequency cases, the average-noise figure is higher than the spot-noise figure. If a filter is chosen such that the ratio of the effective noise bandwidth to the center frequency is small, the difference between the measured noise figure and the actual spot-noise figure will be small.

10,817 NOISE MEASURE OF LOSSY TUNNEL-DIODE AMPLIFIER STAGES by A. Van Der Ziel (U. Minn.); Proc. IRE, Vol. 49, pp. 1211-1212 (L), July 1961

A study of the influence of losses on the noise figure of tunnel-diode amplifiers is presented. The calculations for a stable parallel circuit, based on an extension of Nielsen's approach, are developed. The lumped circuit case is developed for available gain, noise figure and noise measure of the circuit. The same measures are then calculated for a reflection-type amplifier using a circulator. A considerable similarity is observed when compared with the results obtained for a lossy, distributed, active line.

10,818 SHOT NOISE IN TUNNEL DIODE AMPLIFIERS by J. J. Tieman (GE Res. Lab.); Proc. IRE, Vol. 49, pp. 622-623 (L), Mar. 1961

Chang's method of relating the IR product of an I-V characteristic to the noise performance of a tunnel diode amplifier [see abstr. 6261] is questioned. The second derivative of the I-V characteristic does not affect the minimum IR product, nor is a low value of I_m required to assure a low $(IR)_{min}$. Several of Chang's assumptions about tunnel diode characteristics, employed in drawing conclusions about an ideal characteristic for a low possible IR product, are called arbitrary. The second and third derivatives of the I-V characteristic are correct only for Chang's free hand sketches. They are not, however, typical of Ge, GaAs, GaSb or Si tunnel diodes and hence his d^2I/dV^2 disagrees with experiment, and d^3I/dV^3 may even be of opposite sign in the region of interest. The simultaneous occurrence of a small first derivative together with a large second derivative is insufficient to guarantee a small $(IR)_{min}$ since this situation has to apply at V_m and one is not free to choose V_m.

Noise in Tunnel Diode Amplifiers - See 10,760

Noise Temperature of Parametric Amplifiers - See 10,830

Low Noise Amplifier - See 10,822

10,819 DESIGN THEORY OF OPTIMUM NEGATIVE-RESIST-

ANCE AMPLIFIERS by E. S. Kuh and J. D. Patterson (U. California); Proc. IRE, Vol. 49, pp. 1043-1050, June 1961

General amplifiers obtained by imbedding a linear active 1-port device in arbitrary 3-ports are discussed. The active device is assumed to have a representation of a negative conductance $-G_D$ in parallel with a parasitic capacitance C_D. Synthesis methods to approach or achieve the optimum are presented. Other types of amplifier configurations are considered. In each case, the optimum gain-bandwidth formula, synthesis procedure and some useful design curves are given.

Non-Saturating Amplifier Circuit - See 10,839

X-Band Maser Amplifier - See 10,801

X-Band Traveling Wave Maser Amplifier - See 10,802

10,820 A MILLIMETER-WAVE ESAKI DIODE AMPLIFIER by C. A. Burrus and R. Trambarulo (Bell Labs.); Proc. IRE, Vol. 49, pp. 1075-1076 (L), June 1961

Amplification with high gain has been attained with Esaki diodes from 55-85 kMc (5.5 - 3.5 mm wavelength). Formed point-contact Esaki diodes of n-type gallium arsenide were mounted in a reduced-height rectangular waveguide having an LF cutoff of 48 kMc. A contacting piston was used to suppress oscillation, with the input and output separated by a circulator. Stable gains to 35 db were obtained with gain compression occurring at a power output of -35 dbm. Bandwidth was approximately 40 Mc at a peak gain of 20 db. The highest observed frequency of amplification was 85.5 kMc; this limit was imposed by available test equipment. The noise figure near 55 kMc was 16-18 db, which is comparable to a conventional 55 kMc receiver with a similar bandwidth.

10,821 REGENERATIVE PULSE AMPLIFIER by R. K. Richards; U.S. Pat. 2,988,651, Issued June 13, 1961

A single-transistor regenerative pulse amplifier, which requires no clamping circuits or feedback winding on the output transformer, is described. The feedback path consists of two diodes and a resistor in series. An n-p-n transistor is gated by a negative input pulse. The feedback diodes are initially biased into the conducting state and permit feedback. When the output pulse reaches a certain level, the diodes are cut off and the feedback path is opened, providing full output to the load. Signal source loading is minimized since the input is only required to initiate amplifying action. A relatively high PRR is obtained by using a second feedback path to feed the positive going transient to the input and cut the transistor off quickly. A diode between input and ground damps the transformer and prevents oscillation.

Pulse Amplifier for Magnetic Core Memory - See 10,887

10,822 APPLICATION OF SEMICONDUCTOR DIODES TO LOW-NOISE AMPLIFIERS, HARMONIC GENERATORS AND FAST-ACTING TR SWITCHES by R. Gardner, J. C. Greene et al (Airborne Instr. Lab.); U.S. Gov. Res. Rep., Vol. 35, pp. 718-719 (A), June 16, 1961 PB 155 258

A study of the use of semiconductors as low-noise amplifiers, harmonic generators, and fast-acting TR switches is reported. The use of the nonlinear reactance of a reverse-biased p-n junction diode as a low-noise sum-frequency amplifier is analyzed in detail. Experimental results obtained on sum-frequency amplifiers constructed for use at 1 Mc and at 400 Mc are described. The problem of using semiconductor devices as fast-acting TR switches is outlined, and an analysis of pertinent TR system parameters in terms of the series resistance of the semiconductor diode is presented. The power-handling capability of presently available semiconductor devices most suited to this application is discussed briefly. The use of the nonlinear reactance of a reverse-biased p-n junction diode as a harmonic generator is examined theoretically, and preliminary experimental results on a low-frequency prototype harmonic generator are given.

10,823 A NEW DESIGN APPROACH FOR FEEDBACK AMPLIFIERS by M. S. Ghausi and D. O. Pederson (Electronics Res. Lab.); U.S. Gov. Res. Rep., Vol. 36, p. S-34 (A), July 5, 1961 PB 148 501

A new design procedure which permits the realization of desired closed-loop response shape and bandwidth (or rise time) as well as the desensitivity of both the band edge frequency and low frequency response is described. The design procedure, which is based on the root-locus technique, is straightforward. To illustrate the technique, a shunt-shunt feedback configuration is used. The basic amplifier consists of a three-stage common emitter transistor cascade circuit. Typical design examples with experimental results are included.

10,824 TRANSISTOR TONE CONTROL FEEDBACK CIRCUIT by F. D. Waldhauer (RCA); U.S. Pat. 2,994,040, Issued July 25, 1961

A continuously variable tone control circuit for transistor amplifiers is described. The desired frequency attenuation is obtained by current division and negative feedback. A tone control circuit is connected to the output of a common-emitter amplifier. A capacitive current divider network provides an output to a second amplifier and a negative feedback output to the first stage. Continuously variable tone control is obtained by variation in the current division characteristics. The negative feedback raises the first stage output impedance to provide the proper source impedance for the tone control circuit and aids in tone control by making the overall transmission characteristic vary with frequency in the desired manner.

10,825 A COOLED, NEGATIVE CONDUCTANCE, DEGENERATE PARAMETRIC AMPLIFIER by C. T. Stelzied (Calif. Inst. Tech.); Microwave J., Vol. 4, pp. 79-84, July 1961

A simplified theory on the operation of a degenerate parametric amplifier with circulator is discussed. Bandwidth and amplifier noise temperature are derived in terms of varactor and circuit parameters and gain. A varactor figure of merit is presented. The theory is verified for a liquid-nitrogen-cooled 960 Mc parametric amplifier with 20 db gain, 20 Mc bandwidth and 36°K noise temperature.

10,826 DESIGN AND PERFORMANCE OF A 450 MC/S PARAMETRIC AMPLIFIER by D. J. Mudgway (Weapons Res. Estab.); Proc. IRE, Austl., Vol. 22, pp. 167-173, Mar. 1961

The design and performance of a 450 Mc parametric amplifier using the up-converter configuration is described. The bandwidth is 12 Mc and the noise figure and gain of 1.5 db and 9 db, respectively, are in agreement with theoretical prediction. Some of the problems involved in carrying out measurements on the amplifier and in its practical application are discussed.

10,827 NONRECIPROCAL PARAMETRIC AMPLIFIER CIRCUITS by L. D. Baldwin (Genl. Dynamics); Proc. IRE, Vol. 49, p. 1075 (L), June 1961

Two circuits which, while not using a circulator, have similar properties to a single-port reflection amplifier with a three-port circulator are described. Both use two time-varying reactances with a 90° phase shift between them. A common idler circuit is used. In one circuit, a 90° hybrid splits the input signal and shifts one port 90°. Since a similar phase shift is present in the pumping, the idler currents generated are in phase and are dissipated in the idler load. In the reverse direction, the signal phase is shifted 90° in the opposite direction, generating out-of-phase idler currents which cancel, and the signal is reflected without amplification. Except for a slight difference in reverse gain, performance is identical to that of the circulator amplifier. The second circuit uses a 90° phase shift network with the phasing correct for idler cancellation in the reverse direction only at the center frequency. However, the idler circuit bandwidth is less than that of the signal circuit, and the performance obtained is similar to the first circuit.

10,828 BROAD-BAND CAVITY-TYPE PARAMETRIC AMPLIFIER DESIGN by K. M. Johnson (Texas Instr.); IRE Trans., Vol. MTT-9, pp. 187-194, Mar. 1961

The attainment of maximum bandwidth from a nondegenerate parametric amplifier which utilizes a circulator is discussed. Expressions for the gain bandwidth product and maximum possible gain bandwidth product are derived. It is then shown how the Q of the cavities used for the signal and idler circuits may be kept at a minimum without degrading the noise performance of the amplifier. It is shown that the best performance results when the TEM mode is used in coax, or, if waveguide is used, when the operating frequency is far away from the waveguide cutoff frequency. The diode used should have as high a self-resonant frequency as possible and the line admittance should be approximately the diode susceptance. Using a diode with a self-resonant frequency at the idler frequency gives optimum performance. Double tuning the signal circuit to achieve broader bandwidths is also discussed. In this case, the addition of the second tuned circuit gives much broader bandwidths than one would expect from conventional filter theory. Two sample amplifiers are considered and their bandwidth calculated. The effect of double tuning one of the amplifiers is then considered.

10,829 A SOLID-STATE ANALOG TO A TRAVELING-WAVE AMPLIFIER by G. H. Heilmeier (Princeton U.); Proc. IRE, Vol. 49, pp. 1079-1080 (L), June 1961

An exploratory L-band nondegenerate parametric amplifier, providing gains of 4-8 db with bandwidths of 15-25 per cent at a pump frequency of 2,020 Mc, is reported. A measured noise figure of 9.8 db is believed to be partly due to a poor idle frequency termination and internal reflections of the pump frequency signal. A shielded helix was used as the propagation circuit with three parallel stacks of eight pill varactor diodes, each placed end to end, mounted symmetrically in the helix as the active medium. Since the diodes operate under self-biased conditions, they must be carefully selected and positioned to achieve the proper interaction impedance.

10,830 SENSITIVITY OF THE DEGENERATE PARAMETRIC AMPLIFIER by J. T. DeJager and B. J. Robinson (Netherlands Radio Observatory); Proc. IRE, Vol. 49, pp. 1205-1206 (L), July 1961

The noise temperature of a degenerate parametric amplifier is compared with that of a nondegenerate amplifier. The effective bandwidth for noise is halved for the degenerate noise output. Since the degenerate amplifier has its input circuit tuned to half the pump frequency, the output consists of a reflected component at the input frequency and a component converted to the difference between the pump frequency and the signal frequency. These components are equal in amplitude and have equal bandpass characteristics symmetric with respect to the input frequency. If the input is noise, the correlation of these bandwidths leads to an increase in the post-detector fluctuations by a factor of $\sqrt{2}$. The capability of detecting a weak noise signal is only $\sqrt{2}$ better in the degenerate case over a nondegenerate amplifier if the signal bandwidths are equal.

Noise in Reactive Amplifiers - See 10,815

Parametric Amplifier Varactor Diodes - See 10,762

X-Band Traveling Wave Maser Amplifier - See 10,802

10,831 AMPLIFIER CIRCUITS by E. A. Petrocelli and B. Christensen (Westinghouse); U.S. Pat. 2,993,129, Issued July 18, 1961

An amplifier using switching hyperconductive diodes which does not require phasing the input signal with the power supply is described. The input signal is half-wave rectified, filtered and applied through rectifying diodes and current-limiting resistors to a pair of back-to-back hyperconductive diodes. A load and an ac power supply are connected in series across the diodes. The filter output capacitor charges to the breakdown voltage of the diodes and the diodes and capacitor then function as a relaxation oscillator with a frequency higher than the supply voltage. Since firing pulses are present across the hyperconductive diodes throughout a cycle of the supply voltage, no phasing problem exists and load current flows for almost 180° during each power supply alternation.

Millimeter Wave Tunnel Diode Amplifier - See 10,820

10,832 SIMULATING TRANSISTOR AMPLIFIERS by A. R. Berding and R. H. Breedlove (IBM); Electronics, Vol. 34, p. 56, June 1, 1961

A transistor circuit simulator for determining bias point limits, ac gain and input impedance of amplifier stages is described. The simulator is constructed based on the dc (or ac) equivalent circuit of the transistor. Operation parameters can then be determined directly from the measurements of the simulator instead of by solving complex simultaneous equations.

10,833 CORE MATRIX DRIVER EMPLOYING MAGNETIC AMPLIFIERS by J. Yamato and Y. Suzuki (Nippon Tel. and Tel.); Rev. Elect. Commun. Lab., NTT, Vol. 9, pp. 43-49, Jan.-Feb. 1961

A high frequency magnetic amplifier with high efficiency, high S/N, and high output power, developed to drive large scale core memory matrixes in parametron devices, is discussed.

10,834 TRANSISTOR AMPLIFIERS by E. M. Jones (Baldwin Piano); U.S. Pat. 2,994,834, Issued Aug. 1, 1961

A cascaded junction transistor power amplifier circuit in which

the number of stages may be increased to meet load requirements is discussed. The cascaded transistors have common collector junctions making it possible to fabricate plural junction transistors on a single specimen of n-p-n or p-n-p multiple-junction material. The input stage may consist of a small subdivision of the total area, and successive elements in the cascaded series of amplifiers may be formed of proportionally larger areas. In the examples given a pair of transistors having complementary symmetry to one another make up one stage of amplification. The amplifier is relatively insensitive to power supply variation and ripple. It has a high input impedance on the order of 5 megohms and can deliver as much as 70 watts into a 32 ohm load. The dc current supply may also be taken from rectifier junctions integral with the same specimen. This results in a compact, self-contained device suitable for sealing in a heat-dissipating container.

10,835 ELECTRICAL CONTROL CIRCUIT by E. Willems and A. J. W. N. van Overbeek (N. A. Philips); U.S. Pat. 2,986,648, Issued May 30, 1961

A technique for supplying a large controlled power to a load without exceeding the maximum permissible dissipation of a transistor is described. The control is achieved by means of a variable dc voltage supply between the base and emitter. When the positive voltage of the supply is varied, the time in which the current flows can be controlled. If the collector and base voltages and the load impedance are high when the current flows, there is only a very low voltage drop between the emitter and collector electrodes. The power dissipated in the transistor can then be low even though a large power is supplied to the load.

OSCILLATORS

10,836 ON THE COMPUTATION OF SELF-OSCILLATING CIRCUITS WITH SEMICONDUCTING TRIODES [in Russian] by N. I. Asbel' and L. V. Postnikov (NIFTI, Gor'kii U.); Izv. VUZ, Radiofiz., Vol. 4, No. 2, pp. 319-329, 1961

An arbitrary semiconducting self-oscillating system with one degree of freedom is analyzed. On the basis of a piecewise-linear idealization, general relations are obtained which characterize the separation of the phase plane into regions of linearity, the distribution of equilibrium states and their stability. A point transformation of the boundary lines into each other is described for the case of a single-sheeted phase plane.

10,837 IMPULSE-GOVERNED OSCILLATOR TECHNIQUES (4) by C. J. de Lussanet de la Sablonière (Philips); Philips Telecommun. Rev., Vol. 22, pp. 94-101, Jan. 1961

The possible reduction of spurious signals and the size of the holding range of an impulse governed oscillator (IGO) are discussed. The feedback circuit is shown to produce a degenerate effect upon spurious signals resulting from an unwanted ac voltage occurring in the loop circuit, or pickup of an interfering RF signal by the tuned oscillator circuit. Reduction in the holding range size occurs upon rapid fluctuations of the reference frequency. Calculations illustrate the properties of an IGO with negative phase feedback, and an IGO with an Image Selective Circuit.

Tunnel Diode Oscillator Employed as DC to AC Converter - See 10,895

10,838 IMPEDANCE CONTROLLED CROSS-COUPLED ONE-SHOT MULTIVIBRATOR by R. L. Ellsworth (U.S. Army); U.S. Pat. 2,990,480, Issued June 27, 1961

A one-shot multivibrator providing a square wave with fast leading and trailing edges is described. A parallel combination of a resistor, capacitor and diode replaces the usual direct connection from the timing capacitor to the base of the normally conducting transistor. This network increases the apparent input resistance of the transistor during the timing capacitor discharge cycle, allowing a longer pulse to be generated. The added capacitor provides a feedback path allowing the transistor to reach its quasi-stable state faster, speeding up the leading edge. The diode effectively shorts the resistor during the charging cycle of the timing capacitor.

10,839 ANTI-SATURATION CIRCUITS FOR TRANSISTOR AMPLIFIERS by A. D. Scarbrough (Thompson RW); U. S. Pat. 2,990,478, Issued June 27, 1961

An anti-saturation circuit for transistor amplifiers and multivibrators is described. A negative feedback circuit between the collector and base limits the current level to prevent saturation. The feedback circuit includes a low impedance potential source with one side connected to the base, and the other side connected through a diode to the collector. A bypass capacitor is used in the multivibrator circuit to increase trigger speed. When the collector approaches saturation, the diode is biased on and a low impedance feedback path is opened between collector and base. The feedback limits the collector current to a value below saturation.

10,840 EMITTER-TIMED MONOSTABLE CIRCUIT by B. Gilbert (Mullard Semicon. Lab.); Mullard Tech. Commun., Vol. 5, pp. 345-354, July 1961

A type of emitter-coupled monostable circuit in which the timing function is performed in the emitter circuit, and the transistors operate in the emitter current switch mode, is described. Under these conditions the shortest pulses for a given transistor type can be generated. The circuit has good designability, and is relatively insensitive to transistor parameters, supply voltages, and temperature. The circuit can also be used to generate linear sawtooth waveforms.

10,841 THE JUNCTION-TRANSISTOR PUSH-PULL BLOCKING OSCILLATOR by B. Gilbert (Semicon. Measurement Applic. Lab.); Mullard Tech. Commun., Vol. 5, pp. 330-336, June 1961

The operation of a junction-transistor push-pull blocking oscillator is discussed. The expressions derived for the pulse lengths and the mark/space ratio show that this oscillator has several advantages over the single-transistor circuit where accurate pulse lengths and mark/space ratios are required. The mark/space ratio of the output waveform is dependent only on a transformer ratio and the ratio of two voltages so that pulses of defined widths can be produced by synchronizing the circuit by an external source. When another transistor connected in the emitter follower configuration is used for this purpose, synchronizing ranges of 50% are possible. Push-pull blocking oscillators may be used as frequency dividers for ratios of up to about 5.

10,842 TRANSISTORIZED BLOCKING OSCILLATOR FOR TELEMETERING CIRCUITS by H. K. Janssen (Bendix); U. S. Pat. 2,988,709, Issued June 13, 1961

A condition-responsive transistorized blocking oscillator for telemetering use is described. The AF output modulates an RF carrier to indicate environmental changes. An n-p-n transistor contains an RC network in the emitter and base leads. The collector load is the primary of a transformer, with the secondary in the base circuit. When the transistor conducts, blocking oscillator action drives the base into the cutoff. The emitter RC network then charges toward the supply voltage while the base RC network discharges. When the base and emitter voltages are equal, the transistor conducts and the cycle repeats. The timing network controls the transistor turn-on point, permitting pulse frequency control. Using a condition-sensitive element for a resistance provides environmental information.

10,843 ADDITIONAL NEGATIVE-RESISTANCE OSCILLATION MODES by W. N. Carr and T. C. Matty (Carnegie Inst. Tech.); Proc. IRE, Vol. 49, p. 1225 (L), July 1961

Oscillation modes which operate around bias points at the peak and valley of tunnel-diode negative resistance characteristics are reported. Oscillations around the valley point have been achieved with voltage swings of 350 mv peak-to-peak. Operation above a few Mc has not been explored; the lower frequency limit observed was below 1 cps. If two diodes are connected back-to-back, oscillation around the peak point of one diode may extend into the negative resistance region of the second diode providing a swing as large as 750 mv peak-to-peak. Germanium units were used at low temperatures to improve the peak-to-valley ratio to at least 20:1.

Negative Resistance Field Effect Oscillator - See 10,774

10,844 A TRANSISTOR OSCILLATOR HAVING OUTPUT FREQUENCY PROPORTIONAL TO THE D.C. SUPPLY VOLTAGE by A. R. Saha (Jadavpur U.); J. Electronics Control, Vol. 10, pp. 181-190, Mar. 1961

A modified transistor beta phase shift oscillator is discussed and the conditions under which the frequency may be made to vary linearly with supply voltage are derived. A practical oscillator circuit based on these deductions is described. Forward biased p-n junctions in the collector load are used to compensate for variation of gain with supply voltage. The oscillator has a frequency shift of about 3.5 kc per volt of supply voltage. Possible application of the oscillator may be as a wide deviation subcarrier FM oscillator in telemetry equipment.

10,845 VARISTOR NETWORK CONTROLS VOLTAGE-TUNED OSCILLATOR by M. Uno (Chiba U., Japan); Electronics, Vol. 34, pp. 44-47, July 28, 1961

A phase-shift oscillator using SiC varistors to obtain linear frequency control over a wide range is discussed. Differentially connected varistors with a value of $\alpha = 2$ ($I = cE^{\alpha}$) would require an inconveniently high control voltage if a range 10 times the lowest frequency has to be achieved. This difficulty is overcome by using varistors with a value of $\alpha = 3$, and an additional varistor in the voltage control circuit to stabilize the oscillation frequency against temperature changes. A control voltage change of about 20 v is required for a linear oscillation frequency range of ten; the harmonic distortion is negligible over the range; oscillation follows sweep control voltage changes of less than 50 v/sec; temperature coefficient of oscillation frequency is less than a few parts per 1000; frequency and amplitude stabilities for changes in cathode and plate supply voltage of 5 per cent are 2 and 10 per cent, respectively. A varistor capacity of about 300 pf limits the upper frequency to several kc.

Transistor Oscillator Employed as DC to AC Converter - See 10,896

SWITCHING CIRCUITS

10,846 BISTABLE SYSTEMS OF DIFFERENTIAL EQUATIONS WITH APPLICATIONS TO TUNNEL DIODE CIRCUITS by J. K. Moser (New York U.); IBM J. Res. Dev., Vol. 5, pp. 226-240, July 1961

A mathematical analysis for nonlinear circuits which have at least two stable steady states, and therefore are of interest as computing or memory elements, is developed. Circuits containing one or two tunnel diodes are analyzed in detail. The method is based on the study of a certain "potential function" whose extrema are the steady states of the circuit and whose minima correspond to the stable switching states. This study leads to a qualitative description of all solutions in the large and results in quantitative restrictions on the parameters (R, L, C and nonlinear characteristics) which are of practical importance.

10,847 APPLICATION OF BOOLEAN NOTATION TO THE MAINTENANCE OF SWITCHING CIRCUITS by S. Alexander (English Elect.); Electronic Engrg., Vol. 33, pp. 372-374, June 1961

A method for the notation of switching circuits with special regard to its application in the drawing up of test and maintenance schedules is described. The system is based on Boolean algebra which is already used extensively for the design of switching circuits. Several examples including a sample "test schedule" are given.

Fast Acting Diode Switch - See 10,822

10,848 TIME DISCRIMINATOR by A. L. Hall (RCA); U. S. Pat. 2,989,652, Issued June 20, 1961

A transistorized time discriminator which senses the time of occurrence of a pulse signal is described. The input pulse is applied to the bases of two switching transistors (normally off) which are series connected between voltage sources of opposite polarity. A resistor is connected across each transistor and the output is taken from the resistor junction. The output is zero when both transistors are cut off. Each input is shunted to ground by a normally conducting switching transistor. These are cut off in succession by early and late gates. If the input pulse is coincident to a gate, the respective output transistor is switched on and a dc error voltage appears in the output. The polarity of this voltage is indicative of the displacement in time of the input pulse from the crossover area of the early and late gates. If both early and late gates are centered on the pulse, the output is zero.

10,849 SEMICONDUCTOR CIRCUITS UTILIZING A STORAGE

DIODE by H. W. Abbott and L. D. Wechsler (GE); U.S. Pat. 2,976,429, Issued Mar. 21, 1961

A bistable circuit using a diode amplifier, with a power handling capability of 20 w and a power gain of 50, is described. The diode is forward biased during one alternation of an RF power supply to inject carriers and reverse biased during the other alternation to sweep carriers out in a transient reverse current. The injected carriers reduce the diode impedance during the transient reverse current. When a clamped input signal is applied to prevent carrier injection, the resulting high reverse diode impedance provides an amplified output signal. A flip-flop circuit is obtained by using positive feedback, with a continuous on-off repetition rate of 2 kc achieved. A series resonant circuit across the diode provides regenerative feedback to sustain oscillations induced by a positive trigger. A negative trigger permits carrier injection and eliminates the feedback signal.

Tunnel Diode Trigger for Pulse Circuits - See 10,860

10,850 BRIDGE GATING CIRCUIT WITH FLOATING BIAS SOURCE by R. M. MacIntyre (Thompson RW); U.S. Pat. 2,990,477, Issued June 27, 1961

A bridge gating circuit which reduces error voltage output and minimizes signal attenuation is described. A floating bias source prevents signal current flow through the bias source. The bias supply consists of a capacitor and resistor in series. A flip-flop is used as an on-off control and charges the bias capacitor in the off condition. The flip-flop is decoupled from the bridge by diodes when the bridge conducts. The transfer function is equal to the ratio of the output circuit impedance to the sum of the output circuit and associated input circuit impedances.

Diode-Transformer Gate Circuit - See 10,890

10,851 PULSE COMPARATOR CIRCUIT MEASURES FREQUENCY JITTER by K. H. Brackney and D. R. Gosch (GE); Electronics, Vol. 34, pp. 54-56, July 7, 1961

A frequency comparator that will measure jitter of ±64 counts per second using a simple method which involves only counting and complementing is described. It uses two counters and averages counts over 0.5 second. The principle, a block diagram, and the detailed circuitry of the pulse comparator are given. The upper frequency limit of the comparator is 130 kc; however, by using heterodyning the frequency range can be extended.

10,852 HIGH IMPEDANCE TRANSISTOR PICK-OFF CIRCUIT by A. T. Kneale (United Aircraft); U.S. Pat. 2,983,830, Issued May 9, 1961

A pick-off circuit which accurately determines the time at which a positive-going sawtooth voltage equals a reference voltage is described. When the sawtooth voltage reaches the value of the reference voltage, a normally nonconducting diode begins conducting. The current flowing through the diode causes the potential at the base of a transistor to rise and the transistor stops conducting. This cutoff takes place rapidly because of the regenerative feedback produced by a pulse transformer which couples the emitter circuit and the diode circuit. When the transistor conducts again at the trailing edge of the input sawtooth wave, a series of sharp pulses appear at the emitter and a negative square wave is produced at the collector.

10,853 SWITCHING CIRCUITS USING CONSTANT CURRENT SOURCES by R. A. Henle (IBM); U.S. Pat. 2,990,479, Issued June 27, 1961

A high-speed transistor switching circuit, which is independent of the emitter-base breakdown voltage of the transistor used, is described. The emitters of two transistors are connected through diodes to a common point. One base is grounded with the input applied to the other base. A constant current is supplied to each emitter and the common point. The current to the emitters is one-third that to the common point. The current applied to the emitters prevents cutoff while the combination of the constant current and the conduction current prevents saturation. The transistors remain in the most favorable region for rapid response. Since the emitter-base junction is never reverse biased, the emitter-base breakdown voltage is not a factor. A capacitor, connected between the emitters, delivers charge into the emitter of the transistor whose current is increasing at switching time to aid in turn-on.

Inverter Control Circuit Using Switching Transistor - See 10,898

10,854 TRANSISTOR LINE SWITCH by A. E. Pinet (Auto. Elect. Lab.); U.S. Pat. 2,975,305, Issued Mar. 14, 1961

An electronic switch which consumes little power in the blocked state is described. Two transistors of opposite conductivity types are interconnected with transistors of the same type and provided with appropriate polarity voltages. In one stable state, both transistors are cut off and in the other stable state, both transistors are conducting. The signal circuits to be connected by the switch are connected through a diode and capacitor to the emitter-collector path of one transistor. When the transistors are cut off, a high impedance path is presented between the circuits. When the transistors conduct, a low impedance path is presented. Attenuation with the switch open is 8 nepers; with the switch closed 0.08 nepers.

10,855 HIGH VOLTAGE SWITCHING WITH TRANSISTORS (E.M.I., Ltd.); Electronic Engrg., Vol. 33, p. 278 (L), May 1961

A method of switching a high voltage by means of low voltage transistors is presented. A stack of transistors is turned on by the input switching signal and an intermittent short-circuit is provided.

SIGNAL CONVERTERS

Condition Responsive AM Signal Generator - See 10,902

AC to DC Choppers - See 10,911

10,856 PUTTING DIODE MODULATORS TO WORK by G. W. Ogar (Air U., USAF); Electronic Ind., Vol. 20, No. 7, pp. 86-90, July 1961

The operation principle of diode-bridge modulators, which can easily implement many useful electronic functions, is described. An analysis of their various applications (wide band phase shifter, SSB systems and stereo systems) is presented. Detailed block diagrams of the system and an analytic proof are given.

10,857 A JUNCTION TRANSISTOR FREQUENCY DIVIDER by W. D. Ryan and H. B. Williams (Queen's U., Ireland); Proc.

IRE, Vol. 49, p. 1081 (L), June 1961

A junction transistor frequency divider, utilizing the carrier-storage delay effect in the emitter-base diode junction, is described. The use of a transistor instead of a diode reduces the loading effect. Phase synchronization is obtained by cyclically varying the operating conditions so that the device passes through a region in which it is sensitive to a small subharmonic synchronizing signal. Typical storage times limit the lower input frequency to about 100 kc although some power transistors will operate down to 10 kc. The collector voltage waveform is influenced principally by the available charge stored in the base. If a relatively pure subharmonic output is required, a parallel tank circuit may be used as the load.

Parametric Up-Converters - See 10,826

Harmonic Diode Generators - See 10,822

10,858 A CAVITY-TYPE PARAMETRIC CIRCUIT AS A PHASE-DISTORTIONLESS LIMITER by F. A. Olson (USAF Res. Div.) and G. Wade (Raytheon); IRE Trans., Vol. MTT-9, pp. 153-157, Mar. 1961

The properties of a diode parametric frequency converter (negative-conductance type) when used to perform microwave limiting are discussed. Unlike the parametric amplifier, the output power of a converter cannot exceed a certain level, regardless of the amplitude of the input signal. Thus the ability to limit is a fundamental property of regenerative parametric frequency converters. An experimental limiter circuit, consisting of two stages of parametric frequency conversion, provided an output which was constant to within ±1 db over a range of input of 50 db, and had 10 db small signal gain. The phase variation was less than seven degrees over the entire range of input power.

WAVE GENERATORS

10,859 TRANSISTOR PULSE GENERATOR by L. M. Smith (Bell Labs.); U.S. Pat. 2,989,651, Issued June 20, 1961

A point-contact regenerative pulse generator in which the output pulse is stabilized against variations in transistor saturation current and current gain is described. A grounded emitter configuration, with the secondary of a saturable transformer in the base circuit, is used. The primary is in series with a current-limiting resistor and a direct voltage source. This bias current saturates the core, resulting in zero secondary inductance. When the transistor is triggered, the current flowing into the transistor base increases sharply desaturating the core. The secondary inductance then becomes very large, maintaining a constant current flow. After a definite time, the voltage across the secondary drives the core into saturation, permitting the base current to rise almost instantaneously to the cutoff value. The output pulse duration depends solely upon the time required to bring the core from saturation in one direction to saturation in the other direction.

10,860 NEW WAYS TO TRIGGER AVALANCHE PULSE CIRCUITS by H. G. Dill (Hughes Semicon.); Proc. IRE, Vol. 49, p. 1093 (L), June 1961

Use of a tunnel diode to improve the sensitivity and stability of base-triggered and emitter-triggered avalanche circuits is described. The tunnel diode replaces the biasing resistor to ground in a base-triggered circuit. Reverse bias is applied at the emitter to compensate for the forward bias across the tunnel diode. A highly capacitive forward-biased diode between emitter and ground supplies the dc bias. The tunnel diode must be reset to its original state after breakdown. An emitter-triggered stage with the tunnel diode between emitter and ground provides automatic reset of the tunnel diode. Very little energy feeds back into the trigger circuit and the time delay between input and output is 2-4 μsec.

Linear Sawtooth Generator - See 10,840

10,861 TUNNEL-DIODE FAST-STEP GENERATOR PRODUCES POSITIVE OR NEGATIVE STEPS by R. Carlson (Hewlett-Packard); Electronics, Vol. 34, pp. 48-49, July 28, 1961

A generator consisting of a low output impedance power supply and two tunnel diodes is described. The generator is capable of delivering positive and negative 400 mv steps of approximately 0.25 nsec rise time into a 50 Ω load. It can be triggered with $\frac{1}{2}$v signals to produce steps at repetition rates of 0 to 100 kc. Alternatively, it can free run at about 100 kc when the tunnel diode is biased at its current peak point. The duration of the pulse is 2 μsec and is determined by the inductance placed in series with the power supply and the incremental resistance of the tunnel diode. The pulse is flat within one per cent for 100 nsec following the 0.25 nsec rise time. Positive and negative polarities are obtained by connecting two tunnel diodes back-to-back. The conductance of these diodes is sufficiently high in the reverse direction to modify only slightly the forward characteristic of the pair with respect to a single tunnel diode.

FILTERS AND OTHER BASIC CIRCUITS

10,862 EMITTER-FOLLOWER COUPLED MULTISECTION FILTER CIRCUIT by S. Zechter (Philco); U.S. Pat. 2,983,875, Issued May 9, 1961

Active audio frequency filters which utilize emitter follower stages to couple successive inductor-capacitor networks are described. The high input impedance and low output impedance of the emitter follower stage and the isolation between adjacent networks permit the use of smaller inductors than used in the equivalent passive filters. The isolation between adjacent networks is provided by the emitter follower stages and by the use of pole-zero design techniques. The use of emitter follower stages results in voltage gains approaching unity in each section, filters with very low noise output, and a linear response. A typical filter employing emitter follower stages and inductance-capacitance networks has a volume about one eighth that of the corresponding passive filter and less than one third that of the equivalent active filter which utilizes negative impedance converters.

10,863 SERVO FILTER AND GAIN CONTROL IMPROVE AUTOMATIC DIRECTION FINDER by P. V. Sparks (Motorola); Electronics, Vol. 34, pp. 110-113, June 9, 1961

Improved ADF performance obtained by use of a synchronous servo filter and receiver AGC is cited. The AGC circuit provides uniform response over a wide input signal range without

clipping at high modulation levels. The AGC bias controls negative current feedback in each controlled stage by gradually removing the emitter bypass capacitor from the circuit. A synchronous filter at the servo amplifier input separates the 130 cps motor drive voltage from the audio frequencies in the receiver output without introducing phase shift into the signal. A 130 cps switching signal is applied to the bases of two transistors, causing them to operate as an automatic single-pole, double-throw switch. Condensers in each transistor circuit charge to the peak level of the input signal to provide a good square wave to the servo amplifier. The capacitors, in conjunction with an input resistor, act as a low-impedance filter for unwanted frequencies and as integrators at the switching frequency.

10,864 A HIGH Q TUNED CIRCUIT USING A SOLID STATE INDUCTANCE by I. Ladany and R. J. Kearney (U.S. Naval Res. Lab.); J. Electronics Control, Vol. 10, pp. 241-243, Mar. 1961

The use of the inductance and negative resistance of a double base diode to construct a frequency rejection filter with unusual properties is discussed. The Q increases with signal level, the maximum value depending on the tolerance or suppression of nonlinear effects. For a resistor suppression, at a certain signal level, the Q is in excess of 900.

10,865 INVESTIGATIONS OF MAGNETICALLY TUNABLE NARROW BANDPASS NONRECIPROCAL FILTERS USING FERRIMAGNETIC RESONATORS by C. N. Patel (Stanford Electronics Labs.); U.S. Gov. Res. Rep., Vol. 36, p. 37 (A), July 5, 1961 AD 255 743

The possibility of a narrow-bandwidth, small-insertion-loss microwave filter with nonreciprocal characteristics is studied, and the findings are reported. The discussion is limited to single-resonance transmission-type filters. In order to obtain tunability over a wide band of frequencies, samples of ferrimagnetic materials such as crystals of yttrium iron garnet, are used as high-Q microwave resonators. An analysis is presented of an equivalent circuit for coupling between 2 microwave circuits using a YIG sphere as the coupling element when the RF magnetic fields due to the 2 circuits are circularly or, in general, elliptically polarized. The experimental device consisted of a cross guide coupler, like a Bethe hole coupler, with only one off-axis aperture which contained the YIG sphere. The experimental results on various filters with different off-axis locations of the aperture are reported. The filters are tunable over the entire X-band by changing the dc magnetic field. The experimental results obtained are in good agreement with those predicted from the theory.

10,866 TUNABLE FERRITE CORRUGATED WAVEGUIDE FILTERS by M. Crane (Stanford Electronics Labs.); U.S. Gov. Res. Rep., Vol. 36, p. 32 (A), July 5, 1961 AD 255 300

Work on tunable corrugated waveguide filters is described. Corrugated waveguide filters are basically stopband structures with the waveguide acting as a high-pass filter. Two approaches are taken in the design of the tunable corrugated waveguide filter. In the first approach, only the slots incorporated ferrite. In the second approach, the complete structure was filled with ferrite. A corrugated ferrite filter designed with a stopband that covered the frequency range of X-band waveguide is discussed. In the investigation of ferrite filters, an interesting ancillary development is the ferrite waveguide. This structure, a completely filled rectangular waveguide, exhibits a magnetically tunable high-pass filter characteristic.

Magnetic X-Band Filters - See 10,795

Pulse Delay Circuit Using NOR Logic - See 10,875

APPLICATIONS OF SOLID STATE DEVICES

SCIENTIFIC, COMMERCIAL AND SPACE

Application of Masers in Communications and Astronomy - See 10,803

10,867 ELECTRONIC IGNITION SYSTEM DESIGNS by A. V. J. Martin (Electron. Automatisme, Paris); Electronic Ind., Vol. 20, pp. 164-166, July 1961

A transistorized electronic ignition system is described. The primary switch is placed in the base circuit of a power transistor with the collector coupled to the primary winding of the ignition coil. Advantages over classical systems are discussed and designs for an electronic speed meter and an automatic speed regulator are presented.

Transistorized Hearing Aid - See 10,912

Solid State Circuits Applied in Steelmill Controls - See 10,899

Commercial Applications of Diode Modulators - See 10,856

10,868 SATELLITE SOUNDER AND TELEMETER CHART IONOSPHERE ELECTRON DENSITY by S. Horowitz (AF Cambridge Res. Ctr.) and L. Humphrey (GE); Electronics, Vol. 34, pp. 50-53, June 23, 1961

A satellite ionosounder which will soar over the earth in a polar orbit, transmit a high frequency signal, record the reflected returns from the ionosphere and thus provide data for a latitude-time-dependent electron-density profile of the ionosphere is discussed. The ionosounder contains a stepped-discrete-frequency radar transmitter which operates sequentially at 3, 4.2, 5.7, 8, 11 and 15 Mc. The transmitted pulses have a peak power of about 150 w and pulse width of 500 μsec. The radar receiver is a multiple-frequency single-conversion superheterodyne. The satellite equipment can be operated in one of seven different modes and is controlled by a signal from the ground station. Data is recorded and played back at an interrogation station. The telemetry bandwidth is the same as the recorder play back figure and equals record response multiplied by a compression factor (10 in this case).

Automatic Direction Finder for Aircraft - See 10,863

Route Coordinate Generator for Air Traffic Control System - See 10,888

RADIO AND TELEVISION

Rechargeable Transistorized Pocket Radio - See 10,913

Ferrite Rod AM Radio Antenna Arrangement - See 10,799

10,869 MODIFYING VIDICON CAMERA CHAIN FOR SLOW-SCAN TELEVISION SYSTEMS by F. F. Martin and C. T. Shelton (RCA); Electronics, Vol. 34, pp. 101-103, June 9, 1961

Use of a four-second frame time to provide greater resolution and to permit use of a low-power, narrow-band transmitter is described. Transmission of a video picture 250 miles requires 100 watts. The video bandwidth is approximately 40 kc. A lower beam current, with a reduced scanning aperture, can be used since more time is available to discharge the scene. To reduce frame-to-frame carryover, a one-second erase scan is used between the four-second readout scans. An 80 kc wobble current is added to the vertical deflection coil during erase, spreading the electron beam vertically, to prevent interference in the picture. A temperature-compensated, keyed clamp restores the dc component of the video signal. The equivalent resolution is 250 lines compared to 175 lines for the conventional-rate vidicon camera.

TELEPHONY

10,870 REQUIREMENTS FOR ELECTRONIC SWITCHING EQUIPMENT IN TELECOMMUNICATION by H. K. M. Grosser (Philips Telecommun.); Philips Telecommun. Rev., Vol. 22, pp. 78-80, Jan. 1961

The fundamental requirements for electronic switching equipment in telecommunication work are discussed. The three major differences in the requirements for computers and switching systems are presented. One of the main problems is matching numerous low-speed inputs to the high processing capacity of electronic equipment. The switching speed is determined by traffic requirements and a PRF of 20 kc in the common control circuit is found to be ample. The primary emphasis is on reliability. A survey is given of the characteristics of basic circuits developed for use in electronic switching equipment.

10,871 TRANSISTORIZED CARRIER EQUIPMENT INSTALLED BY COPENHAGEN TELEPHONE COMPANY (PART I) TERMINAL AND LINE EQUIPMENT by J. D. Christensen (Copenhagen Tel.) and S. E. Andersen (Philips); Philips Telecommun. Rev., Vol. 22, pp. 108-116, May 1961

A number of frequency segregated 12-channel systems operated on deloaded and unloaded VF cables between a main exchange and its satellites are described. With this equipment, carrier working within a multi-exchange area is now being introduced in Denmark. The article explains how this was made economically possible with transistor circuitry.

10,872 TRANSISTORIZED CARRIER EQUIPMENT INSTALLED BY COPENHAGEN TELEPHONE COMPANY (PART 2) SELECTION OF VF CABLE PAIRS AND CROSSTALK BALANCING by C. N. Jensen (Copenhagen Tel.); Philips Telecommun. Rev., Vol. 22, pp. 117-123, May 1961

Referring to installation work carried out in northern Sjaelland (Denmark), the measures that have been taken in deloading and balancing a number of pairs in a random spliced VF cable, to make them suitable for carrier telephony up to 108 kc, are discussed. The results obtained are reviewed, and information is given on a new VF cable containing six carrier quads.

RADAR

Radar Transceivers for Satellite - See 10,868

10,873 TIME DISCRIMINATOR by A. I. Mintzer (RCA); U.S. Pat. 2,975,299, Issued Mar. 14, 1961

A circuit for sensing the time of occurrence of a signal for use in automatic tracking radar is described. A pair of normally closed diode switches, connected in bipolar fashion, are opened in immediate succession. A video pulse is transformer coupled to the switches with the correct polarity to be passed by the switch when open. A common circuit receives the switch outputs and derives an integrated signal having a sense and amplitude indicative of the time of occurrence of the input signal relative to a reference pulse. The diode switches are opened by early and late gate pulses which are generated by applying a unidirectional gate pulse to a short-circuited delay line having a length equal to one-half the gate duration. When the input video signal is centered at the crossover point of the bipolar gate signal, the integrator output is zero.

TELEMETRY

Satellite Ionosphere Data Telemetry System - See 10,868

Blocking Oscillator for Application in Telemetering Systems - See 10,842

MICROWAVES

10,874 A STRIPLINE FREQUENCY TRANSLATER by E. M. Rutz (Emerson Res. Lab.); IRE Trans., Vol. MTT-9, pp. 158-161, Mar. 1961

A frequency translator which operates at C-band frequencies is discussed. The modulators in the frequency translator are crystal diodes and the modulation is obtained by periodic variation of the reflection characteristic of the crystal modulators. The conversion loss of the frequency translator is 6.5 db at 8 mw input power. The unwanted sidebands are at least 25 db below the translated signal.

Microwave Antennas - See 10,807

COMPUTERS

Differences in Computer and Telecommunications Switching Systems - See 10,870

10,875 PULSE CONTROL APPARATUS by J. Dobbie (Westinghouse); U.S. Pat. 2,977,486, Issued Mar. 28, 1961

A pulse delay circuit, using NOR circuits, which delays the output by a variable time interval is described. The pulse in-

put is applied to two NOR circuits with one output connected directly to a feedback NOR unit and the other output connected to the feedback unit through an RC time delay network and a Zener diode. A gating pulse source can also be applied to the feedback unit. The RC network determines the time interval until the Zener breakdown voltage is reached. Pulse delay is obtained through the logic functions of the NOR units.

10,876 DESIGN OF LOGIC CIRCUITS USING THIN FILMS AND TUNNEL DIODES by T. A. Smay and A. V. Pohm (Iowa State U. Sci. Tech.); Electronics, Vol. 34, pp. 59-61, Sept. 15, 1961

Logic circuits using thin ferromagnetic films and tunnel diodes are discussed. Because of its negative resistance characteristic, the tunnel diode can be biased to operate at two stable voltage levels for a given current condition, while the single-domain ferromagnetic film has two stable magnetization orientations in the absence of external fields. Two types of toggling circuits are presented including schematics, characteristic curves, switching waveforms, and a theoretical discussion of operating principles. Both the tunnel diode and the thin ferromagnetic film operate at low voltage and moderate current levels and have high switching speeds. The primary difficulty in using such devices at present is the amount of amplification required to bring the sense winding signal up to a usable level. Improved deposition of films may result in greater energy transfer.

Current-Steering Diode Matrix Switch - See 10,884

Magnetic Amplifiers for Parametron Circuits - See 10,833

10,877 A LOW-COST PRE-SET TRANSISTORIZED COUNTER by R. R. Painter and R. A. Christensen (RCA); Semicon. Prod., Vol. 4, pp. 33-36, May 1961

The design and construction of a low-cost, general purpose, transistorized counter which accepts incoming information in the form of mechanical displacements from a microswitch, light-intensity variations from a photocell, or electrical signals are described. The two-decade counter may be pre-set to count numbers up to 100 at counting rates up to 10,000 per second. Numbers greater than 100 can be counted by the use of additional decades having no input circuit.

10,878 RANDOM PULSE GENERATOR TESTS CIRCUITS, ENCODES MESSAGES by B. K. Ericksen and J. D. Schmidt (GE); Electronics, Vol. 34, pp. 56-59, June 23, 1961

An improved pseudo-random sequence pulse generator, consisting of an n-stage shift register, is presented. The modulo 2 sum of the content of several stages of the shift register is formed and fed into the first stage as a reset pulse. The content of any stage can be taken as the output. A specific scheme contains approximately 30 shift register stages and has a maximum shift rate of 1.5 Mc. The modulo 2 sum of any 10 of the 30 or more shift stages is formed through a high speed (25 Mc) complementary flip-flop. The contents of these 10 stages are scanned by the output pulses of the blocking oscillators. The major design features of the shift register, the high speed flip-flop and blocking oscillator are included.

Modular Serial Word Generator - See 10,914

10,879 LOGIC CIRCUIT FOR A RADIO FREQUENCY CARRIER INFORMATION HANDLING SYSTEM by F. Sterzer and D. J. Blattner (RCA); U.S. Pat. 2,977,484, Issued Mar. 28, 1961

High-frequency adder and half-adder circuits useful in pulsed RF carrier computer systems are described. The circuits were designed for a PRF of 500 Mc at a carrier frequency of 3000 Mc. A hybrid circuit, in rat race form, is constructed of strip transmission line with two input arms and sum and carry output arms. The lines, which contain terminating transducers, are connected to a circular strip line with an expander in shunt with the carry output line. The input RF energy is phased to arrive at the circular strip junctions in the proper phase. The circuits are interconnected to form full adders. Adder and half-adder action is obtained by reflection, division and absorption of the input RF energy.

10,880 ELECTROLUMINESCENT-PHOTOCONDUCTIVE PATTERN RECOGNIZER ORGANIZES ITSELF by J. A. O'Connell (Genl. Tel. and Electronics); Electronics, Vol. 34, pp. 54-57, July 14, 1961

A sandwich module using flow table principles to recognize a 12-bit digital word is described. The device consists of a recognition panel, a storage panel and an input panel. The digital input is divided into four 3-bit words which are applied to successive recognition gates where they are compared with a pattern optically coupled-in from the storage panel. An ON condition is shifted from stage to stage when the digital information presented to the stage matches a pattern of binary words that it has been programmed to accept. Different recognition patterns are obtained by altering the pattern of illuminated controlling photoconductors in the flow table panel. Under single-shot operation, speeds of 3-4 msec per logical decision have been obtained. Under continuous operation, the speed is 5 - 10 times slower per decision element because of the slow photoconductor decay time.

10,881 MAGNETO-OPTICAL READOUT OF MAGNETIC RECORDINGS by T. Lentz and J. Miyata (Natl. Cash Register); Electronics, Vol. 34, pp. 36-39, Sept. 1, 1961

A device utilizing the longitudinal Kerr effect to read back magnetic bit patterns recorded on a thin ferromagnetic film is described. Bit densities from 40-4000 bits/linear inch are reported using an 800A vacuum evaporated cobalt film recorded by the standard magnetic method. High level noise problems arising from phototube shot-noise and magnetic film surface imperfections are overcome by splitting the information modulated light beam and feeding a differential amplifier. Film coercivity of 30 and 100 oe are related to resolution capability. Maser light sources may provide even higher bit densities.

10,882 SERIAL MATRIX STORAGE SYSTEMS by M. Lehman (Israel Ministry Def.); IRE Trans., Vol. EC-10, pp. 247-252, June 1961

The application of coincident-current techniques, usually associated with parallel ferrite-core stores, to the operation of serio-parallel or purely serial memories is discussed. A block diagram outline of one possible physical realization of a serial system is presented and the conditions under which such a store is economically justified are discussed. The distinguishing feature of the system discussed is that coincidence is established in the memory matrix between two currents representing an address signal and a time signal, respectively. It is shown how the properties of the time-controlled series store may lead to the adoption of a word asynchronous design for serial digital computers. In such a machine, timing is not controlled or determined by limited store access. The serial techniques facili-

tate the incorporation of autonomous transfers, automatic floating point operations, high speed multiplication, division and shift orders and asynchronous transfers into small serial computers.

10,883 A MAGNETIC ASSOCIATIVE MEMORY by J. R. Kiseda, H. E. Petersen, W. C. Seelbach, and M. Teig (IBM Res. Ctr.); IBM J. Res. and Dev., Vol. 5, pp. 106-121, Apr. 1961

A computer storage system in which data flows in and out of the memory on the basis of content rather than location (address) is described. A small experimental model of this system, using ferrite cores as novel associative memory storage elements, is described.

10,884 A 0.7 MICROSECOND FERRITE CORE MEMORY by W. H. Rhodes, L. A. Russell, F. E. Sakalay, and R. M. Whalen (IBM); IBM J. Res. and Dev., Vol. 5, pp. 174-182, July 1961

The design and performance of a newly developed magnetic core memory is described. A two-dimensional array organization and partial switching of toroidal cores were employed in the design of this low-power, high-speed memory. The memory features a unique combination of a current-steering diode matrix and a load-sharing magnetic switch for an economical and high-performance drive system. The operating memory has a storage capacity of 73,728 bits and executes instructions reliably up to a repetition rate of 1.47 Mc. The discussion includes a description of the organization, the series-parallel delay line clock, the control of critical timing pulses, and the actual measured performance.

10,885 DIODE STEERING INCREASES SPEED OF MAGNETIC MEMORIES by A. Melmed, R. Shevlin, and W. Orvedahl (NYU and U. Chicago); Electronics, Vol. 34, pp. 68-70, Sept. 15, 1961

A method of incorporating diodes into magnetic memory systems to increase their speed is described. A junction diode is used as the steering element for word selection in a word-organized core memory. Its recovery current is used to half select the same word during the second half of a READ or STORE operation. A detailed description of the memory system consisting of over 400,000 cores is given. Diode steering reduces the problems raised by partially selected word lines. It leaves control over the word-line parameters external to the core stack, so that the difficulty introduced by variation in line impedance with digit content may be overcome. The advantage of this selection system over the more conventional twin-diode scheme lies in conversion of the formerly wasteful diode recovery time into useful operation time. The magnetic-core memory system may be used in general purpose digital computers.

10,886 OBTAINING NONDESTRUCTIVE READOUT WITH FERROELECTRIC MEMORIES by A. B. Kaufman (Litton Systems); Electronics, Vol. 34, pp. 47-51, Aug. 25, 1961

A barium titanate ferroelectric memory cell with nondestructive readout is described. Electrodes are deposited on a polycrystalline element, with operation similar to an electromechanical filter operated near or at its resonant frequency. The memory cell is made in two parts with mechanical coupling between the parts. The motor element is permanently polarized and exhibits electrostrictive properties, expanding and contracting with an applied sine wave clock voltage. The second part is the memory element which is polarized in a specific direction by an applied electric field. Readout is accomplished through the remanent piezoelectric effect. By using additional memory cells in a strip, a serial word readout may be obtained from a single clock pulse. The mechanical propagation of the motor pulse down the strip excites each memory cell in turn. Individual memory cells have been operated in excess of one Mc.

10,887 PULSE AMPLIFIER INCLUDING TRANSISTORS by T. E. Einsele and H. von der Heyden (IBM); U.S. Pat. 2,994,003, Issued July 25, 1961

A drive pulse amplifier for a magnetic core memory which operates into a controlled load circuit to decrease power dissipation and increase rise time is described. The collector is connected through a high resistance and the core matrix to a high potential, and shunted through a diode to a low potential. When the transistor cuts off, the diode conducts, connecting the collector to the low potential. When the collector current exceeds the diode current, the diode cuts off and the low potential is switched out of the collector circuit. The rise time is determined by the line inductance and the low potential supply. The transistor is driven into saturation before the low potential is switched out, reducing power dissipation.

Magneto-Optical Readout of Magnetic Recordings - See 10,881

Microminiature Magnetic Shift Register - See 10,915

Shift Register in Random Pulse Generator - See 10,878

10,888 FUNCTION GENERATOR CIRCUITS by W. B. Sander (Tasker Instr.); U.S. Pat. 2,976,430, Issued Mar. 21, 1961

A function generator circuit which translates an input signal into any number of independently varying output signals, each of which is specified as a different function of the input, is described. A twin diode network is used for each output. The input is applied to a high-gain inverter amplifier with the output applied to the diode networks. The diodes are connected back-to-back through a common resistance to a potential source. The amplifier output is applied to one diode with the other diode connected through a feedback resistor to the amplifier input. The input diode is normally biased off, and the output is determined by the voltage divider action of the diode load resistor and the output diode impedance. At a predetermined input amplitude, the input diode becomes forward biased, and the output then follows the amplifier output. The transition point can be accurately set by selection of the circuit voltages and impedances. The circuit is used as a route coordinate generator in an Air Traffic Control System.

10,889 DETECTING TRANSMISSION ERRORS IN PHASE-SHIFT-KEYING SYSTEMS by L. C. Widmann (GE); Electronics, Vol. 34, pp. 76-79, Sept. 8, 1961

Field operating tests to determine the quality of new communication and data transmission systems are described. In the phase-shift-keying systems tested there is an inability to distinguish between phase-lock at 0° and phase-lock at 180°. The error detecting and polarity correcting unit described detects phase-lock at 180° and corrects message inversion. A nine-bit test message is transmitted; the received test message then is compared with a replica of the original. A block diagram and detailed description is given of major sub-units, including appropriate waveforms. Inputs to the equipment are: the message to be checked; bit-timing pulses in phase with the bits in the message to be checked; bit-timing pulses halfway between con-

secutive in-phase bit-timing pulses; and character-timing pulses. Berkeley decimal counting units count the number of messages received, the number of message errors, and the number of digit errors.

10,890 DIODE-TRANSFORMER GATING CIRCUIT by K. H. Olsen (Digital Equip.); U.S. Pat. 2,977,485, Issued Mar. 28, 1961

A low-cost, high-speed gating circuit for digital data processing systems is described. The input signal is applied to a transformer primary with the output taken from the secondary. A diode in series with the secondary is gated to block or pass the signal. A complementary signal to a flip-flop circuit is provided by the use of two gate circuits with a common input for the complement pulse. The gate outputs are connected to the flip-flop inputs and the control signals are derived from the flip-flop outputs.

POWER

10,891 CONTROLLED RECTIFIER PRODUCES QUARTER-MEGAWATT PULSE POWER by H. G. Heard (Radiation at Stanford); Electronics, Vol. 34, pp. 54-55, June 23, 1961

An all solid-state modulator that produces a peak power output of 250 kw is presented. The modulator uses Si diodes for high-voltage rectifier, backswing, hold-off and inverse-diode circuits. The switch is a p-n-p-n Si-controlled rectifier. The trigger generator uses two-layer and four-layer diodes. When a positive trigger signal from the trigger generator is applied to the gate electrode of the controlled rectifier, the rectifier is turned on; at the termination of the trigger pulse it is turned off. The average rating of the rectifier is 50 a, though peak current may reach as high as 5000 a for short pulse operation. Units with average current rated at 100 a are available and 200 a units are under development.

10,892 REGULATED POSITIVE-NEGATIVE SUPPLY DELIVERS LOW-VOLTAGE DIRECT CURRENT by D. T. Birch and K. E. Chellis; Electronics, Vol. 34, p. 62, July 28, 1961

A common power supply using a series transistor with a shunt dc amplifier and a Zener diode to supply the reference voltage is discussed. Its output is adjustable from 11 to 15v and is "nearly constant" from no load to 300 ma, or from 90-140v ac line voltage variations. Values of regulation and stabilization factors are not given. Ripple at no load is 2 mv, and a full load is 5 mv.

10,893 A DC POWER SUPPLY USING TRANSISTORS AND ZENER DIODE REFERENCE SOURCES by R. E. Aitchison and C. T. Murray (U. Sydney); Proc. IRE Austl., Vol. 22, pp. 26-27, Jan. 1961

A variable dc power supply using Zener diodes as a reference source is described. The unit consists of two separate power supplies: a 12v, 250 ma constant voltage supply, and a 1 μa to 10 ma constant current supply. A constant 6v, 0-1 ma reference supply is also provided. RC filters are used instead of chokes. The Zener reference system uses cascaded Zener diodes to provide low ripple and high stability. The internal resistance of the constant voltage supply is 0.02 Ω and maximum ripple is 35μv. The constant current supply has a maximum ripple of 30μv and an internal resistance of 10 meg at 25μa and 50 kohms at 10 ma. The internal resistance of the 6v reference supply is 10 Ω with a maximum ripple of 90μv.

Transistorized Power Supplies - See 10,916

10,894 TRANSFORMER AND SHUNT TRANSISTORS REGULATE DC POWER SUPPLY by J. T. Keefe (Sola Elect.); Electronics, Vol. 34, pp. 99-101, May 19, 1961

A constant voltage ferroresonant transformer which can be used in dc power supplies to provide a high degree of regulation is described. Improved regulation can be achieved when a shunt transistor regulating circuit is added. The regulating circuit consists of a temperature-compensated Zener diode circuit to sense the output voltage. Shunt transistors turn on when the output voltage is too high and turn off when the output voltage is low. Current through the shunt circuit adds to the load current, increasing the voltage drop through the leakage reactance of the constant voltage transformer, providing regulation. A complete schematic of the regulating circuit is included.

10,895 CONVERTER EFFICIENCY AND POWER OUTPUT OF A TUNNEL-DIODE RELAXATION OSCILLATOR by S. Wang (U. California); Proc. IRE, Vol. 49, pp. 1219-1220 (L), July 1961

The efficiency and power output of a tunnel diode oscillator operated as a dc to ac converter are considered. Such a converter is useful in conjunction with thermoelectric generators since both are low impedance devices and the voltage required to bias the tunnel-diode into the negative resistance region is obtainable from single-cell thermoelectric generators. For high conversion efficiency, it is desirable to make the ratio of peak-to-valley current as large as possible. Experimental results agree with the theoretical analysis presented.

10,896 TRANSISTOR OSCILLATOR by T. C. G. Wagner (Minn. - Honeywell); U.S. Pat. 2,990,519, Issued June 27, 1961

A dc to ac converter which reduces the power dissipated in the transistors during switching is described. Two transistors have their emitters connected to each end of a transformer primary. The bases are connected to a center-tapped feedback winding with a synchronizing pulse input to the center-tap. The synchronizing pulse frequency is twice the oscillator frequency. The pulses drive the transistors quickly through the transition from a low-voltage, high-current state to a high-voltage, low-current state, reducing power dissipation in the transistors during this period. A capacitor across the primary slows down the voltage reversal across the transformer to permit the synchronizing effect. Diodes in the emitters prevent overswing during the time both transistors are cut off.

10,897 ELECTRICAL INVERTER CIRCUITS by J. F. Roesel, Jr. and R. W. Lucky (Westinghouse); U.S. Pat. 2,977,550, Issued Mar. 28, 1961

A self-excited inverter circuit in which the output frequency is independent of the input magnitude and can be varied over a wide range is described. A switching transformer, connected in parallel to the output transformer, has separate windings connected to the bases of the switching transistors. A variable capacitor is connected in series with the transformer winding and one transistor collector. The output frequency is set by the capacitor. When one transistor conducts, a portion of the

collector current charges the capacitor. When the capacitor is charged, current flow through the switching transformer ceases and the resulting potential change switches the transistors.

Transistor Power Amplifier - See 10,834

10,898 INVERTER CONTROL CIRCUIT SAVES POWER by D. W. R. McKinley (Natl. Res. Counc., Ottawa); Electronics, Vol. 34, p. 56, Aug. 4, 1961

An inverter control circuit which reduces standby current drain to less than one ma is described. The sensing element consists of a pair of back-to-back Si diodes which provide bias voltage to trigger a switching transistor, closing a relay. Under no load, the relay is open and the input to the inverter is disconnected. Under load, a dc bias developed across one sensing diode switches the transistor and closes the relay. A capacitor across the relay stores enough energy to hold the relay closed until the inverter voltage builds up. Load current through the other sensing diode holds the relay closed until the load is removed.

CONTROL

10,899 SEMICONDUCTORS IMPROVE RELIABILITY OF STEEL-MILL CONTROL EQUIPMENT by T. E. DeViney (Square D); Electronics, Vol. 34, pp. 104-107, June 9, 1961

Use of solid-state circuits to replace electromechanical devices for controlling motors on a steel strip welding and coiling line is described. Three dc drive motors drive a processor, a set of tension rolls and an up-coiler. A looping pit allows slack in the strip for decoupling from the up-coiler. Depth of the loop is regulated by a photoelectric control. Light, directed across the pit, is intercepted by the loop, regulating the amount of light striking the photodetector. The output is amplified by a temperature-compensated silicon transistor and used to control the field strength of the up-coiler motor. The motor shunt fields are supplied by separate silicon controlled rectifier bridges with magnetic amplifier firing circuits. Acceleration and deceleration are controlled by separate transistor circuits, regulated by a feedback signal taken from the field current of the motor being controlled.

Motor Speed Control Circuit - See 10,917

10,900 DESIGNING SOLID-STATE SYNCHROS WITH HALL-EFFECT COMPONENTS by Z. R. S. Ratajski (Genl. Precision); Electronics, Vol. 34, pp. 59-63, Sept. 8, 1961

A study and development of Hall effect components with the object of replacing windings and wear-prone contacts in synchro devices by semiconductors operating with permanent magnets is described. When used for signal generation important parameters are the stability of signal, low noise (low Hall voltage at zero field), low magnet or resistance and temperature effects, high signal-to-noise ratio, and linearity and symmetry of the signal. When Hall generators are used for power transfer, other parameters are important: high Hall voltage output at low impedance, high power transfer efficiency, heat dissipation capacity and maximum operating temperature. Some compromise must be made in selection of Hall materials: those recommended for signal generators are indium phosphide, Ge and Si; those for power transfer are InSb and InAs. A brief theoretical discussion of the principles involved in Hall effect synchro circuits is given and some examples of Hall effect devices are presented. Advantages to be gained by application of Hall effect components are: simple design and fewer parts, increased reliability, reduced friction of the rotating member, further miniaturization capability, reduced production cost and new areas of application with dc and ac power supplies.

10,901 TRANSISTOR AMPLIFIER CONTROLS REMOTE APPLIANCES (C. M. W., Staff of Electronics); Electronics, Vol. 34, p. 59, May 26, 1961

A transistorized ultrasonic unit which can be used for remote control of TV sets as well as other consumer appliances is presented. The unit uses seven transistors, five of which form a five stage cascade amplifier tuned to a symmetrical double peaked curve at the control frequencies, 38.285 kc and 41.805 kc. The output stage contains two class B detector-amplifiers, each tuned to one of the two control frequencies. The use of a double fulcrum relay in the output circuit allows two channel control as well as providing mechanical cancellation of broad-band noise signals.

INSTRUMENTATION

Piezoelectric Transducing Elements - See 10,809

10,902 INCREMENTAL SENSOR by K. P. Congdon (Avco); U.S. Pat. 2,977,487, Issued Mar. 28, 1961

An incremental sensing system to detect extremely small signal variations is described. A sensing bridge, energized by a constant signal source, is maintained in an unbalanced state. The bridge output is a condition responsive AM signal which represents the variations in the condition being sensed. The signal is amplified and applied to a reverse biased diode having a load circuit time constant much less than the period of the input signal, enabling the diode to act as a wave follower gate, passing only the peak portions of the input. The diode output is amplified and shaped in a transistor amplifier to produce a related AM output signal of increased percentage modulation. The intelligence can then be recovered in any standard demodulator. The gating action of the diode permits elimination of unwanted signals below a certain level.

10,903 TRANSISTOR MULTIRANGE D.C. MILLIVOLTMETER by K. Holford (Mullard Res. Labs.); Mullard Tech. Commun., Vol. 5, pp. 311-316, June 1961

A portable dc millivoltmeter having a maximum sensitivity of 10 mv full-scale deflection and an input resistance of 1 meg per volt is described. The circuit uses four BCZ11 transistors and a 9 v battery, and consumes 0.7 ma. Output indication is by means of a 100 μa moving-coil meter. The effect of ambient temperature change upon both the calibration accuracy and the zero stability is considered. A theoretical justification is given for the balance system adopted for the long-tailed-pair input stage.

10,904 THERMISTORS AS CRYOGENIC TEMPERATURE SENSORS by P. E. Martin and H. Richards (Martin); Program Cryogenic Engrg. Conf., pp. 43-44 (A), Aug. 1961

Data on the use of thermistors as sensors for temperature meas-

urements in liquid nitrogen and liquid hydrogen are presented. The primary interest is from the engineering viewpoint, but this is of necessity backed by the laboratory measurements where the cryogenic temperatures can be controlled by maintaining constant pressure in small cryostats. Thermistors are economical, fast, reproducible, and small enough to act as point sensors. There are possible disadvantages. The leads are fragile and easily torn away in a stream. Each thermistor needs to be calibrated, and this under exact conditions as in use. Nevertheless, thermistors are recommended, and if reasonable precautions are followed, thermistors are capable of temperature recordings better than fifty millidegrees over limited ranges.

10,905 GAS-FILLED ULTRAVIOLET DETECTOR WARNS OF FIRE AND EXPLOSIONS by D. H. Howling and R. C. Roxberry (McGraw Edison); Electronics, Vol. 34, pp. 52-55, May 26, 1961

An ultraviolet radiation detector tube that features stable high-power gain and sensitivity in the spectral region of 1900-2900 A is discussed. The tube consists of two symmetrical electrodes which permit operation on both ac and dc. The tube is normally operated at 700 v rms with instantaneous striking voltage at approximately 700 v. A typical value of current sensitivity of the tube at 60 cps is 2.3×10^8 a/w. Maximum permissible ambient temperature is around 200°C. Probability of false alarm due to noise has been calculated; the interval between false alarms turns out to be approximately 8.7×10^5 years. An experimental aircraft fire detector circuit using 3 of these detector tubes is presented.

Solid State Infrared Counter - See 10,789

Electronic Speed Meter - See 10,867

10,906 INFRARED CURTAIN SYSTEM DETECTS AND COUNTS MOVING OBJECTS by P. A. Tove and J. Czekajewski (U. Uppsala, Sweden); Electronics, Vol. 34, pp. 40-43, Aug. 4, 1961

The use of infrared light beams to detect and register the passage of moving objects is described. Signals are produced by phototransistors when the infrared beams in two closely-spaced curtains are interrupted. The pulses are applied to logic circuits to register events. A mechanical register with a time indicator provides direct printing of the data. For remote data collection, AM pulse signals are created when an event occurs. The pulses are modulated at two different frequencies, depending on the direction of travel of the moving object. A third modulation frequency is used for check pulses. Bandpass filters in the receiver route the pulses to separate registers for permanent recording.

ENERGY CONVERSION AND HEAT PUMPING

Thermal and Electrical Circuit Effects on Entropy of Thermoelectric Devices - See 10,786

Solar Energy Converters - See 10,783

High Temperature Solar Cells - See 10,782

GaAs Solar Cells - See 10,784

Thermoelectric Air Conditioner for Submarines - See 10,788

NEW PRODUCTS

10,907 INDIUM ANTIMONIDE (Cominco Products Inc., Electronic Materials Dept., 933 West 3rd Ave., Spokane 4, Wash.)

Indium antimonide available in both single crystal and polycrystalline forms with a wide range of electrical properties is announced. N-type polycrystalline material is available in three electron mobility grades: 100,000 to 200,000 (Grade 12), 200,000 to 400,000 (Grade 24), and 400,000 plus (Grade 40) cm^2/volt-sec at 78°K. This material is supplied in bars of semicircular cross-section approximately 4.5 cm wide by 1.3 cm thick, weighing about 30 gm per cm. Boat grown and vertically pulled single crystals are available in two electron mobility grades: 300,000 to 500,000 (Grade 35S), and 500,000 plus (Grade 50S) cm^2/volt-sec at 78°K. Doped (both n and p type to 10^{18}) materials and fabricated shapes from all stocks can be supplied to customer specifications.

10,908 MICROETCH VARACTOR DIODES (Philco Corp., Lansdale Div., Lansdale, Pa.)

A new series of microetched germanium varactor diodes capable of providing simultaneous operation at maximum frequency and high voltage is disclosed. The new diodes, comprising types L-4110, L-4111, and L-4112 have very high cutoff frequencies and exhibit a greatly increased capacitance variation over the whole operating voltage range. Designed primarily as efficient harmonic generators at frequencies up to 3 Gc, 6 Gc, and 10 Gc (in order of ascending cutoff frequency), they may also be used as parametric amplifiers or RF tuning devices.

10,909 HIGH TEMPERATURE RECTIFIER HOUSINGS (Advanced Vacuum Products, Inc., 430 Fairfield Ave., Stamford, Conn.)

Ceramic-to-metal housings for power and controlled semiconductor rectifiers capable of withstanding temperatures to 1700°F are announced. Metallized alumina ceramic brazed to metal hardware forms a molecular bond stronger than the ceramic itself. The devices show strength in the order of 15,000 psi, thermal shock resistance at temperatures of 1000°F, and high thermal conductivity characteristic of a vacuum seal leak tested at 1×10^{-9} cc/sec.

10,910 MINIATURE FERRITE ISOLATORS (Sylvania Electric Products, Inc., 1100 Main St., Buffalo 9, N.Y.)

Miniature, lightweight coaxial ferrite isolators capable of operating under environmental conditions as severe as those imposed on ferrite devices of conventional size are announced. Typical of these new devices is an X-band isolator with an isolation-to-insertion-loss ratio of 20 to 1 and a 10 per cent bandwidth, weighing four ounces. The overall length of the unit, including TNC connectors, is 2-11/16 inches. Furnished for any frequency from 4.0 Gc to 11.0 Gc, they can be designed and built to customer specifications within four weeks.

10,911 ELECTRONIC CHOPPERS (Solid State Electronics Co., 15321 Rayen St., Sepulveda, Calif.)

A series of solid state electronic choppers (or modulators) de-

signed to alternately connect and disconnect a load from a signal source or for use as ac to dc demodulators is announced. They are capable of linearly switching ro chopping voltages over a dynamic range extending from a fraction of a millivolt to ten volts, and can be driven from dc to a huncred kc. Solidly encapsulated in epoxy resin and available in both germanium and silicon units, they will withstand shocks of up to 500 G for 11 milliseconds, vibration at 30 G of from zero to 2000 cps, and acceleration to 700 G. Applications are in low level voltage measurements, dc amplifier stabilization, high-speed servomechanisms, thermocouple instrumentation, low-level switching, and many other uses.

10,912 EYEGLASS HEARING AID (Otarion Listener Corp., Box 711, Ossining, N.Y.)

A six-transistor eyeglass hearing aid, the Super-9, weighing less than 2/3 ounce and said to be the world's most powerful, has been introduced. Able to provide for 40 to 85 decibel hearing losses, it will operate efficiently at temperatures of from freezing to 120 degrees Fahrenheit. The hearing aid is designed with RX circuitry that allows a choice of tone and response depending on the type of hearing deficiency.

10,913 RECHARGEABLE POCKET RADIO (Gulton Industries, Inc., 212 Durham Ave., Metuchen, N.J.)

A pocket-size transistor radio powered by a rechargeable nickel-cadmium battery is announced. The six-transistor Ever-Play radio can be recharged in any electrical outlet, and one charge stores power for up to 15 hours of full volume playing with none of the fade-out associated with conventional batteries.

10,914 SERIAL WORD GENERATOR (Servo Corp. of America, 111 New South Rd., Hicksville, L.I., N.Y.)

A fully transistorized modular serial word generator ("5500") featuring selectable word length and bit rates to 1 Mc is announced. Flexible basic design allows selection of clock rate, data coding, serial word length, and bit duration for the pulse data output. Positive and negative non-return-to-zero data output is also provided. While two standard instruments are supplied, providing word lengths of up to 40 and 80 bits, greater capacity and multiple-channel units are available on special order. Fully modular construction enables addition or change of standard plug-in modules for wide functional flexibility. Applications include: design and test of shift registers, memory elements, digital input-output equipment, code conversion systems, digital to analog converters, etc.

10,915 MICROMINIATURE MAGNETIC SHIFT REGISTER BIT (Magnetics Research Co., Inc., 179 Westmoreland Ave., White Plains, N.Y.)

A microminiature register bit module for use in space vehicles weighing 2 grams and occupying only 1/16 cubic inch per bit is announced. Operable from a single missile battery supply at low current drains, standard electrical designs are available for shift rates up to 250 kc, and providing 5 volt flat topped output pulses at 1:0 ratios of better than 8 to 1. The units are used for parallel to serial and serial to parallel conversion of information, buffer storage, and counting.

10,916 MODULAR POWER SUPPLIES (Power Sources, Inc., Northwest Industrial Park, Burlington, Mass.)

Modular transistor regulated power supplies are announced. Operable at full ratings without heat sink at up to 35°C ambient temperatures and with mounting base temperature of 65°C, they are available in a full line of specifications ranging from 4.5-6.0 volts to 45-55 volts. These plus-in packages operate isolated from the ac line, providing adjustable output. They are short circuit protected by current limiting and provide automatic recovery after short removal.

10,917 MOTOR CONTROL (Industrial Control Co., Central Ave. at Pinelawn, Farmingdale, L.I., N.Y.)

The 309-A, a solid-state, wide range speed control driving a 1/20 HP motor directly from the 60 cps line, is announced. Shaft speed is indicated on a panel meter and ranges from 100 to 5000 rpm with maximum load torque of 10 oz-in at any speed. A tachometer stabilizes shaft speed against changes in line voltage and load, and speed remains constant within two per cent regardless of load variation. The control will reverse and dynamically brake the motor for fast stops and can be furnished with mating gear boxes for different shaft speeds. Maximum power drain is 150 watts.

SUBJECT INDEX

G

H

I

J

AUTHOR INDEX

AUTHOR INDEX *(Continued)*

CAPSULE
CLASSIFICATION OUTLINE
for
COMPUTER ABSTRACTS ON CARDS

C0 ELECTRONIC COMPUTERS — GENERAL

- C0.1 History and Prediction
- C0.2 Surveys and Visits; State of the Art
- C0.3 Summaries of Technical Conferences
- C0.4 Bibliographies, Abstracts, and Reviews
- C0.5 Texts
- C0.6 Standards and Suggested Standards
- C0.8 Personnel
- C0.9 Education

C1 LOGIC AND SWITCHING THEORY

- C1.0 General
- C1.1 Basic Theory and Principles
- C1.2 Truth Functions (Switching or Boolean Functions)
- C1.3 Combinational Switching Networks
- C1.4 Non-Deterministic and Unreliable Switching Networks
- C1.6 Iterative Switching Networks
- C1.7 Theory of Automata
- C1.8 Sequential Switching Theory and Networks

C2 DIGITAL COMPUTERS AND SYSTEMS

- C2.0 General
- C2.1 System Design and Machine Organization
- C2.2 Applied Logic Design
- C2.3 Digital Arithmetic Methods and Systems
- C2.4 Error Detection and Correction in Computing Systems
- C2.5 Reliability, Maintenance, Mechanical Construction, and Production of Computers
- C2.6 General-Purpose and Special-Purpose Digital Computers (Alphabetically)
- C2.7 General-Purpose Digital Computers (by Country and Type)
- C2.8 Special-Purpose Digital Computers (For Real-time Control and Data Acquisition Systems see Section C12.)

C3 DEVICES AND BASIC LOGIC AND WAVEFORMING CIRCUITS

- C3.0 General
- C3.1 Electromechanical and Passive Linear Electrical Components
- C3.2 Electron Devices and Electronic Logic Circuits (including Microwave)
- C3.3 Semiconductor Devices and Logic Circuits
- C3.5 Parametrons and their Logic Circuits; Parametric Amplifiers
- C3.6 Nonlinear Magnetic Devices and Logic Circuits
- C3.7 Cryogenic (Superconductive) Devices and Logic Circuits
- C3.8 Other Devices for Logic and Their Circuits
- C3.9 Basic Sequential and Waveforming Circuits

C4 STORAGE AND INPUT-OUTPUT

- C4.0 General
- C4.1 Principles and Theory of Storage Organization
- C4.2 Static Magnetic Random-Access Storage
- C4.3 Static Non-Magnetic Random-Access Storage
- C4.4 Dynamic (Volatile) Random-Access Storage
- C4.5 Reference Storage (Contents Not Changeable by the Machine)
- C4.7 Sequential-Access Storage in Fixed Media or Elements (Usually Dynamic)
- C4.8 Storage on Moving Media
- C4.9 Input-Output

C5 PROGRAMMING AND CODING

- C5.0 General
- C5.1 Basic Principles and Techniques of Programming
- C5.2 Machine Programming and Coding Techniques
- C5.3 Programming Languages
- C5.4 Automatic Programming
- C5.6 Concurrent Programming; Multi-Problem Handling
- C5.8 Program Monitoring and Debugging
- C5.9 Non-Mathematical Algorithms; Data-Handling Algorithms

C6 FORMAL AND NATURAL LANGUAGES, INFORMATION RETRIEVAL, AND HUMANITIES

- C6.0 General
- C6.1 Formal Languages and Systems
- C6.2 Symbol Manipulation
- C6.4 Natural Languages, Linguistics, and Mechanical Translation
- C6.6 Information Retrieval
- C6.8 Humanities and Social Sciences

C7 BEHAVIORAL SCIENCE AND ARTIFICIAL INTELLIGENCE

- C7.1 Pattern and Character Recognition and Detection
- C7.2 Speech Recognition and Production
- C7.3 Psychology and Behavioral Science
- C7.5 Probabilistic and Self-Organizing or Adaptive Systems
- C7.7 Learning, Problem Solving, and Game Playing
- C7.8 Man and the Machine

C8 MATHEMATICS

- C8.0 General
- C8.1 Number Representation and Arithmetic; Number Theory
- C8.2 Functional Approximation to Data
- C8.3 Computation of Functions
- C8.4 Algebra and Analysis
- C8.6 Calculus and Differential Equations
- C8.8 Combinatorial Mathematics

C9 PROBABILITY, INFORMATION THEORY, AND COMMUNICATION SYSTEMS

- C9.1 Probability
- C9.2 Statistics
- C9.3 Operations Research and Game Theory
- C9.4 Simulation
- C9.5 Information Theory and Noise (Interference)
- C9.7 Communication and Broadcast Systems and Radar

C10 SCIENCE, ENGINEERING, AND MEDICINE

- C10.0 General
- C10.1 Electrical Science and Engineering
- C10.2 Mechanics; Mechanical and Civil Engineering
- C10.3 Aeronautical Engineering and Design
- C10.4 Astronomy, Space, and Geophysics
- C10.6 Chemistry and Chemical Engineering
- C10.7 Classical and Atomic Physics
- C10.8 Nuclear Physics
- C10.9 Medicine and Biology

C11 ANALOG AND HYBRID COMPUTERS

- C11.1 Direct Analogs
- C11.2 Analog Computer Techniques and Systems
- C11.3 Analog Computer Components (Subassemblies)
- C11.5 Analog Computer Mathematical Methods and Programming
- C11.7 Hybrid (Analog-Digital) Computers
- C11.9 Analog-Digital Conversion

C12 REAL-TIME SYSTEMS AND AUTOMATIC CONTROL; INDUSTRIAL APPLICATIONS

- C12.0 General
- C12.1 Control System Theory
- C12.2 Sampled-Data System Theory
- C12.4 Data Acquisition and Transmission Systems
- C12.5 General-Purpose Real-Time Systems
- C12.6 Real-Time Control Computers (on-line)
- C12.8 Industrial Engineering and Production Techniques; Automation

C13 GOVERNMENT, MILITARY, AND TRANSPORTATION APPLICATIONS

- C13.1 Government and Politics
- C13.3 Military Applications
- C13.6 Transportation Operations
- C13.7 Aviation
- C13.8 Railroads

C14 BUSINESS APPLICATIONS

- C14.0 General
- C14.1 Business Data Processing Techniques
- C14.3 Management Science
- C14.5 Application of Computing (Data-Processing) Machines in Specific Businesses

"Every 24 hours enough technical papers are turned out around the globe to fill seven sets of the twenty-four volume *Encyclopaedia Britannica*. And the output is rising every year. This year's crop: some 60 million papers . . . the laboratory scientist, busy with work of his own, no longer can find enough hours in the day to keep up with all that is published in his field. Even staying on top of the indexes and abstracts of these papers has become an insurmountable task for the lab men. One result is that company after company has found itself duplicating research work that others have done and fully chronicled."

From the *Wall Street Journal*
Tuesday, December 20, 1960

COMPUTER ABSTRACTS ON CARDS

A quick cumulative reference to the Technical Literature on Electronic Computers

C 2.25/1.249

1539 COMPUTER DESIGN OF MULTIPLE-OUTPUT LOGICAL NETWORKS by T. C. Bartee (Lincoln Lab., M.I.T.); IRE Trans. on Electronic Computers, Vol. EC-10, pp. 21-30, March 1961

An important step in the design of digital machines lies in the derivation of the Boolean expressions which describe the combinational logical networks in the system. Emphasis is generally placed upon deriving expressions which are minimal according to some criteria. A computer program which automatically derives a set of minimal Boolean expressions describing a given logical network with multiple-output lines is discussed. The program accepts punched cards listing the in-out relations for the network, and then prints a list of expressions which are minimal according to a selected one of three criteria. The basic design procedure and the criteria for minimality are described.

COMPUTER ABSTRACTS ON CARDS is designed to provide the engineer or scientist with a cumulative reference file to the technical literature on electronic computers, *organized by subject matter*. As a subscriber you would receive, every other month, several hundred 3″ x 5″ cards containing abstracts of recently published papers in the computer field. These abstracts summarize the contents of the papers, enabling you to determine what work has been reported on a given subject and showing you where you can find more detailed information on that subject. In addition to the abstract and the journal reference, each card has a classification number which makes it easy for you to file the card in a *logical sequence* with all previously issued cards. In this way you can continuously group together abstracts of related references, just as the Dewey Decimal System enables a librarian to group together books on related subjects.

This abstract card file corresponds in some ways to the card file which enables the librarian to locate any book or periodical in the library. However, it has additional advantages which result from the information provided by the abstracts themselves and from the logical (as opposed to alphabetical) organization which permits one to browse through references on related topics as one might browse through the books on a library shelf. An alphabetical Pre-Index is provided with this service to direct the user to the part of the file which is devoted to a given topic. In addition, the same abstracts are supplied in a non-cumulative form with subject and author indexes. Taken together the card file, the Pre-Index, and non-cumulative version of the abstracts make it easy to locate information by:

Logical Sequence
Alphabetically by Subject
Alphabetically by Author

COMPUTER ABSTRACTS ON CARDS covers the following topics in the field of electronic computers:

- Logic and Switching Theory (Boolean Functions, Switching Networks, Automata)
- Digital Computers and Systems (Design, Arithmetic Methods, Equipment, Error Detection)
- Devices (Electromechanical, Electron Tube, Semiconductor, Magnetic, Cryogenic, etc.)
- Logic and Waveforming Circuits
- Storage and Input-Output
- Programming and Coding (Programming Languages, Automatic Programming, Algorithms)
- Languages (Natural and Formal Languages, Mechanical Translation)
- Information Retrieval
- Pattern Recognition and Artificial Intelligence
- Mathematics (Number Theory, Numerical Analysis, Probability and Statistics)
- Operations Research and Game Theory
- Information Theory and Noise; Communications Systems
- Analog and Hybrid Computers
- Real-Time Systems and Automatic Control
- Applications of Computers in Science, Engineering, Industry, Government, Business, etc.

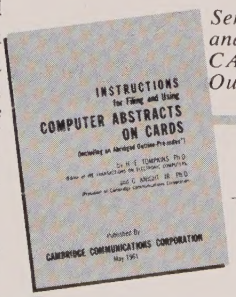

Send for free booklet — "Instructions for Filing and Using COMPUTER ABSTRACTS ON CARDS" — including Abridged Classification Outline and Pre-Index.

CAMBRIDGE COMMUNICATIONS CORPORATION
238 Main St., Cambridge 42, Mass.

Please send me a copy of "Instructions for Filing and Using COMPUTER ABSTRACTS ON CARDS".

NAME _____

TITLE _____

COMPANY _____

ADDRESS _____

CITY _____ ZONE _____

STATE _____

in'for·ma'tion re·triev'al, *n.* **1.** rapid location of technical information on specific topics.

information retrieval system for the solid state:

SOLID STATE ABSTRACTS ON CARDS

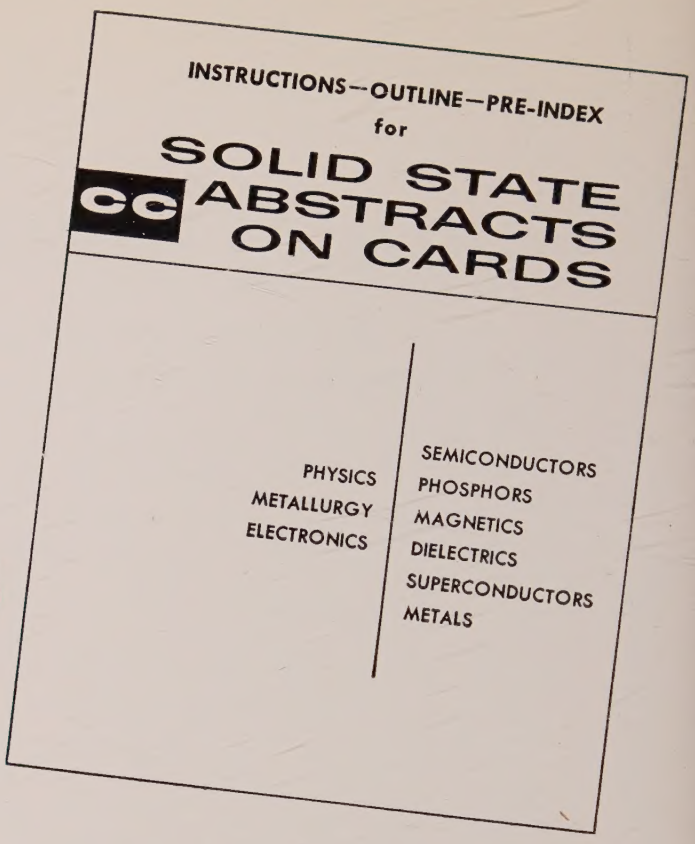

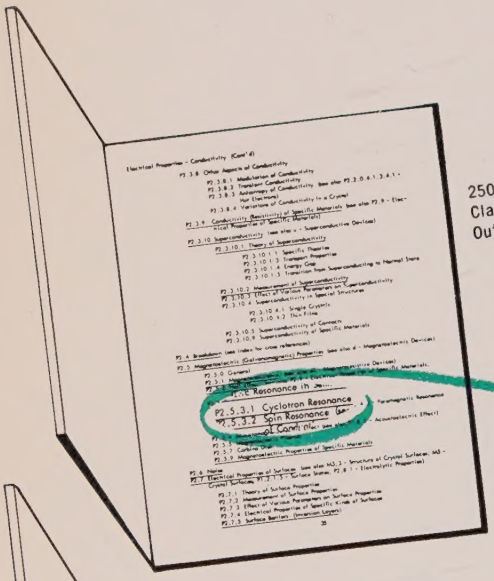

2500-Topic Classification Outline

Send for your free copy of our new 120 page book describing this unique system which is now being used in more than 300 solid state laboratories throughout the world.

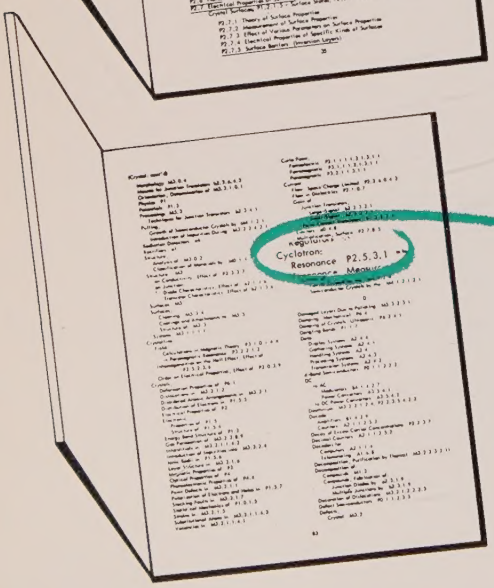

4000-Entry Alphabetical Pre-Index

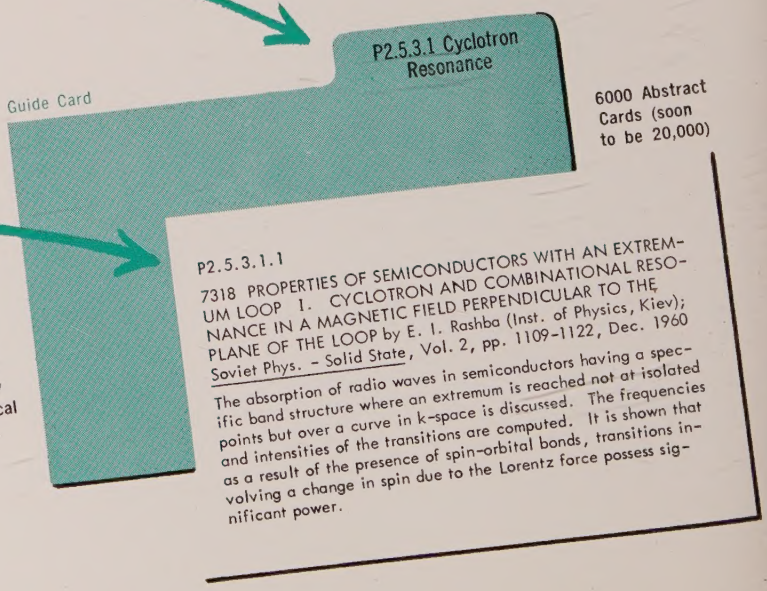

CAMBRIDGE COMMUNICATIONS CORPORATION

236 MAIN STREET • CAMBRIDGE 42, MASSACHUSETTS • **Tel. 491-0710**